Linda Helander

Hexylaminolevulinate Photodynamic Treatment of Cancer Cell Lines

Thesis for the degree of Philosophiae Doctor

Trondheim, June 2015

Norwegian University of Science and Technology
Faculty of Medicine
Department of Cancer Research and Molecular Medicine (IKM)

NTNU – Trondheim
Norwegian University of
Science and Technology

NTNU
Norwegian University of Science and Technology

Thesis for the degree of Philosophiae Doctor

Faculty of Medicine
Department of Cancer Research and Molecular Medicine (IKM)

978-82-326-1022-8 (print)
978-82-326-1023-5 (digital)
1503-8181

Doctoral theses at NTNU, 2015:183

Printed by NTNU Grafisk senter

Norsk sammendrag:

Heksylaminolevulinat fotodynamisk behandling av kreftcellelinjer.

Fotodynamisk terapi (PDT) er en behandlingsmetode som kan brukes på både kreft og pre-kreft. Metoden er allerede i bruk på klinikker og flere pasienter ved hudavdelingen her på St.Olav blir behandlet med PDT hver uke. Metoden er en tostegsbehandling der det først enten blir tilsatt en fotosensitizer eller en forløper til en fotosensitizer. Fotosensitizer vil i hovedsak akkumuleres i kreftvev og den gjør cellene sensitive for vanlig synlig lys. Etter at kreftvevet har blitt lyssensitivt påføres det lys med tilpasset bølgelengde. Dette er som regel rødt lys.

Selv om PDT er i bruk på klinikker er det et behov for optimalisering og større kunnskap om de effekter metoden gir. Vi har valgt å studere heksylaminolevulinat (HAL) basert PDT på cellenivå. Denne varianten av PDT er godkjent for diagnose av blærekreft og den aktive fotosensitizeren er protoporfyrin IX (PpIX). I denne avhandlingen har vi sett på effektene fra ulike parametere i lyset og fokusert på hvilken type celledød som blir indusert samt effekter på proteiner.

Fra de fire studiene i avhandlingen har vi funnet ut at HAL-PDT med rødlys effektivt dreper rotteblærekreft-celler, hovedsakelig gjennom nekrose og at fraksjonering av lysdosen med 45 sekunder lys etterfulgt av 60 sekund mørke ikke gir endret utslag på hverken mengde celledød eller type i forhold til sammenhengende belysning.

Videre så har vi sett at effekter fra HAL-PDT er avhengig av hvilken cellelinje som er i bruk. Alle de fem cellelinjenes dose- responskurver varierte både i form og lysdoseområde. Vi så også at lav lysintensitet ikke var like effektiv som høy lysintensitet for sub-letale doser og vi fikk resultater som indikerer at lav lysintensitet induserer apoptose i større grad enn PDT med høy lysintensitet. PpIX kan aktiveres av både rødt og blått lys, men det ser ut til at rødlys HAL-PDT gir mer apoptose enn blålys HAL-PDT.

I de to siste studiene var fokuset på proteinendringer. Blålys HAL-PDT på rotteblærekreftceller viste at det ble indusert post-translasjonelle modifikasjoner, noen proteiner endret mengde og at en del proteiner ble karbonylerte etter HAL-PDT.

I den siste studien viste vi at økt lysdose gir økt induksjon av reaktive oksygen arter (ROS). Vi identifiserte over 1900 proteiner som var reversibelt oksidert på cystein sete, i stor grad som følge av ROS. Ut fra disse studerte vi en undergruppe som vi var ekstra sikre på at var endret som følge av HAL-PDT. Over halvparten av disse viste seg å være assosiert med programmert celledød og flere av disse er igjen kjent for å

være redoksregulert. Redoksregulering av proteiner er et voksende fagfelt og mekanismens betydning i cellers signalverden øker. For å verifisere at noen av de proteinene vi identifiserte kan være en sentral triggermekanisme for HAL-PDT indusert apoptose behøves det en del mer forskning.
Oppsummert så bidrar denne avhandlingen til en bedre forståelse av effektene etter HAL-PDT og den peker på viktigheten av å bruke optimale parametere for selve belysningen og den åpner for at reversibel oksidering av cystein seter kan være en sentral mekanisme for indusering av apoptose etter HAL-PDT.

Navn kandidat: *Linda Helander*
Institutt: *Institutt for kreftforskning og molekylærmedisin*
Veiledere: *Hovedveileder: Professor Hans E. Krokan; medveiledere:*
dr. Odrun A. Gederaas, professor Duan Chen og professor em. Anders Johnsson
Finansieringskilde: *stipend fra FUGE Midt-Norge*
Finansiell støtte: *Svanhild og Arne Must's fond for medisinsk forskning*

Ovennevnte avhandling er funnet verdig til å forsvares offentlig
for graden PhD i Molekylærmedisin
Disputas finner sted i Auditoriet MTA,Medisinsk teknisk forskningssenter,
Tirsdag 30. Juni 2015 , kl. 12.15.

Hexylaminolevulinate photodynamic treatment of cancer cell lines

Linda Helander

Table of Content

Acknowledgements

The work presented in this thesis has been carried out at the Department of Cancer Research and Molecular Medicine, Faculty of Medicine at NTNU. I am grateful for the funding granted the Functional Genomics Program of Research Council of Norway, and the Svanhild and Arne Must fund for medical research which has allowed me to study HAL-PDT on cancer cells.

Foremost, I would like to express my gratitude to my supervisor prof. Hans Krokan. Your support, critical questions and eye for details has made this thesis possible and raised its scientific level. I've learned a lot from you, both scientifically and about the world of academia. Thank you, Hans.

This thesis would probably never come to the end without the long distance collaboration with dr. Kristjan Plaetzer (Priv.Dozent.). The discussions during the Salzburg visits and by video calls have been an invaluable source for motivation and learning. Thank you, Kristjan.

I also would like to thank my co-supervisors: prof.em. Anders Johnsson for admirable and experienced guidance throughout both my master and doctoral thesis; dr. Odrun Gederaas for applying for the funding, introducing me to PDT colleagues and her lab protocol routines; and prof. Duan Chen for guidance (that made me see both the broader picture and important details) when I've asked for it.

A special thank goes to the PROMEC-gentlemen: prof. Geir Slupphaug for including me to your group and doing scientifically immersion into our papers, dr. Lars Hagen for always answering my questions and guiding me through the proteomics experiments and Animesh Sharma for coffee breaks and doing magic with the datasets. Another special thank goes to prof.em. Thor Bernt Melø for being a positive and patient scientific support throughout both my master and doctoral thesis; and to my co-PhD, dr. Yan Baglo, I admire your working capacity and value our discussions and talks.

My sincere gratitude goes to co-authors and both past and present colleagues for contributing to the work, for answering all questions I've thrown at you and for the fun chats over slightly bad coffee. Thank you for providing a good scientific and social including environment.

Family and friends gets my warmest gratitude for being supportive and enduring this journey with me. And to my life partner, Vidar, and children, Gard and Embla: tusen takk for at dere har holdt ut opp- og nedturene. Dere er tryggheten, utfordringen og livsgleden min. Jeg gleder meg til fortsettelsen.

Trondheim, January 2015

Linda Helander

List of papers

Paper I:

Photo induced hexylaminolevulinate destruction of rat bladder cells AY-27.

Ingvild Kinn Ekroll*, Odrun Arna Gederaas, Linda Helander, Astrid Hjelde, Thor Bernt Melø and Anders Johnsson

Photochem Photobiol Sci. 2011 Jun;10(6):1072-9.
doi: 10.1039/c0pp00393j

Paper II:

Red versus blue light illumination in hexyl 5-aminolevulinate photodynamic therapy: the influence of light color and irradiance on the treatment outcome in vitro.

Linda Helander*, Hans E. Krokan, Anders Johnsson, Odrun A. Gederaas and Kristjan Plaetzer

J Biomed Opt. 2014 Aug;19(8):088002.
doi: 10.1117/1.JBO.19.8.088002

Paper III:

Photodynamic therapy with hexyl aminolevulinate induces carbonylation, posttranslational modifications and changed expression of proteins in cell survival and cell death pathways.

Yan Baglo, Mirta M. L. Sousa, Geir Slupphaug, Lars Hagen, Sissel Håvåg, Linda Helander, Kamila A. Zub, Hans E. Krokan and Odrun A. Gederaas *

Photochem Photobiol Sci. 2011 Jul;10(7):1137-45.
doi: 10.1039/c0pp00369g

Paper IV:

Reversible oxidation of thiol proteins after hexylaminolevulinate mediated photodynamic therapy.

Linda Helander, Animesh Sharma, Hans E. Krokan, Kristjan Plaetzer, Barbara Krammer, Odrun A. Gederaas, Geir Slupphaug and Lars Hagen.*

Manuscript, submitted

Abbreviations

AIF	Apoptosis inducing factor
ALA	Aminolevulinate
ATP	Adenosine triphosphate
BCC	Basal cell carcinoma
DNA	Deoxyribonucleic acid
GSH	Glutathione
HAL	Hexylaminolevulinate
HPD	Hematoporphyrin
LD	Lethal dose
LDL	Low density lipoprotein
LED	Light emitting diode
MMP	Mitochondrial membrane permeabilization
MPTP	Mitochondrial permeability transition pore
mTOR	mammalian target of rapamycin
PBR	Peripheral benzodiazepine receptor
PDD	Photodiagnosis
PDT	Photodynamic therapy
PpIX	Protoporphyrin IX
PS	Photosensitizer
ROS	Reactive oxygen species
SOD	Superoxide dismutase

Background

This background is subdivided into three main topics: photodynamic therapy (PDT), cell death and oxidative stress. Each subject is large, diverse and integrated with each other. Hopefully the separation into topics makes the introduction of this thesis easier to comprehend. PDT is the method used in this thesis and will be described in general terms first and then more detailed on the most relevant topics for this thesis. Cell death and oxidative stress are both important effects of PDT and have been aspects of this thesis.

1.1 Photodynamic therapy (PDT)

Photodynamic therapy is a form of cancer treatment based on light activation of a photo-sensitive compound, a photosensitizer (PS). This treatment is approved for clinical use with different photosensitizers in several countries for different types of tumour malignant and non-malignant conditions.

1.1.1 PDT in general

Several different photosensitizers have been tested for PDT and some of them have been approved for clinical use. Two main features of a photosensitizer are that it absorbs light within the visible range and that it accumulates preferably in cancerous cells/tissue. A good PS has a high ratio for entering a long-lived excited state after light absorption, has high cancer to normal tissue ratio and quite rapid clearance from the organism. The first step in PDT is to administer a PS or a PS precursor; the second step is to illuminate the target with appropriate light. These two steps results in oxidative stress at the cellular level which can induce cell death. When dealing with the subject PDT it is important to know that there are some differences between effects *in vivo* and *in vitro*, as well as at organism and cellular levels, respectively. *In vivo* treatment is much more complex since PDT will induce an inflammatory response and vascular shut down in addition to

direct target kill. PDT will be described in more detail in the subsequent paragraphs.

1.1.1.1 History of PDT

The history of PDT has been well reviewed by others and only a brief account will be given here (Agostinis et al., 2011; Dolmans et al., 2003; Honigsmann, 2013; Krammer & Plaetzer, 2008; Moan & Peng, 2003). It started 3000 years ago as phototherapy when the Indians, the Egyptians and the Chinese applied light alone on humans for therapeutic purposes. Phototherapy was used to treat diverse disorders such as psoriasis, vitiligo and skin cancer. In 1903 Niels Finsen was awarded the Nobel Prize for his use of light in treatment of *lupus vulgaris* and was accordingly acknowledged as the founder of modern phototherapy. The combination of photoactive components and light to treat a disorder was first described in one of India's sacred books 1400 BC. Both Indians and Egyptians treated vitiligo by natural psoralens in combination with solar light.

Further progress did not occur until 1974 when PUVA (treatment with psoralens and UVA light) was reported to be an efficient psoriasis treatment. Around 1900, researchers observed that the combination of certain chemicals and light in the visible range could induce cell death. Oscar Raab and his supervisor Hermann von Tappeiner carried out ground-breaking work and this group introduced the term photodynamic in 1907. In 1913, Friedrich Meyer-Betz injected himself with hematoporphyrin (HPD) and became light sensitive for over two months; this was the first time hematoporphyrins were used on humans. Hans Fischer received the Nobel Prize in 1930 for his work on porphyrins. Porphyrin-induced fluorescence from tumours was first observed and published by Albert Policard in 1924. HPD was partially purified and sold under the trade name Photofrin which became a widely used photosensitizer for clinical PDT.

A major breakthrough for PDT came in 1975 when Dougherty and co-workers reported that combination of HPD and red light reduced tumour in mice (Dougherty et al., 1975). In the same year Kelly and co-workers reported elimination of bladder cancer in mice after treatment with HPD and light and in 1976 this group started the first human trial with HPD to treat bladder cancer (Kelly, 1975; Kelly et al., 1975). Due to

the impurity of HPD and the long lasting light sensitivity when using Photofrin an intensive search for better photosensitizers was undertaken. In 1979, Zvi Malik and co-workers published a paper describing how aminolevulinate (ALA) increases endogenous production of protoporphyrin IX (PpIX) constituting the basis for ALA-based PDT, but without the light part of PDT (Malik & Djaldetti, 1979; Malik et al., 1979).

Two years later Kennedy and Pottier started to study ALA-induced porphyrin production and in 1987 they treated the first patient with ALA-PDT (Kennedy & Pottier, 1992; Kennedy et al., 1990; Pottier et al., 1986). After these publications several other researchers began to study the basics and possible application of ALA in PDT. In 1993 PDT was for the first time approved as cancer treatment, when Photofrin-based PDT was approved as treatment against bladder cancer in Canada. At the present, several photosensitizers are clinically approved, see Table 1.

1.1.1.2 Mechanisms of PDT; photochemical reaction

There are three essential components in PDT: photosensitizer (PS), light and molecular oxygen. None of the components is toxic alone, but when combined appropriately they can together initiate a photochemical reaction which can generate oxidative stress and cause toxicity and cell death. PDT is a two-step procedure. After administration of a PS the tumour locus is irradiated with light of appropriate wavelength. In the subsequent text phototoxicity and the photochemical reaction will be described.

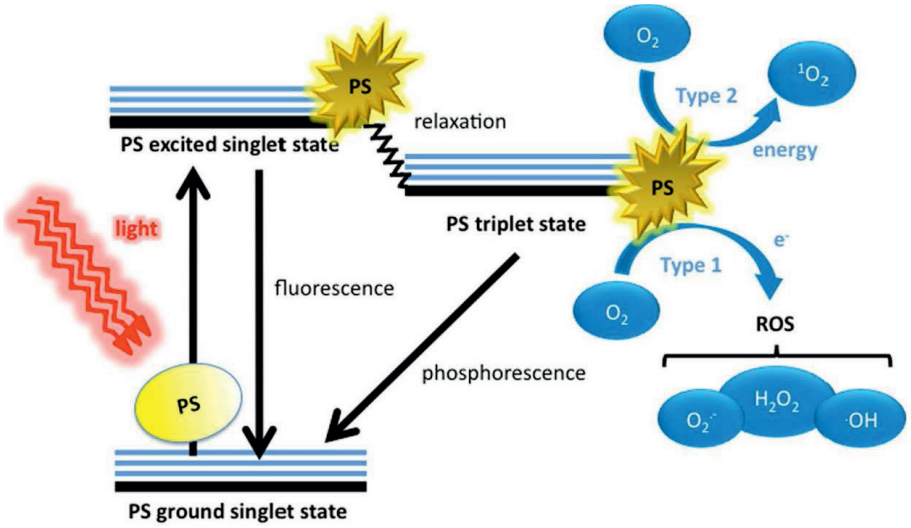

Figure 1: A Jablonski diagram. For details, see text below. Adapted from (Dai et al., 2012)

The Jablonski diagram in Figure 1 is often used as an illustration of the interaction of light with molecules, the photophysical processes. A photosensitizer in the ground state is in a singlet state configuration. In the singlet state the molecule is characterized by paired electrons. Electrons can only have two orientations; +1/2 and -½ (often denoted as "spin up" and "spin down", ↑ and ↓) and paired electrons are in antiparallel direction and thus have a total spin quantum number S=0, and a magnetic quantum number of 1, M=2S + 1. Ground state is the preferred energetic state for a molecule and in ground state, S_0, all the electrons are in their energetically lowest possible orbital. When a PS absorbs a light quantum of appropriate energy (wavelength) one of its electrons shifts to a higher energetic level S_x (where x = 0, 1, 2, 3… and denotes the level of increased energetic state). Since all excited states are energetically less preferable than the ground state, the PS will return to S_0 after a short time period (typically 10^{-15}-10^{-12} second (Plaetzer et al., 2008)). The de-excitation of a molecule can take place in several ways.

All excited energetic states S_x are sub-sectioned into several vibrational levels and an electron in a high vibrational level of an excited state will rapidly return to the energetically lowest level of that state through vibrational relaxation. The excess energy

in vibrational relaxation is lost as heat. If the PS was in S_x where x >1 it can after vibrational relaxation drop to the first excited singlet state, S_1.

The relaxation from S_1 to S_0 can take place in three different ways: emission of a photon (fluorescence), heat radiation or by crossing into a triplet state and further interact with other molecules. Fluorescence will always occur from the lowest vibrational state in S_1 and is therefore not dependent on the wavelength of the absorbed light, the photon has a fixed wavelength, and the emitted photon has always lower energy (wavelength) than the absorbed one (Plaetzer et al., 2009).

The third possibility for relaxation is when the PS crosses from S_1 into an isoenergetic level of the triplet state, T_1. In triplet state the electrons are unpaired and have thus S = 1 and M =3. The crossing from S_1 to T_1 is spin-forbidden and is a non-radiative process called inter system crossing, ISC. Most PSs have a high quantum yield for this process. Triplet states are generally characterized with a relative long lifetime, up to seconds. De-excitation from T_1 takes place either by a radiative process called phosphorescence or by a photochemical reaction. The effects of PDT come from photochemical reactions.

The term phototoxicity is used for the process where a non-toxic compound is converted into an oxidant or produces an oxidant after absorption of light. Phototoxicity can be separated into two main photochemical reactions; type I and type II. These photochemical reactions are the starting points for the effects of PDT and therefore optimal PSs have a high yield for triplet excited state and photochemical reactions.

Type I photochemical reaction is when the PS de-excites from T_1 to ground state by transferring electrons (or protons) to oxygen or other nearby molecules. This result in radical anions (or cations, respectively) and these radicals are likely to react with molecular oxygen to form reactive oxygen species (ROS), especially superoxide anions. After the first type I photochemical reaction, several secondary reactions can occur and result in a diversity of oxidants, as has been thoroughly reviewed (Plaetzer et al., 2009).

Type II photochemical reaction is when the PS de-excites from T_1 to ground state by energy transfer, not by transfer of electrons/protons. The energy transfer has to be to a molecule in triplet state. Naturally occurring molecules in triplet state is rare, but molecular oxygen is in triplet state in its ground state, $^3O_2$. So, during type II

photochemical reaction singlet oxygen, $^1O_2$, is formed which is highly reactive.

Both type I and type II reactions happen in parallel and are competing reactions. The ratio between the two reactions depends mostly on the type of PS in use and on the concentration of molecular oxygen (Foote, 1991; Ochsner, 1997; Plaetzer et al., 2009). For most PSs used in PDT, type II reactions is the dominant reaction (Plaetzer et al., 2009; Weishaupt et al., 1976).

1.1.1.3 Molecular and cellular mechanism involved in PDT

As described in 1.1.1.2, PDT generates oxidants and especially singlet oxygen. High amounts of oxidants can overload the anti-oxidative defence system of the cell/organism and create oxidative stress. Oxidative stress will induce several stress responses in the affected cells. Depending on the type of cellular damage and amount of damage, the cell could experience different types of effects including survival, autophagy, apoptosis and necrosis. Cell death and oxidative stress are the main effects in cells after PDT and will be described in section 1.2 and 1.3, respectively.

1.1.1.4 PDT in the clinical use

PDT on patients is more complex than PDT on cell cultures. In addition to directly *target cell damage*, eradication of tumour in patients will be supported by *vascular damage* and *immune responses*. The significance of the three effects is still under discussion and will not be treated comprehensively in this subsection. Direct tumour cytotoxicity is briefly described in the previous subsections, and will be described in more detail in section 1.2. An overview of direct cell damage and the two indirect mechanisms causing tumour damage (immune response and vascular damage) are sketched in Figure 2 and a brief description of both indirect damage pathways follows.

Figure 2: Mechanisms of tumour eradication in clinical PDT. First PDT generates oxidative damage that can kill cancer cells directly. The induction of apoptosis and/or necrosis stimulates release of both inflammatory mediators and tumour associated antigens. This results first in a non-specific immune response followed by slowly developing adaptive immunity. In addition, PDT induces destruction of tumour vascularity which can contribute to tumour eradication through lack of oxygen and nutrients. Figure is adapted from (Pizova et al., 2012).

Enhanced anti-tumour immunity after PDT:

PDT induces oxidative stress which further triggers a variety of signal pathways, including signalling via Toll-like receptors. Toll-like receptors are central in innate

immune responses. Other central molecules for initiation of immune response are the expression of heat shock proteins, transcription factors such as nuclear factor κB (NF-κB) and activator protein 1 (AP-1) which are all reported to have increased activity after PDT (Castano et al., 2006; Garg et al., 2011; Garg et al., 2010; Mroz et al., 2010; Pizova et al., 2012; Sanovic et al., 2009; Verwanger et al., 2002).

In addition, PDT-induced degradation of membrane lipids and generation of arachidonic acid metabolites, which together with histamine and serotonin released from damaged vasculature (activated mast and enterochromaffin cells) will lead to invasion and infiltration of leukocytes in the tumour (Pizova et al., 2012). After activation, leukocytes will take part in tumour destruction and activate the complement system. The complement system is a major effector system of innate immunity and plays a role even in adaptive immunity. Activation of the complement system after PDT seems to play an important role in PDT-induced immune responses (Garg et al., 2010; Pizova et al., 2012).

Subsequent to activation of innate immune responses comes development of adaptive immunity. Necrotic cells release inflammatory cytokines (Festjens et al., 2006).When the dying tumour cells release their antigens in the inflamed area, the antigens will be taken up by antigen-presenting cells. This promotes initiation of specific antitumor immunity. PDTs ability to induce antitumor responses is a mechanism pursued by scientists aiming to generate anticancer vaccines in several studies (Castano et al., 2006; Garg et al., 2010; Pizova et al., 2012).

The opposite of enhanced anti-tumour immunity, immunosuppression, has been demonstrated (Mroz & Hamblin, 2011; Pizova et al., 2012) and appears to be correlated with increased treated area (Pizova et al., 2012). Frost and co-workers demonstrated that a decrease of light intensity prevented PDT-induced immunosuppression (Frost et al., 2011). This may indicate that when PDT overwhelms the patients stress response system, immunosuppression instead of enhanced immunity will be triggered. A way of improving the PDT effect might be by combining PDT with immunotherapy (Kwitniewski et al., 2008; Pizova et al., 2012).

PDT and tumour vascularity:

Unlike normal tissue, tumour tissue needs to continually generate new blood vessels to supply the growing tumour tissue. Abnormal vascularity is one of the hallmarks of

tumour tissue. PDT can in some cases be used to target the tumour angiogenesis and the tumour blood vessels and this will contribute significantly to the final treatment outcome (Chen et al., 2006; Krammer, 2001; Middelburg et al., 2014). The targeting of blood vessels is either through passive or active targeting approaches (Chen et al., 2006).

Passive vascular targeting PDT: The time period when the applied PS is mainly localized in the blood vessels (usually short time after administration) gives a temporal therapeutic window for vascular targeting (Chen et al., 2006; Senge & Radomski, 2013). In addition, the physicochemical properties of the PS may contribute to passive vascular targeting, where properties like lipophilicity and high affinity for vascular components, such as LDL-receptors, enhance the vascular targeting (Maziere et al., 1990).

Active vascular targeting PDT: Either structural modification of the PS or a targeted drug delivery system can cause the PS to be retained in the neovascular system producing a specific vascular effect. The targeting moieties are peptides, antibodies or other ligands that recognize molecules that are selectively expressed on newly synthesized blood vessels (Bhuvaneswari et al., 2009). All molecules with higher expression in tumour blood vessels than normal ones may potentially be targets for PDT.

Clinical use of PDT to treat cancer goes back to the late 1970's and since then more than 200 clinical PDT trials have been performed (Agostinis et al., 2011). Currently, the main PS and pro-PS in clinical use are: hematoporphyrin derivative (Photofrin®), mTHPC (5,10,15,20-Tetra(3-hydroxyphenyl)chlorine, Foscan®, Fospeg® and Foslip®), δ-aminolevulinate and its derivatives (Levulan®, Metvix®, Hexvix® and Cysview®), benzoporphyrin derivative monoacid ring A (Verteporfin® and Visudyne®) and mono-L-aspartyl chlorine e6 (NPe6, Talaporfin®, Laserphyrin®) (Senge & Radomski, 2013). The different cancer types that are treated with PDT include; skin cancer (pre-cancerous actinic keratosis, basal cell carcinoma, Bowens disease), head and neck tumours, digestive system tumours, urinary system tumours, intraperitoneal malignancies, non-small cell lung cancer, mesothelioma and brain tumours (Adigbli & MacRobert, 2012; Agostinis et al., 2011; Baldea & Filip, 2012; Bissonnette, 2011; Bozzini et al., 2012; Calin et al., 2011; Ikeda et al., 2011; Karrer et al., 2013; Kharkwal

et al., 2011; Krammer & Plaetzer, 2008; Lee & Baron, 2011; Oosterlinck et al., 2004; Zhao & He, 2010). Cure rates may exceed 90%, but PDT may also be used as palliative treatment. PDT has nice cosmetic results compared to invasive treatment and the preservation of tissue function after PDT is good. Since none of the approved PSs are localized in the nucleus, the genotoxicity is minimal. It is therefore safe to repeat the PDT treatments and for PSs with rapid clearance from the body, the treatment can easily be repeated after a week. In addition to being a cancer treatment, PDT is also used in the cosmetic industry for skin rejuvenation (Karrer et al., 2013; Nootheti & Goldman, 2007) and as medical treatment against acne (Bissonnette, 2011; Choi et al., 2010; Kjeldstad & Johnsson, 1986; Lee et al., 2007; Taub, 2004).

Table 1: Overview over photosensitizers that have been applied in patients, and where they are approved or in trials. The table was updated in 2011 and is adapted from (Agostinis et al., 2011).

PHOTOSENSITIZER	STRUCTURE	WAVELENGTH, nm	APPROVED	TRIALS	CANCER TYPES
Porfimer sodium (Photofrin) (HPD)	Porphyrin	630	Worldwide		Lung, esophagus, bile duct, bladder, brain, ovarian
ALA	Porphyrin precursor	635	Worldwide		Skin, bladder, brain, esophagus
ALA esters	Porphyrin precursor	635	Europe		Skin, bladder
Temoporfin (Foscan) (mTHPC)	Chlorine	652	Europe	United States	Head and neck, lung, brain, skin, bile duct
Verteporfin	Chlorine	690	Worldwide (AMD)	United Kingdom	Ophthalmic, pancreatic, skin
HPPH	Chlorin	665		United States	Head and neck, esophagus, lung
SnEt2 (Purlytin)	Chlorin	660		United States	Skin, breast
Talaporfin (LS11, MACE, NPe6)	Chlorin	660		United States	Liver, colon, brain
Ce6-PVP (Fotolon), Ce6 derivatives (Radachlorin, Photodithazine)	Chlorin	660		Belarus, Russia	Nasopharyngeal, sarcoma, brain
Silicon phthalocyanine (Pc4)	Phthalocyanine	675		United States	Cutaneous T-cell lymphoma
Padoporfin (TOOKAD)	Bacteriochlorin	762		United States	Prostate
Motexafin lutetium (Lutex)	Texaphyrin	732		United States	Breast

Abbreviations: ALA, 5-aminolevulinic acid; AMD, age-related macular degeneration; Ce6-PVP, chlorin e6-polyvinypyrrolidone; HPD, hematoporphyrin derivative; HPPH, 2- (1-hexyloxyethyl)-2-devinyl pyropheophorbide-a; MACE, mono-(L)-aspartylchlorin-e6; mTHPC, m-tetrahydroxyphenylchlorin; nm indicates nanometers; SnEt2, tin ethyl etiopurpurin.

Even though much time has passed since PDT was first reported (early 1900's) it has not been included in mainstream clinical treatments (Agostinis et al., 2011). PDT is often used as alternative treatment, palliative treatment or in combination with other treatments. There is also a difference between countries in the use of PDT. The reasons for this delay are complicated. Hopefully a better understanding of dosimetry, utilization

of LED technology, a better improved PSs (with rapid clearance from the body, high specificity and absorption in red/far red range), and more clinical trials will improve PDTs potential as treatment modality.

1.1.1.5 The ideal photosensitizer

There are some features making one PS better than others, as outlined (Plaetzer et al., 2008): "The ideal photosensitizer is characterized by (1) high light absorption within the optimal window for PDT (approximately 650 nm to 850 nm), (2) a high quantum yield for the triplet state, (3) a rather high photo-stability, (4) amphiphilicity, (5) high selectivity for the target tissue, (6) a low tendency to form aggregates, (7) no dark toxicity and mutagenicity, (8) no side-effects, and rapid clearing from the body after PDT, and, (9) a safe and reproducible PDT protocol." (end of citation). Unfortunately, the ideal PS does not exist. In the studies in the present thesis the PS protoporphyrin IX (PpIX) has been used. PpIX fulfils many of the features describing the ideal PS, as elaborated upon in the subsequent sub-section.

1.1.2 ALA-based PDT

One of the differences between ALA-based PDT and other PDTs are that in ALA-based PDT a precursor of the PS is added rather than the PS itself. In ALA-based PDT either ALA or an ester derivative of ALA is added. Exogenously added ALA (derivative) will enter the heme synthesis and endogenous protoporphyrin IX will be produced (Kennedy & Pottier, 1992). PpIX is the active PS in ALA-based PDT. Among all tested ALA derivatives, three are approved for clinical PDT: 1) ALA (Levulan®), 2) methyl ALA (MAL, Metvix®) and 3) hexyl ALA (HAL, Hexvix® and Cysview®). The largest functional difference between these compounds is their lipophilicity and consequently the uptake mechanism of the pro-drug into the cells. In the studies in this thesis, HAL has been used and HAL-PDT will be described in the next sub-section.

1.1.2.1 Heme biosynthesis

Heme is an essential molecule in most organisms and is an integral part of hemoproteins. Hemoproteins have diverse biological roles such as oxygen transport, catalysis and electron transfer/transport. The biosynthesis of heme is well studied and knowledge of this synthesis is essential in ALA-based PDT (Hamza & Dailey, 2012; Heinemann et al., 2008; Herman et al., 1998; Krammer & Uberriegler, 1996; Layer et al., 2010; Webber et al., 1997b). A defect in any of the eight enzymes in the conserved heme biosynthesis pathway, except the two first ones will lead to a metabolic type of disorder named porphyria (Besur et al., 2014). In ALA-based PDT the first and rate limiting step in the heme synthesis is bypassed by adding exogenous ALA.

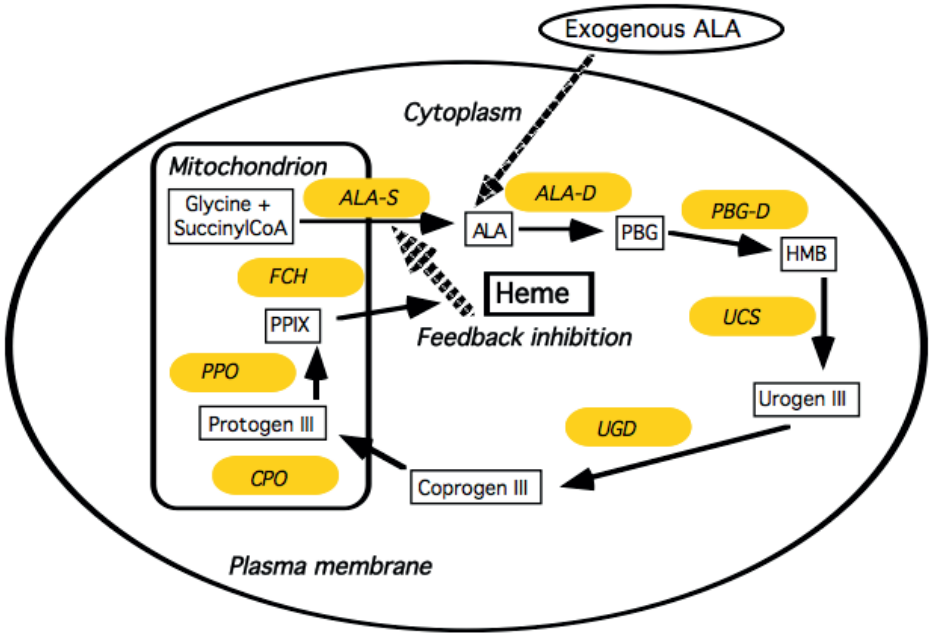

Figure 3: The heme synthesis in mitochondria. For details, see text below. Enzymes in the pathway are highlighted in yellow and the products in black boxes. Adapted from (Ying-Ying Huang, 2009).

Normally, ALA is formed enzymatically by ALA synthase (ALA-S) from glycine and succinyl coenzyme A inside mitochondria, see figure 3. ALAs activity is regulated by negative feedback from heme and is the initial and rate limiting, committed step in

heme biosynthesis. The produced ALA is then exported out of the mitochondrial matrix and two ALA molecules are asymmetrically condensed by ALA dehydratase (ALAD) into porphobilinogen. Four porphobilinogen molecules are deaminated and polymerized by porphobilinogen deaminase (PBGD) into hydroxymethylbilane, a linear tetrapyrrole. The linear tetrapyrrole is converted into uroporphyrinogen III, a cyclic tetrapyrrole, by uroporphyrinogen III synthase (UROS). The last cytoplasmic enzyme in this pathway is uroporphyrinogen decarboxylase (UROD) which decarboxylates uroporphyrinogen III into coproporphyrinogen III. Coproporphyrinogen III is translocated into the mitochondrial matrix by adenine nucleotide transporter (ANT) and ATP binding cassette transporter B6 (ABCB6) (Azuma et al., 2008; Chavan et al., 2013). The next step in heme synthesis is catalysed by coproporphyrinogen oxidase (CPOX) which oxidatively decarboxylates the substrate into protoporphyrinogen IX. The penultimate step is catalysed by protoporphyrinogen oxidase (PPOX), and is oxidation of protoporphyrinogen into protoporphyrin IX (PpIX). The terminal step is the insertion of ferrous iron into PpIX to produce heme, catalysed by ferrochelatase (FECH).

PpIX accumulation and selectivity:

In ALA-based PDT there is a difference in PpIX accumulation in tumour tissue and normal tissue. PpIX is a hydrophobic photosensitizer and the goal in ALA-based PDT is to get a high accumulation of PpIX in target cells and a high target:normal ratio (up to 90:1 is reported) (Abels et al., 1994). Most likely the selective accumulation of ALA-induced PpIX in tumours cannot be explained by a single factor, but rather by a complex interaction of several factors. The factors contributing to accumulation and their interaction may further vary with location in organism, disease type, degree of differentiation, stage and grade of the disease and of course by the route of administration [reviewed in (Michael R. Hamblin, 2008)].

Table 2: Potential factors affecting selective PpIX accumulation in tumours, adapted from (Michael R. Hamblin, 2008).

Global factor	**Specific factor**
Altered metabolic turnover in heme synthesis	Enhanced activity of pre-PpIX enzymes Decreased activity of post –PpIX enzymes Benzodiazepine receptor expression
Altered cellular properties of neoplasms	5-ALA uptake Proliferation Differentiation Mitochondrial content Cell density Iron pool/transferrin receptor
Environmental receptor	pH Temperature Lymphatic drainage Tissue pressure Vascularization Tissue integrity

Central points in the heme synthesis for ALA-based PDT:

The most important part is to bypass the negative feedback on ALA synthase. By adding exogenous ALA or ALA derivative this problem is bypassed. There are a few studies showing that an ALA ester enters the heme synthesis as ALA after an esterase has cleaved off the ester-tail (Di Venosa et al., 2006; Perotti et al., 2004).

For selectivity of cancer cells: There is increased PBG-S and -D and reduced ferrochelatase activity in tumour cells compared to normal cells (Michael R. Hamblin, 2008). The PBR receptor (benzodiazepine) is important for transport of coproporphyrinogen from cytoplasm to mitochondria and PBR is abundant in neoplastic cells (Mesenholler & Matthews, 2000; Michael R. Hamblin, 2008).

Catabolism of porphyrins:

One of the major advantages with ALA-based PDT compared to PDT with other PSs is the relatively rapid elimination of porphyrins and thereby short period of enhanced light sensitivity for patients. All redundant porphyrins are cleared from the patient in 24-48 hours (Kennedy & Pottier, 1992; Webber et al., 1997a). Red blood cells have a lifetime of only 120 days. This results in excessive heme that the organism must remove. Since

PpIX is the last intermediate in heme biosynthesis, only lacking ferrous iron, it makes sense that we have a system for its degradation and removal. The liver is central in metabolism of heme and porphyrins, both for synthesis and degradation (Bloomer, 1998). In the liver, heme is catabolized to bilirubin through sequential action of heme oxygenase and biliverdin reductase and subsequently excreted in the bile. The excretory pathways of the different porphyrins are determined primarily by their hydrophilicity. Protoporphyrin IX, which is hydrophobic, is excreted almost entirely in the bile.

Properties of Protoporphyrin IX:

Protoporphyrin IX is a tetrapyrrole which is biochemically used as a carrier molecule for divalent cations, such as Fe^{2+}, Mg^{2+} and Zn^{2+}. This protein is ambiphilic, as shown in Figure 4, and has therefore a high affinity for membranes. The porphyrin core is hydrophobic and the propionate side chains constitute the hydrophilic part of PpIX. PpIX tends to form supramolecular assemblies such as bilayer structures and vesicles. When PpIX is located in aqueous solution it easily aggregates and the nature of the aggregation is pH-dependent (Kessel et al., 2001; Scolaro et al., 2002). In addition, it has been shown that PpIX has a high affinity for parts of the mitochondrial permeability transition pore (MPTP) (Agostinis et al., 2004; Kessel et al., 2001; Oleinick et al., 2002).

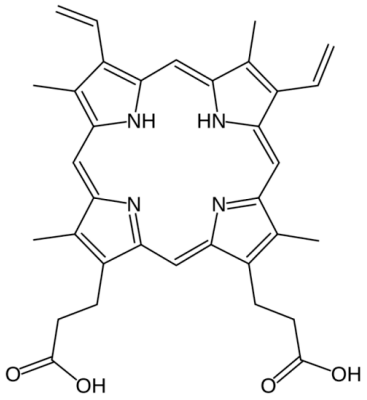

Figure 4 : The chemical structure of protoporphyrin IX.
Molecular mass: 562.658 g/mol.
Molecular formula: $C_{34}H_{34}N_4O_4$.
Picture adapted from http://commons.wikimedia.org/wiki/File:Protoporphyrin_IX.svg.

PpIX is an endogenous photosensitizer and has a typical porphyrin absorption spectra with a high absorption capacity around 400 nm and four Q-bands in the range 500-650 nm, as shown in Figure 5. When excited, PpIX emits fluorescence mainly

around 635 nm and has an additional small fluorescence peak around 705 nm. The exact wavelength for PpIX spectrum depends on e.g solvent and pH (Scolaro et al., 2002). The typical lifetime of triplet state PS is up to seconds (Plaetzer et al., 2008)). PpIX has a singlet oxygen yield about 56 % (Redmond & Gamlin, 1999).

The process when PpIX is changed into a non-fluorescent form is known as photobleaching or photodegradation. PpIX can be photodegraded through oxygen dependent mechanisms as described by Cox and co-workers in 1982 (Cox et al., 1982; Cox & Whitten, 1982). When PpIX is excited (subsection 1.1.1.2) the oxidants produced in the photochemical reactions can oxidize ground-state PpIX. Oxidation of PpIX can result in photoproducts which absorb and emit light at slightly longer wavelengths (Cox & Whitten, 1982; Ericson et al., 2003; Krieg & Whitten, 1984; Moan et al., 1997).

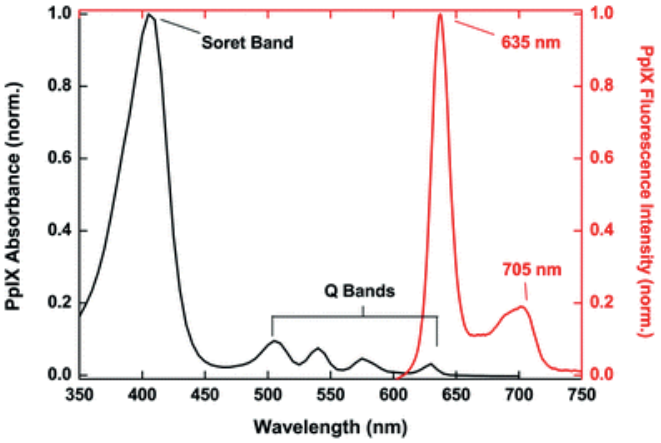

Figure 5: A characteristic absorption and fluorescence spectrum for protoporphyrin IX. Absorption spectrum is presented in black line, left axis and fluorescence in red line, right axis. The figure is adapted from (Valentine et al., 2013).

1.1.2.2 HAL-PDT

In the studies in this thesis an esterified derivate of ALA with a tail length of six carbons has been used. The derivative is named hexylaminolevulinate (HAL) and is shown in figure 6. Hexylaminolevulinate has been launched under the trade names Hexvix and

Cysview (PhotoCure, Oslo, Norway) and is approved for photodiagnosis (PDD) of bladder cancer in all EU/EAA countries and the US, respectively. HAL-PDD was recommended for bladder cancer detection in the guidelines of the European Association of Urologists in 2004 and 2005 (Oosterlinck et al., 2004; van der Meijden et al., 2005).

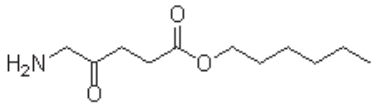

Figure 6: Chemical structure of hexylaminolevulinate. Chemical formula: $C_{11}H_{21}NO_3$. Molecular weight: 215.29. Picture is adapted from http://www.medkoo.com/Anticancer-approved/Structures/img-hexaminolevulinate.gif

The characteristics, application and perspectives for the use of ALA derivatives have been thoroughly reviewed (Fotinos et al., 2006). How ester derivatives of 5-ALA enter the heme synthesis is still not fully solved. Whether ALA esters enter the heme synthesis as 5-ALA after esterases have cleaved off the ester tails, enter directly or after other degradation reactions is still debated (Tunstall et al., 2002), but there are results supporting esterases to have a crucial role (Di Venosa et al., 2006; Perotti et al., 2004). HAL has been shown to be superior to ALA both regarding porphyrin formation and drug penetration (Kiesslich et al., 2014; Lange et al., 1999; Marti et al., 2003).

1.1.3 Light

Light is electromagnetic waves and light/photon energy is given by

$$E = h f = h c / \lambda ;$$

E (energy) h (Planck's constant) and c (speed of light is constant, c= f λ; f (frequency) λ (wavelength).

From this equation, we see that the energy decreases with increasing wavelength. Electromagnetic radiation is energy which can be emitted and absorbed by charged particles. It has a wavelike behaviour and consists of both an electric and magnetic field. The electromagnetic spectrum ranges from gamma rays ($\lambda \sim 10^{-13}$ m) to radio waves ($\lambda \sim 10^{3}$ m). Visible light is only a small part of the spectrum ranging between UV-light

and infrared radiation and ranges from 400 nm to 800 nm.

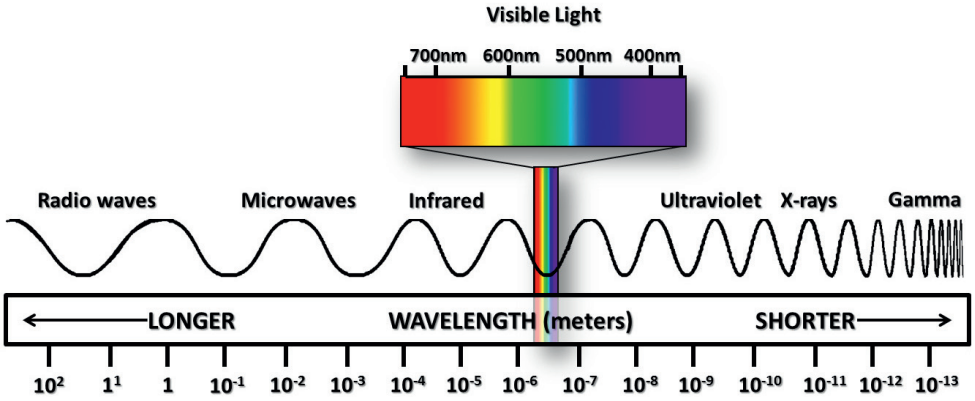

Figure 7: Electromagnetic spectrum, including visible light and its colours and corresponding wavelengths. Figure is adapted from (2015-01-28): http://www.ces.fau.edu/nasa/module-2/radiation-sun.php

Most PSs used in PDT absorbs light in the red range (600-700nm). The first law of photochemistry says that light must be absorbed by a compound before a photochemical reaction can take place. Since absorption defines the critical step for photochemical reaction and the amount of incoming photons determines the likelihood of absorption, a simplified description of light dose is the two factors: light intensity and illumination time.

Light dose (J/cm^2) = light intensity (W/cm^2) * time (sec), 1 Ws = 1 J.

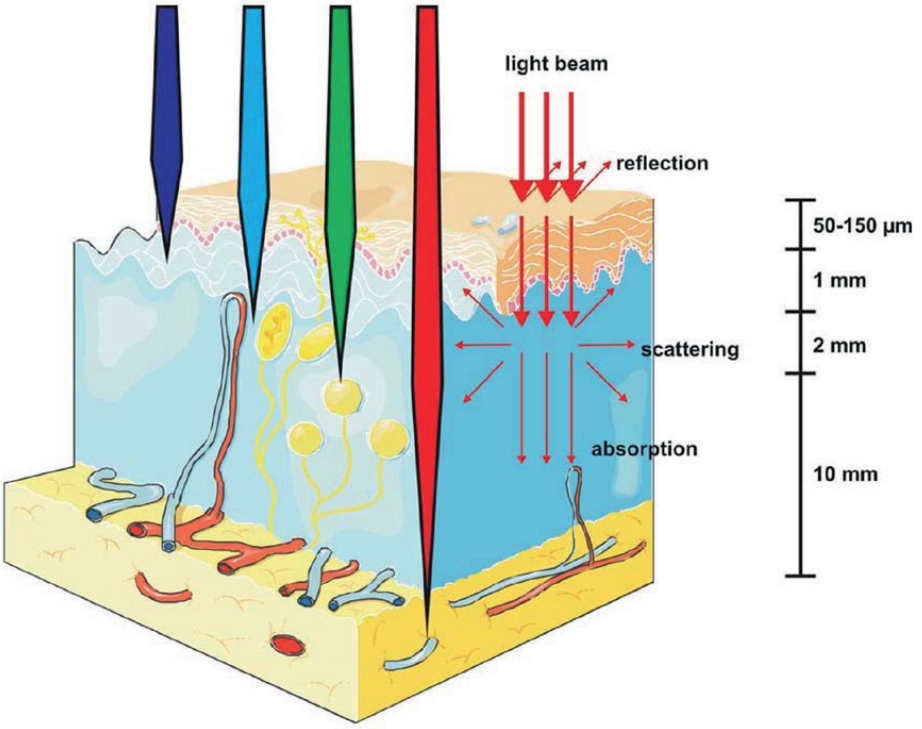

Figure 8: Light propagation through tissue and the penetration capacity of the different light colours. Figure is adapted from (Agostinis et al., 2011).

Light in tissue:

When applying light for PDT on patients one has to consider the interactions between light and tissue. The same processes applies also for PDT on cell lines, but makes less impact since the light usually is applied from below the cell dish/plate/flask. There are four main processes for light targeting tissue; refraction, reflection, scattering and absorption, as shown in Figure 8 and Figure 9.

Snell's law describes refraction of light in the interface between two media with different refractive indices and Fresnel's law describes reflection in the same interface. Both processes are determined by their relative values of refractive indices and are proportional to the incidence angle. Both processes can be minimized by applying the light beam perpendicular to the interface. The most pronounced effect on light intensity and direction comes from *scattering* of light. Scattering is a complex process which

widens the light beam and thereby reduces the light intensity in addition to changing the light beam direction (and wavelength, depending on the particle size). The last process is absorption. Absorption causes light intensity to reduce with increasing penetration depth and is described by Lambert-Beer's law, which has an exponential form.

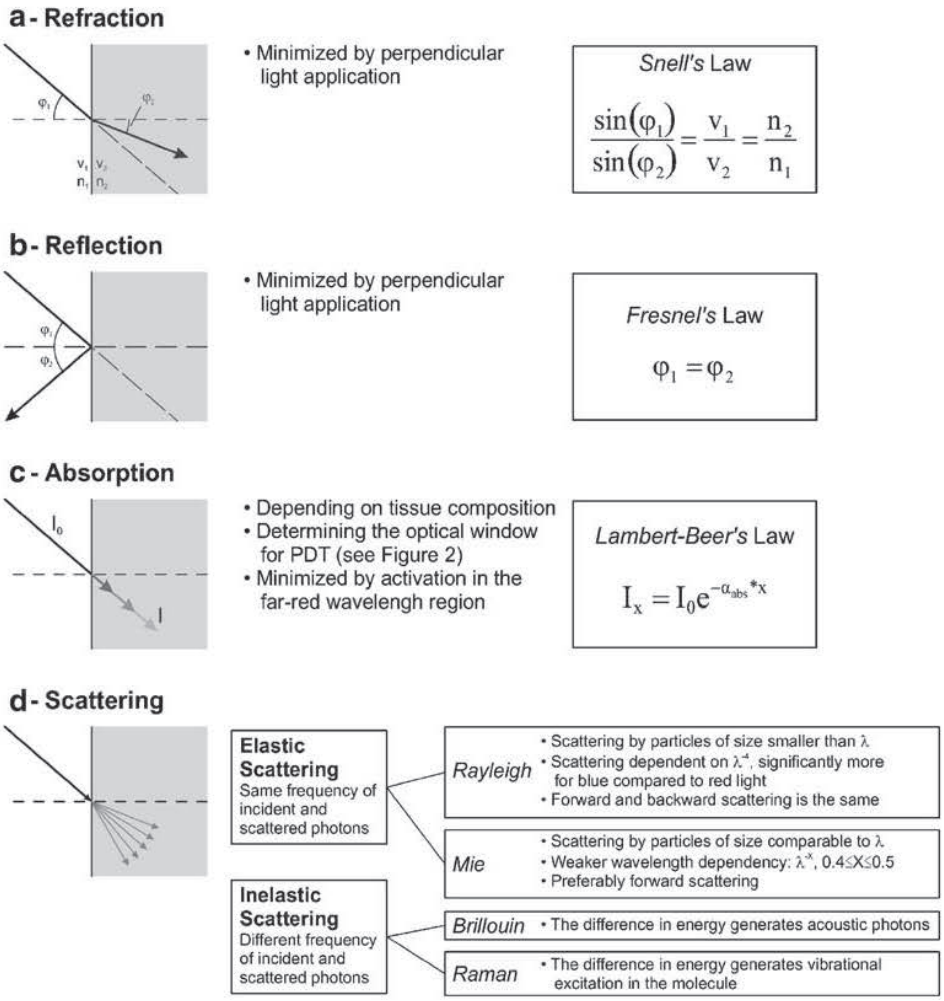

Figure 9: The different interaction mechanisms between tissue and light with the corresponding physical laws. Figure is adapted from (Plaetzer et al., 2009).

Tissue consists of several molecules/chromophores, which absorb incoming light. The most important ones are water, oxyhemoglobin (HbO_2) and deoxyhemoglobin, melanin

and cytochromes. The combined absorption spectrum of these chromophores defines the optical window for PDT in tissue as seen in Figure 10 (Plaetzer et al., 2009). The optical window (600-1400nm) from these absorption spectra is further reduced since light above 850 nm does not contain enough energy to excite a PS into triplet state with high enough energy to produce singlet oxygen. The lowest energy difference between ground state $^3O_2$ and $^1O_2$ is 0.98 eV which corresponds to a wavelength of 1270 nm, the natural phosphorescence of $^1O_2$. The triplet state PS has to exceed this energy and due to thermal losses in the photophysical process, the upper wavelength limit for PDT to efficiently produce $^1O_2$ is 850 nm (Juzeniene et al., 2006; Plaetzer et al., 2009).

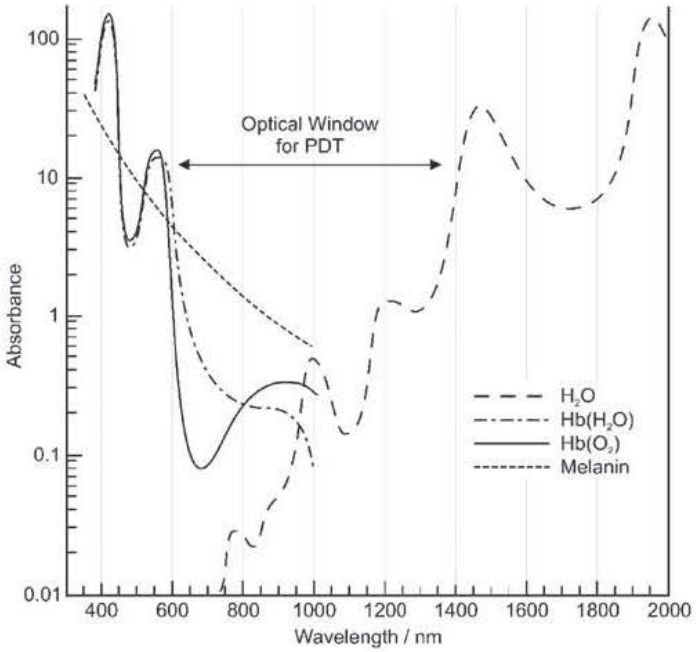

Figure 10: The 'optical window' for PDT. The absorbance spectrums for some tissue components are presented. Absorption of light by tissue components limits the wavelength range suitable for PDT to about 650–1400 nm. This range is further reduced, since PS triplet-state molecules excited by λ>850 nm have too low energy to produce singlet oxygen efficiently. Figure is adapted from (Plaetzer et al., 2009).

The penetration depth of light into tissue also depends on the wavelength of the incoming light, as presented in Figure 8. Penetration depth is defined as 1/e of the incoming light, and from Beer-Lamberts law in Figure 9, we see that penetration depth

increases with increasing wavelength. This is measured in different tissue for different wavelengths. Blue light penetrates about 1-2 mm into tissue and red light about 5-6 mm (Juzenas et al., 2009; Juzeniene et al., 2006).

1.1.3.1 Light sources for PDT, particularly LED

Different types of lamps have been used and are used for PDT (Brancaleon & Moseley, 2002). There are different types of broad band lamps, more narrow wavelength range and monochromatic. Broad band lamps have the advantages that they are cheap and easy to use, have high light intensity and can illuminate large areas. However, they produce heat, have broad spectra and cannot easily be used for optical fibres. Lasers have the advantages of monochromatic light, limited heat production, are easily used with optical fibres, can deliver high light intensity both as pulses and continuously. However, most lasers are expensive and are not so straight forward to handle. The third and perhaps best suited light source option is LED (light emitting diode). LEDs have narrow bandwidth, are cheap, can be used for fibre optics, produce minimal heat, and can illuminate large areas. Perhaps the largest disadvantage is the upper limitation in light intensity from LEDs. Since LED based arrays are the main light source in this thesis a brief introduction of LEDs is required.

A light emitting diode is a semiconductor light source which converts electrical energy into light energy. When voltage is applied, electrons can recombine with electron holes within the semiconductor and this recombination releases energy in form of photons. This effect is termed electroluminescence and the colour of the emitted light is defined by the energy gap in the semiconductor (defined of the material forming the p-n junction). A problem is that LED efficacy drops with increasing current applied, known as droop; this limits the output light intensity and results in heating when higher current is applied. The cause of the droop is still debated, but many points to the Auger recombination. In simple words: instead of emitting a photon when an electron recombines with a hole, a second electron (Auger electron) is ejected out of the atom.
LED performance is temperature-dependent and conventional LEDs are made from a variety of inorganic semiconductor materials. Most materials used in LEDs have high

refractive indices and this restricts the output direction from a LED. Most LEDs emit light straight forward in a cone shape with cone walls around 15°.

A new form of illumination source for PDT is the flexible organic LEDs (OLED). The organic LEDs have a broader wavelength range, are flexible and emit diffuse light. These features make it possible to develop light emitting patches/bandage where the patient easily can carry the power source in his/her pocket (Attili et al., 2009).

1.1.4 Summary of PDT

PDT is a two-step process where the factors are non-toxic separately, but when combined they become cytotoxic. The PS localizes quite specifically to cancer cells (high tumour:normal ratio) and is activated by visible light. Activated PS generates oxidants through oxygen dependent photochemical processes. An oxidant level beyond the cells anti-oxidative defence capacity may result in oxidative stress, oxidative damage and cell death. Cell death will be described in section 1.2 and oxidative stress in section 1.3. It is important to keep in mind that there is a difference between PDT on patients and on cell cultures, especially regarding the complexity of the target and thereby the responses. Light is perhaps the easiest factor to adjust in PDT and the applied light dose is given by the light intensity multiplied by the illumination time. One of the most utilized PDT types is ALA-based PDT. Exogenously added ALA (or derivative, such as HAL) enters the heme synthesis and endogenous PpIX accumulates in target cells. PpIX is activated both by blue and red light, clears rapidly from the organism and has a high cancer: normal ratio. HAL-PDT show superior properties (e.g. PpIX production and tissue penetration) compared to ALA-PDT and have been used in this thesis.

1.2 Cell death

At the start of this thesis introduction it was stated that PDT may eradicate cancer through interfering with angiogenesis, immune responses and direct cell kill. In this subsection the direct cell kill in form of the different cell death pathways will be

addressed. The studies included in this thesis comprise only *in vitro* level research and consequently direct cell kill is a main focus in the thesis. This subsection will give an introduction to the cell death pathways apoptosis, autophagy and necrosis. To understand these pathways is important both for knowing the cause of several diseases and for development of possible therapeutic strategies, including improvement of PDT. Cell death induced by PDT has been studied in quite a few laboratories (Castano et al., 2005; Kushibiki et al., 2013; Mroz et al., 2011; Plaetzer et al., 2002; Yoo & Ha, 2012), but since PDT is a diversified treatment and cancer a diverse disease, a detailed understanding of mechanisms is far from complete. First, necrosis will be addressed, subsequently autophagy, last and in more detail apoptosis will be addressed. Throughout this subsection the role of PDT (and especially HAL-PDT) will be included. The morphological properties of each pathway are illustrated in Figure 11.

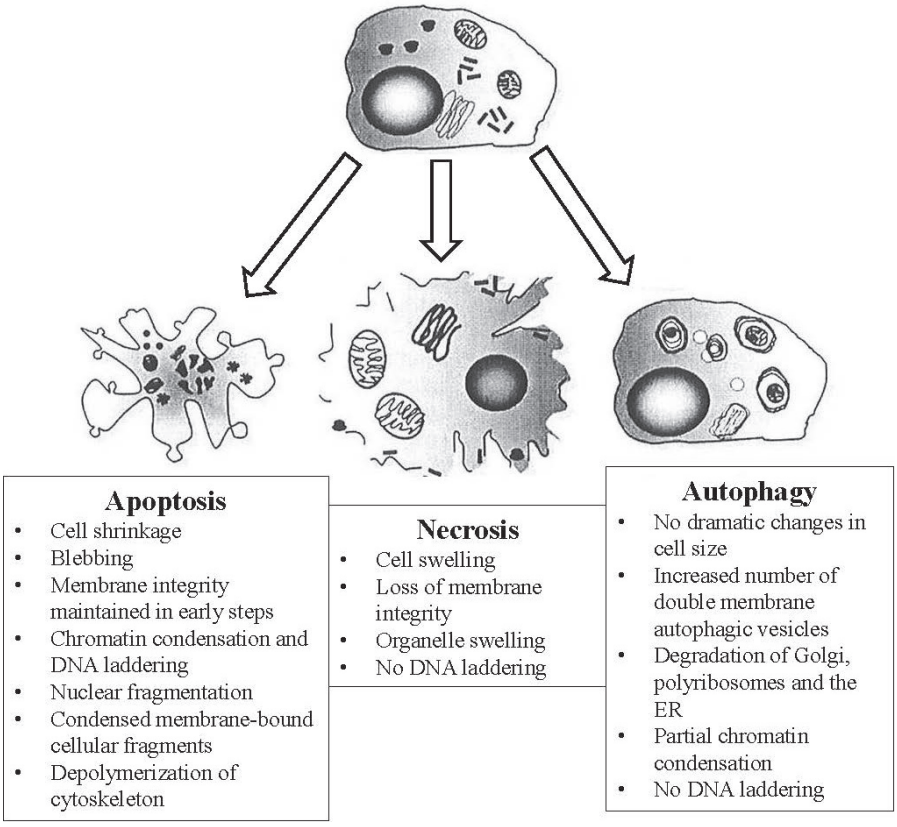

Figure 11: This figure illustrates the morphological properties of each cell death pathway. Modified from (Henriquez et al., 2008).

1.2.1 Necrosis

Necrosis is a cell death pathway with some distinct morphological properties as depicted in Figure 11. Whether necrosis is the main cell death pathway induced by PDT depends on several factors, such as type of sensitizer used, applied light dose and cell line examined. This is not fully understood yet and will not be discussed further in this subsection. Anyhow, necrosis is an important cell death pathway in PDT and will be briefly discussed.

Necrosis is mostly caused by external factors such as toxins, severe injuries and infections and has frequently a damaging effect on the surrounding tissues as well. Briefly; extensive stress to the cell may cause necrosis, while less stress causes apoptosis or repair. Necrosis also has a more damaging outcome for the surrounding cells than the more controlled apoptosis. Necrosis is often referred to as an accidental death mode (Henriquez et al., 2008; Kroemer et al., 2007). In recent reviews [(Vanden Berghe et al., 2014) and references therein] the perception of necrosis has changed to an active choice probability and controllable cell death mode. Perhaps it is necessary to distinguish between accidental and programmed necrosis. Accidental necrosis normally occurs within 2-4 hours after the triggering injury (Kroemer et al., 2007), such as illumination during PDT. Necrotic cells have the property to induce local inflammation (Kroemer et al., 2007). This happens mainly because necrotic cell eventually burst and intracellular substances come in physical contact with neighbouring cells. Since inhibition of other cell death pathways can lead to necrosis, it is by some suggested as a back-up pathway (Henriquez et al., 2008).

The extent of the injury mainly determines the final phenotypic appearance of the cell. Main features of necrosis are listed in Figure 11; swelling of organelles and the cell, loss of membrane integrity and no DNA laddering. Necrosis has few known specific biochemical markers (Baumann, 2012). Membrane impermeable markers tagged for an intracellular target are often used to detect necrosis and electron microscopy can be used for identifying necrotic cells.

Different mechanisms can lead to necrotic cell death, including high doses of ROS (Henriquez et al., 2008). This overview will only highlight some of the ROS-mediated mechanisms, since PDT generates ROS through photochemical reactions.

Excess of ROS can rapidly damage cells by oxidizing essential components, such as lipids, proteins and DNA, thus disturbing vital cell functions (Henriquez et al., 2008; Kroemer et al., 2007). ROS also function as signal molecules in pathways leading to both apoptosis and necrosis (Henriquez et al., 2008). Several studies indicate that low formation of ROS induces apoptosis, while high formation of ROS induces necrosis, [reviewed in (Henriquez et al., 2008; Schieber & Chandel, 2014)], e.g. low and high doses of PDT. Another way by which ROS can induce necrosis is by inhibiting apoptosis through suppressing caspase activation [(Henriquez et al., 2008) and references therein]. This is possible since catalytic activity of caspases is receptive to redox regulation.

Thus far, few biochemical hallmarks of necrosis have been established (Baumann, 2012) and it is only recently that the view of necrosis as an accidental death mode is changing into a possibly programmed death mode (Vanden Berghe et al., 2014). Necrosis is a total cell collapse with some distinct morphological changes, caused by severe stress, such as high dose PDT, and it evokes inflammation.

1.2.2 Autophagy

PDT induces oxidative stress and autophagy is well known to be induced by ROS (Garg et al., 2013; Kessel & Reiners, 2007; Kessel et al., 2006; Reiners et al., 2010). Autophagy is a catabolic process involving degradation of intracellular components by lysosomal mechanisms, which become up-regulated under stress conditions. The autophagy process is regulated and plays an important role in cell maintenance, growth, development and future destiny (Navarro-Yepes et al., 2014). The best known function of autophagy is degradation and recycling of nutrients from not so important cellular components to more important components of the cell during cell starvation. But it also has a very important role in clearance of ROS damaged organelles and irreversibly oxidized proteins. The understanding of autophagy has improved considerably in the last decade (Ravikumar et al., 2009). Even though autophagy is mainly looked upon as a cell survival mechanism, some evidence points towards that it has a role in cell death (Fulda & Kogel, 2015; Tsujimoto & Shimizu, 2005b).

There exist different types of autophagy, including chaperon-mediated autophagy, microautophagy and macroautophagy (Ravikumar et al., 2009). Macroautophagy is the process where cells form double membrane vesicles called autophagosomes and is the type of autophagy which will be emphasized in this thesis and further on referred to as autophagy.

1.2.2.1 Mechanisms of autophagy:

Autophagy starts by a flat membrane cistern wrapping around cytoplasmic organelles and/or a part of the cytosol. This forms a closed double membrane bound vacuole called autophagosome. These maturate stepwise by fusing with endosomal and/or lysosomal vesicles, generating amphisomes or autolysosomes, respectively (Tsujimoto & Shimizu, 2005a). Autolysosomes finally digest the sequestered cellular components by lysosomal hydrolases (Kroemer et al., 2007; Tsujimoto & Shimizu, 2005a). For a more detailed description of the autophagosome formation, the reader is referred to (Ravikumar et al., 2009).

Autophagy is regulated by PI3 kinase type I and III (Tsujimoto & Shimizu, 2005a). PI3 kinase Type I is activated by growth factors, such as insulin. The type I pathway is inhibited through PDK1 and Akt, which regulate mammalian target of rapamycin (mTOR). PI3 kinase type III promotes the nucleation of autophagic vesicles. mTOR is regulated by many proteins, so it is likely that the autophagy process is very complex. Additionally was an mTOR independent autophagic pathway found in 2005 (Sarkar et al., 2005).

1.2.2.2 Autophagic cell death

The role of autophagy in cell death remains incompletely explored. The functional relationship between necrosis/apoptosis and autophagy is complex and may either contribute to cell death or be a part of the cellular defence against acute stress (Booth et al., 2014; Marino et al., 2014; Nikoletopoulou et al., 2013). An overview of the role of autophagy in cell death will be given in the following text.

Autophagic cell death is morphologically defined as a type of cell death occurring in the absence of chromatin condensation and presence of massive autophagic vacuolization of the cytoplasm, see Figure 11. But according to (Kroemer et al., 2009) and (Tsujimoto & Shimizu, 2005a) the term "autophagic cell death" simply describes cell death with autophagy. An increased number of autophagosomes are sometimes seen in dying cells, but this is often not the result of autophagy-mediated cell death (Ravikumar et al., 2009). The functional interaction between apoptosis and autophagy is indicated by the following observation: Enhancing autophagy gives an anti-apoptotic effect, whereas blocking of autophagy increases cells sensitivity to pro-apoptotic insults.

Knowledge on the molecular basis of autophagic cell death has advanced tremendously in recent years, but remains incompletely understood (Birgisdottir et al., 2013; Fulda & Kogel, 2015; Zhang, 2015). Autophagic cell death is dependent on autophagy proteins involved in the formation of autophagosomes (Shimizu et al., 2004; Yu et al., 2004). The details of the autophagosome formation and the different ways to cell death are well reviewed by Fulda and Kögel (Fulda & Kogel, 2015). The perhaps three most central players for this process are the autophagic molecules Beclin-1 (also called Atg6), Atg5 and Atg7. Their binding to other molecules are required for activation of different stages of the pathway. One research group has shown that autophagic death of mouse cells, L929, is dependent on Jun N-terminal kinase (Jnk) (Yu et al., 2004). How Jnk and autophagy is linked was not determined, but the importance of Jnk to autophagic cell death was confirmed by unpublished results in Bax/Bak deficient mouse embryonic cells (Tsujimoto & Shimizu, 2005a). Also, Bak/Bax deficient mouse embryo cells require anti-apoptotic protein basal-cell lymphoma-extra large (Bcl-x_L) or Bcl-2 to perform autophagic cell death (Tsujimoto & Shimizu, 2005a). It is also shown that starvation induces Jnk1 activity which phosphorylates Bcl-2, thereby disrupting the interaction between Beclin-1 and Bcl-2 and inducing autophagy (Wei et al., 2008).

1.2.3 Apoptosis

Apoptosis has been extensively studied and many well written reviews are available (e.g.(Cohen, 1997; Elmore, 2007; Green & Reed, 1998; Hengartner, 2000; Nagata, 1997; Porter & Janicke, 1999; Thompson, 1995; Zimmermann & Green, 2001)). The role of apoptosis in PDT has also been well reviewed (e.g. (Agostinis et al., 2004; Kessel & Luo, 1998; Kessel & Reiners, 2007; Kessel et al., 2006; Kiesslich et al., 2013; Oleinick et al., 2002; Plaetzer et al., 2005))

Programmed cell death was first described by Lokshin and Williams in 1965 (Lockshin & Williams, 1965) and apoptosis was morphologically identified by Kerr et al in 1972 (Danial & Korsmeyer, 2004; Galluzzi et al., 2014; Kerr et al., 1972). Apoptosis is a mode of cell death executed by an intracellular program and has distinct morphological features (Danial & Korsmeyer, 2004; Galluzzi et al., 2014). During apoptosis the cell shrinks and condenses, the cytoskeleton collapses, the nuclear envelope disassembles, the nuclear chromatin condenses and breaks up into fragments, the cell surface blebs into apoptotic bodies and the cell surface becomes chemically altered in such a way that it can be recognized by neighbouring cells/macrophages and phagocytosed. See Figure 11 and Figure 12 for morphological hallmarks and picture. Apoptotic cells *in vivo* are rapidly phagocytosed, thus few apoptotic cells are seen in tissue and it has minimal effect on the neighbouring cells. If the apoptotic cells are phagocytosed before the late phase, they will not evoke an inflammatory response (Rock & Kono, 2008).

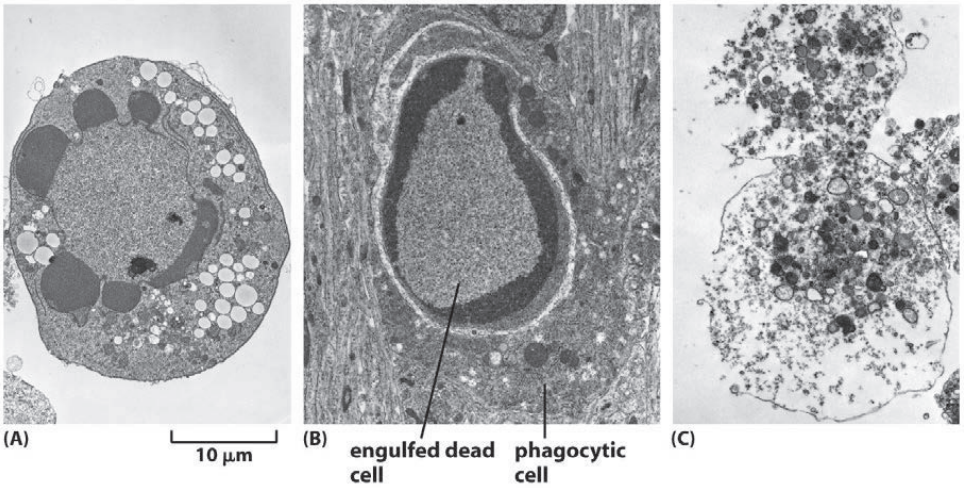

Figure 12: This images show apoptotic and necrotic cells. A) presents an apoptotic cell grown in a culture dish, B) shows an apoptotic cell in tissue that has been endocytosed by a phagocytic cell, C) a necrotic cell grown in culture dish. Adapted from (Alberts et al., 2008).

In animal development the apoptotic process removes unwanted cells and regulates the cell number. In adult tissue, apoptosis plays an important role in the tight regulation of cell death and division. In different control processes, the outcome is often apoptosis when the cell damage is severe enough, thus apoptosis is a part of the cell quality regulation.

Apoptosis is divided into two main pathways, the extrinsic and intrinsic pathway, depending on which stimuli trigger the onset of apoptosis. The extrinsic pathway is the process in which extracellular signals trigger apoptosis by binding to specific death receptors. The intrinsic pathway is when intracellular apoptotic signals trigger to the onset of apoptosis. The intrinsic pathway can be sub-divided into different pathways, depending on where the apoptotic signal cascade origins and its progress.

1.2.3.1 In general

Some features of the different apoptotic pathways are common and are often used as markers for apoptosis in research.

Apoptosis is biochemically recognizable. Some of the common apoptotic events will be addressed in the subsequent text. One of the early events in the apoptotic process is the

flipping of a phospholipid, phosphatidylserine, from inner membrane to the outer membrane surface. Phosphatidylserine can be labelled by fluorescent tagged Annexin V and measured by different fluorescent techniques. Other cells read the exposed phosphatidylserine as an “eat me” signal and phosphatidylserine inhibits cytokines.

Apoptotic cells often lose their electrical potential across the inner mitochondrial membrane and release cytochrome *c* from mitochondria into cytosol. Both of these events can be labelled by different techniques. Extensive release of cytochrome c clearly happens before swelling and rupture of mitochondria (Danial & Korsmeyer, 2004).
During apoptosis chromosomal DNA is cleaved into fragments of distinct sizes by endonucleases (Kitazumi & Tsukahara, 2011). Chromosomal DNA is cleaved in the linker region between nucleosomes, which results in DNA fragments of distinct sizes. DNA fragmentation can be recognized by a characteristic gel electrophorese pattern or the new DNA ends can be marked by the TUNEL assay (Loo, 2011).

The different apoptotic pathways origin from separate sites in the cell, but will largely assemble at the same effector caspases and result in caspase-dependent cell death. There are some less common caspase-independent mechanisms death modes. Both the caspase dependent and independent pathways have some common mechanisms. This crosstalk makes substitutions of one pathway with another possible. Despite all these complexities, apoptosis uses some main mechanisms: The caspase cascade coordinates the process of the characteristic changes in morphology during apoptosis; there are two separate main pathways for trigging this cascade, the intrinsic and extrinsic pathway. Below, the caspase cascade will be briefly described and subsequently both the intrinsic and extrinsic pathway will be described.

1.2.3.2 The caspase cascade

The mechanisms of the caspase cascade are well studied (Chan et al., 2000; Choi et al., 2002; Cohen, 1997; Fuentes-Prior & Salvesen, 2004; Furre et al., 2006; Granville et al., 1998; Janicke et al., 1998; Kurokawa & Kornbluth, 2009; Salvesen & Riedl, 2008; Thornberry & Lazebnik, 1998; Wang et al., 2003). Caspases are proteases that have cysteine at their active site and cleave their target protein at specific aspartic acid

residues. Caspases are synthesized as inactive pro-caspases which are typically activated by proteolytic cleavage. Pro-caspase cleavage is catalysed by other active caspases and splits the pro-caspase into a large and a small subunit. The two subunits assemble into a heterodimer and the assembly of two such dimers gives an active tetramer.

Once activated, caspases cleave other pro-caspases in an amplifying cascade. This proteolytic cascade starts with an initiator pro-caspase, which cleaves an executioner pro-caspase (also called an effector pro-caspase), which again cleaves another executioner/effector pro-caspase or a target protein (Shalini et al., 2014). The caspase cascade is destructive, self-amplifying and irreversible. Which caspases that are involved, depend on cell type and stimulus, but perhaps the most central caspase is caspase-3, which is an effector caspase (Choi et al., 2002; Janicke et al., 1998; Porter & Janicke, 1999).

Two separable pathways are well documented to activate the pro-caspases, the intrinsic and the extrinsic pathway.

1.2.3.3 Intrinsic pathway

The intrinsic pathway is usually trigged as a response to different types of stress, such as DNA damage, toxins, radiation, hypoxia, oxidative stress or hypoxia, or absence of nutrients or extracellular survival signals (Movassagh & Foo, 2008). The main feature of the intrinsic pathway is the permeabilization of the outer mitochondrial membrane and the resulting release of apoptogenic molecules into cytosol (Figure 13). Since PpIX, the photosensitizer in HAL-PDT, is produced in mitochondria and induced singlet oxygen has a short diffusion length intracellularly, mitochondria is a likely target and consequently the intrinsic pathway would be the likely mechanism initiated.

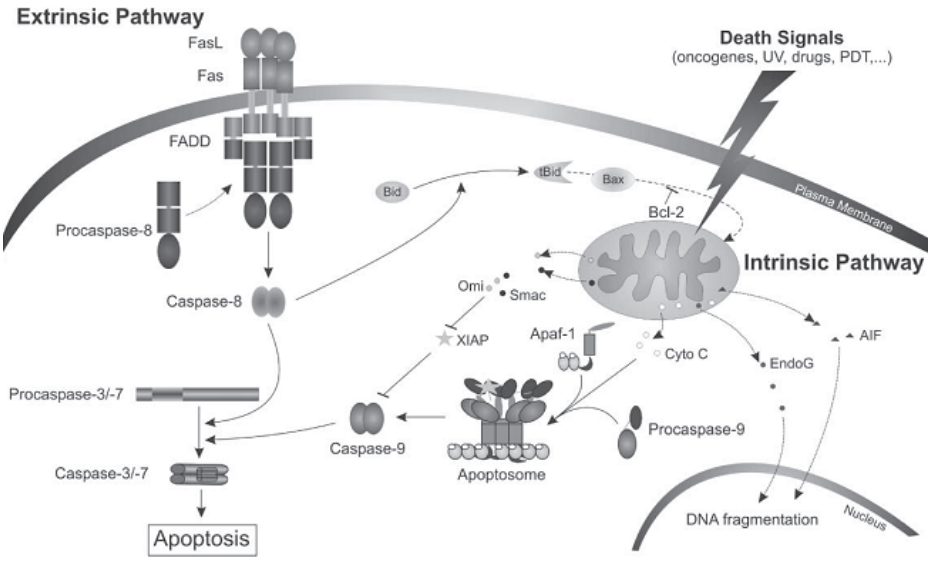

Figure 13: Extrinsic and intrinsic apoptosis. "Different pathways of caspase activation leading to apoptosis. The extrinsic or death receptor pathway of caspase activation is initiated by the binding of a member of the tumour necrosis-factor (TNF)-family of death-receptor ligands to their cognate receptors (in this picture FasL and Fas). Through their death domain, oligomerized receptors, recruit adaptor protein (FADD), which in turn recruits pro-caspase-8 and/or pro-caspase-10 to form the death inducing signalling complex (DISC). As part of the DISC pro-caspase-8 becomes autocatalytically activated and in turn cleaves effector pro-caspase-3/-7. The effector caspases then process different substrates leading to apoptotic cell death. A separate pathway of caspase activation involves the mitochondrion as a central organelle and is therefore called the mitochondrial or intrinsic pathway. Different death signals, including PDT, can induce the permeabilization of the outer mitochondrial membrane leading to the release of apoptogenic molecules, such as cytochrome c, Smac/DIABLO and endonuclease G from the intermembrane space of the mitochondrion. The release of these molecules is tightly controlled by different members of the Bcl-2 family. The release of cytochrome c promotes, in the presence of dATP/ATP, the formation of the apoptosome, which includes Apaf-1 (apoptotic protease activating factor-1) and pro-caspase-9. Autocatalytic activation of caspase-9 triggers the activation of effector caspases, ensuring apoptotic cell death. A cross-talk between those two pathways is provided by cleavage of the BH3-only protein Bid by activated caspase-8. Truncated Bid in turn promotes Bax oligomerization and insertion into outer mitochondrial membrane, leading to subsequent cytochrome c release"(citation end). Figure and text adapted from (Agostinis et al., 2004).

Cytosolic cytochrome c binds to Apaf-1, which in presence of dATP or ATP leads to pro-caspase-9 activation in an oligomeric complex called the apoptosome (Alberts et al., 2008; Movassagh & Foo, 2008). Caspase-9 activates down stream caspases, including pro-caspase-3, which triggers apoptosis. In parallel with cytochrome c, other mitochondrial intermembrane proteins are also released into cytosol, such as EndoG

(endonuclease G), AIF (apoptosis inducing factor) and Smac. EndoG and AIF further translocate to the nucleus and promote caspase-independent DNA breakdown. An irreversible loss of mitochondrial function (e.g. caused by PDT) could also release apoptotic proteins (Green & Reed, 1998; Kessel & Luo, 1998; Kroemer et al., 2007; Orrenius et al., 2007; Ott et al., 2007; Sinha et al., 2013).

The release of these apoptotic proteins is thought to occur through mitochondrial membrane permeabilzation (MMP), which is defined as a sudden permeabilization of the inner mitochondrial membrane for molecules below 1500 Da. The opening of this MMP pore causes a change in the ion gradient and the outer mitochondrial membrane bursts due to osmotic swelling (Kroemer et al., 2007).

The intrinsic apoptotic pathway is tightly regulated by the Bcl-2 family of proteins (B cell lymphoma 2). This family of proteins is also involved in the extrinsic apoptotic pathway and apoptosis triggered from Ca^{2+} imbalance or the unfolded protein response in endoplasmic reticulum. The pro-apoptotic family members (Bax, Bid, Bak and Bim) and the anti-apoptotic members (Bcl-2 and Bcl-X_L) are found at different subcellular localizations and are activated either by relocalization, up regulation or post translational modification.

1.2.3.4 Extrinsic pathway

The extrinsic pathway of apoptosis is trigged when extracellular signal proteins bind to death receptors on the cell-surface. Death receptors are transmembrane homotrimers that belong to the tumour necrosis factor (TNF) receptor family (e.g. Fas, TNF-RI and TRAIL receptor). The ligands are also homotrimers and belong to TNF family of signal proteins (e.g. FasL, TNF-α and TRAIL). The ligand to receptor binding results in reorganization of the inactive Fas complex and stimulates recruitment of adaptor protein, such as Fas-associated via death domain (FADD), which in turn activates procaspase 8 and/or 10. Caspase 8/10 activates the death-inducing signalling complex (DISC), which activates the apoptotic caspase cascade by activating the initiator caspase. Once the caspase cascade has been initiated, the extrinsic pathway is similar to the intrinsic pathway.

1.2.4 Summary of cell death

Apoptosis, autophagy and necrosis are three different death pathways, caused by different stimuli and executed by different mechanisms. At the same time there exist links between all three pathways and functional interaction between them. All three pathways contribute to the pathogenesis of several diseases and represent possible targets for treatment. Probably all three death pathways are involved in PDT-induced cell death, but at varying degrees. The main goal of PDT is to kill the cancer cells and for this matter all three pathways may do the job. But since they will affect the adjacent regions differently a combined action of them could give additional effects not obtained by a single mechanism. Consequently, knowledge of what is activated after PDT is well worth studying.

1.3 Oxidative stress

Oxidative stress is basically when the amount of oxidants (e.g. ROS) exceeds the capacity of the antioxidants defence system. As described in section 1.1.1.2 Mechanisms of PDT; photochemical reactions PDT generates ROS through photochemical reactions. This is probably the main direct effect of PDT. Subsequently, this oxidative stress causes cell death through mechanisms triggered by oxidative stress and consequences thereof. The focus of this section will be oxidative stress induced by PDT, oxidative stress in general, oxidation of proteins and lastly redox signalling.

1.3.1 Oxidative stress induced by PDT

As illustrated with the Jablonski diagram in Figure 1 the excited photosensitizer de-excites either by energy transfer to oxygen (type II reaction) creating singlet oxygen ($^1O_2$) or by transferring electrons/protons (type I reaction) to a molecule in the vicinity, thus generating radicals. Molecular details of the oxidants produced by PDT are illustrated in Figure 14 and the subsequent text.

The radical anion/cations formed by type I reaction are likely to further react with oxygen through secondary photochemical reactions, forming reactive oxygen species (ROS). When a PS transfers an electron directly to oxygen, superoxide anions are produced. The not so reactive superoxide molecules can react with each other resulting in the more reactive hydrogen peroxide (H_2O_2). Hydrogen peroxide can easily pass through membranes and is therefore not restricted to one cellular compartment. The lifetime (half-life of 1 ms) of H_2O_2 is also much longer than many ROS' and combined with the membrane permeability it is a very potent ROS for producing cellular damage (Cheeseman & Slater, 1993).

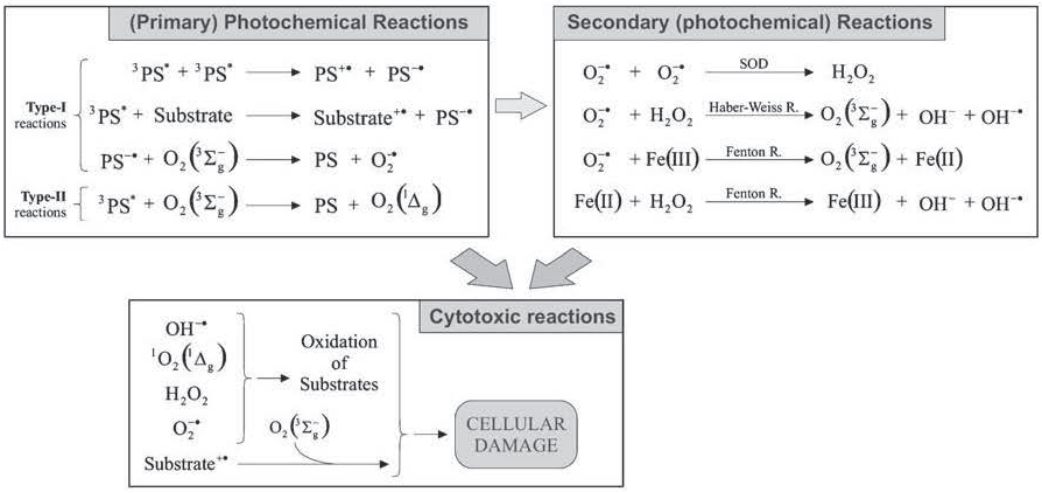

Figure 14: "Overview of photochemical reactions during PDT. Several types of primary and secondary photochemical reactions cause production of reactive oxygen species and dose-dependent cellular damage. H_2O_2, hydrogen peroxide; $^1O_2$ ($O_2(^1\Delta_g)$), singlet oxygen (excited state); O_2 ($3\Sigma^-_g$), triplet oxygen (ground state); $O_2^{-\bullet}$, superoxide anion; $OH^{\bullet}$, hydroxyl radical; SOD, superoxide dismutase; $X^{-/+}$, anion/cation species; $X^{\bullet}$, radical species."(citation end). Figure and text adapted from (Plaetzer et al., 2009).

From photoreaction type II, singlet oxygen is produced by energy transfer from the excited PS to ground state oxygen. Singlet oxygen is very reactive and can diffuse trough membranes, but it has a short lifetime of about 0.1 µs (Moan, 1990; Moan & Berg, 1991). The diffusion length is maximum 30 nm intracellularly (Plaetzer et al., 2009). Consequently, the intracellular localization of the PS is determining the site of

cellular damage during PDT. Nearly all PSs used in PDT have a high quantum yield for $^1O_2$ formation (~0.3-0.5) (Juzeniene et al., 2006; Moan & Berg, 1991; Moan & Juzenas, 2006).

A mix of type I and type II reaction occurs during PDT and depending on the PDT dose, the induced oxidative stress could be quite massive. In the following sections a more general discussion on oxidative stress will be given.

1.3.2 Oxidative stress in general

During oxidative stress, cell components can be damaged, including DNA, RNA, lipids and proteins. The effect of oxidative stress depends on its extent. Small changes can be overcome by the cell, but severe oxidative stress may cause cell death (Stadtman & Levine, 2002). It has been shown that moderate oxidative stress causes apoptosis and stronger stress causes necrosis (Lennon et al., 1991), see figure 15. Depending on the type of damage, oxidative stress can be harmless, pathogenic (Dalle-Donne et al., 2006b) or may promote aging. To cover all of the aspects of oxidative stress in this thesis would require comprehensive efforts beyond the scope of the present review (Rahal et al., 2014). Consequently, further discussion is restricted to oxidative stress on proteins.

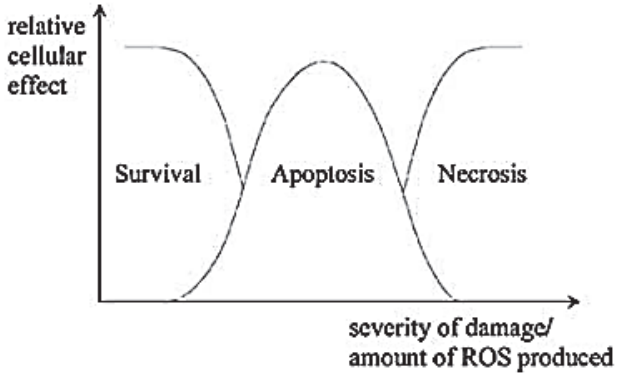

Figure 15: A simplified illustration of how increasing degree of oxidative stress/PDT-induced damage activates different cellular responses. The basic view is that the response is dose-dependent with a transition from (low dose) survival (and autophagy) to apoptosis to necrosis (high dose). Figure adapted from (Plaetzer et al., 2005).

Redox reaction - In a redox reaction both reduction and oxidation take place and redox refers to all chemical reactions where atoms get their oxidation state altered. During oxidation of the molecule, there is a loss of electrons; an increase in oxidation state. Likewise, during reduction there is a gain of electrons; a decrease in oxidation state.

Reactive oxygen species (ROS) are oxygen-containing molecules which are chemically reactive. ROS are highly reactive due to unpaired electrons in the outer valence shell.

A radical/free radical has either unpaired electrons or an open outer shell configuration. So in other words; a ROS is a free radical which contains oxygen.
Singlet oxygen is not a free radical and is thereby not a ROS. Nevertheless, it is very reactive and can react with most molecules due to its quantum state.
The most reactive radicals tend to be less selective, unlike less reactive radicals, which tend to be more selective.

Often the term oxidant (oxidizing agent) is used. This is a wider concept and includes all molecules which remove electrons from another molecule in a redox reaction. By using this term, incorrect use of the terms ROS and radicals is avoided. In addition, the term pro-oxidant is worth noticing. Pro-oxidants are chemicals which

induce oxidative stress either through creating oxidants or by inhibiting antioxidant systems.

Oxidative stress - A biological system will normally be in a balanced redox state when the antioxidant defences efficiently cope with the background level of oxidants. If either the antioxidant defence system decreases its capacity or the level of oxidants is raised, the biological system will enter a state of oxidative stress.

Antioxidant defence system - Oxidative stress is also called the paradox of aerobic life. Organisms have developed strategies of antioxidant defence that handle the negative effects of oxidative stress, The defence strategies involved may be subdivided into three levels; protection, interception and repair (Sies, 1993).

Nonenzymatic antioxidants include both lipophilic and hydrophilic compounds; the lipophilicity depends on the location of action. The basic process is deactivation of the damaging compound. For radicals this means to transform them into a non-radical end product. The other basic process is translocation of the damaging compound from a sensitive target site to a less deleterious cell compartment.

Enzymatic antioxidants exist in all eukaryotic organisms. There are three major antioxidant enzymes: superoxide dismutase (SOD), catalase and glutathione (GSH) peroxidase (Sies, 1993). All of these enzymes are quite general and they have an effect on a broad range of substrates. In addition there are several types of specialized antioxidant enzymes that react with and detoxify specific oxidants.

1.3.3 Oxidative stress on proteins

Proteins are a major target for oxidants due to their abundance in the cell; in dried cells and in tissue protein constitutes about 70 % of the weight. In addition, proteins have a high rate constant for reaction with oxidants (Davies, 2005), especially with singlet oxygen (Davies, 2003). Since proteins have several different and specific biological functions, oxidative modification of proteins can result in various functional consequences. In general, oxidative modifications of proteins may result in reduced function, or even loss of their normal function. Some oxidants result in limited and

specific damage, while others cause widespread and relatively non-specific damage. Generally the most reactive oxidants are the least selective ones (Davies, 2005).

When proteins are damaged they may become targeted for degradation (Chang et al., 2000). Proteolysis down to amino acids is carried out by different endogenous proteases and lysosomal pathways (Chang et al., 2000; Stadtman & Levine, 2000). Furthermore, it has been shown that protein oxidation occurs very early after cells are exposed to oxidative stress and that this oxidation happens before the decrease of cellular ATP and the subsequent cell death (Ciolino & Levine, 1997). Different oxidative modifications of proteins are involved in different diseases including neuro-generative disorders and cancer. For a more extensive treatment of this subject, the reader is referred to (Berlett & Stadtman, 1997).

Radical attacks on proteins can generate secondary reactive species ultimately resulting in cell death. The propagation of radical reactions on proteins is well known and described in (Hawkins & Davies, 2001) and will not be further elaborated upon in this thesis. Consequences of protein oxidation at the cellular level are presented in Figure 16, but the focus will be on the different modifications and the role of oxidative protein modifications in cellular signalling. There are two main sites of oxidative damage on proteins (Berlett & Stadtman, 1997): oxidation of the protein backbone and oxidation of amino acid residue side chains. In brief, oxidation of protein backbone leads to intra- and inter-protein crosslinking and peptide backbone cleavage (Barelli et al., 2008; Berlett & Stadtman, 1997). The side chain oxidation is more complex, as described subsequently.

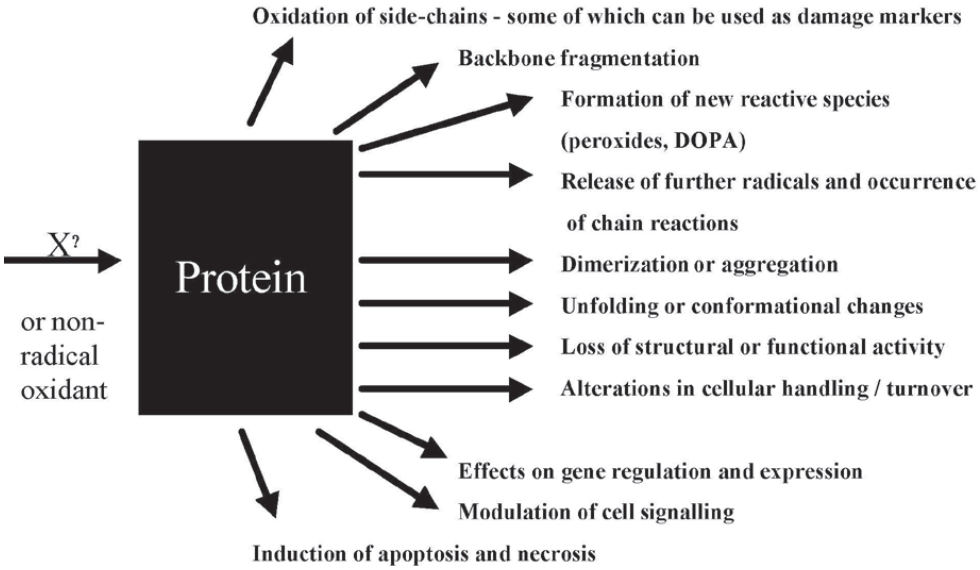

Figure 16: A schematic overview of cellular consequences after protein oxidation. The figure is adapted from: http://scholar.googleusercontent.com/scholar?q=cache:OMuFFKHxkWoJ:scholar.google.com/&hl=no&as_sdt=0&as_vis=1 which was based on (Davies & Truscott, 2001; Hawkins & Davies, 2001).

There are 20 different amino acid side chains when rare amino acids and post translational modifications are excluded. Many radicals lack electrons and consequently they react preferably with electron-rich side chains (Trp, Tyr, His, Met, Cys and Phe). Most of the oxidative modifications on side chains result in increase of hydrophilicity of the target residue. The structural effects are displayed Figure 17. Due to the high number of potential oxidative reaction sites and products it is practical to divide the amino acids into four groups: with cystine and cysteine residues, aliphatic amino acids, aromatic amino acids and methionine. The first group will be discussed last and more in depth.

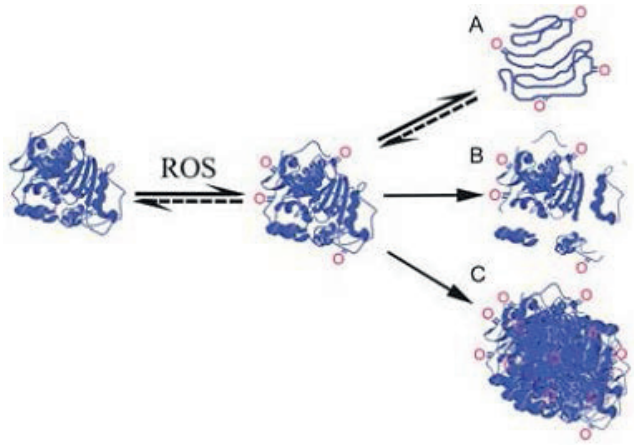

Figure 17: This figure presents schematically visualized effects of oxidative stress on protein structure: A) unfolding (partial or total); B) backbone cleavage; and C) aggregation. The unfolding can be reversible, see text 1.3.4. Backbone cleavage may be from direct oxidation or indirect due to increased susceptibility to proteolysis. Figure is adapted from(Tornvall, 2010).

Amino acids with aliphatic side chains (glycine, alanine, valine, proline, leucine and isoleucine) are oxidatively modified primarily by hydrogen abstraction and the major products formed are peroxides, alcohols and carbonyls. These modifications are irreversible. The most studied product is probably carbonyls. Carbonylated proteins are generally dysfunctional, can be caused by multiple reactions, measured by several techniques and may occur in several disease states (Dalle-Donne et al., 2003). The content of carbonylated proteins increases with age and at the end of a life cycle about one out of three proteins carries a carbonylation (Stadtman & Levine, 2000). The increase in carbonylation is drastic in the last third of a lifespan (in the range of *C.elegans* to human), which usually is after the reproducible phase (Levine, 2002; Levine & Stadtman, 2001; Stadtman & Levine, 2000). The importance of keeping the carbonylation low during reproducible age is documented in a plant study where they found that the carbonylation increased during life, but was reduced before pollination [(Nystrom, 2005) and references therein]. Carbonylation has a role in age related diseases as well, probably mostly due to the loss of protein function (Dalle-Donne et al., 2006a; Dalle-Donne et al., 2006b). At high content, carbonylated proteins are likely to cause substantial disruption of cellular function (Levine & Stadtman, 2001).

Amino acids with aromatic side chains (phenylalanine, tyrosine, tryptophan and histidine) are oxidatively modified mainly through addition, but abstraction can occur. Oxidation of aromatic side chains is irreversible. Electron abstraction on aromatic side chains results mainly in hydroxylated products. In contrast, addition of electrons results in a great diversity of products (since the end product often has incorporated elements from the relevant oxidant). The same types of end products seem to be formed both in the presence and absence of oxygen (Davies, 2005).

Methionine residues of proteins are very sensitive to oxidation from any kind of ROS/oxidant (Stadtman & Levine, 2000). Oxidation of methionine can be reversed enzymatically, unlike the oxidative modifications on non-sulphur-containing amino acids. Methionine oxidation results either in methionine sulfone or in methionine sulfoxide. Since sulphur centres are easily oxidized, the side chains of methionine and cysteine are the main oxidations sites under mild oxidative conditions, while carbonylation is more pronounced under severe oxidative stress (Tornvall, 2010). More details on methionine oxidation are extensively reviewed in (Davies, 2005).

1.3.4 Cystine and cysteine; thiol proteins

Oxidation of thiol proteins is the main focus in the last manuscript of this thesis. A thiol is an organosulfur compound that contains a carbon-bonded sulfhydryl (–C–SH or R–SH) group (where R represents an alkane, alkene, or other carbon-containing group of atoms). The –SH functional group itself is referred to as either a *thiol group* or a *sulfhydryl group* [http://chemistry.about.com/od/organicchemistryglossary/g/Thiol-Definition.htm (2015-01-28)].

There are three sulphur containing amino acids; cysteine, cystine and methionine, but methionine cannot make disulphide bonds. In addition, methionine is a thiol-ester due to the methyl group attached to the sulphur. Cystine is a dimeric amino acid made up of two cysteine molecules linked by disulphide bond. Oxidation of cystine is less studied than oxidation of cysteine and therefore is most of the thiol oxidation below equivalent with cysteine oxidation.

Oxidized cysteine residues can exist in a range of specific modifications. The main modifications are shown in Figure 18. Oxidative thiol protein modifications can be reversible or irreversible. Sulfinic and sulfonic acid are irreversible modifications while intermolecular disulphide, glutathionylation, intramolecular disulphide and sulfonamide are reversible thiol modifications. Often the irreversible modifications are induced under more severe oxidative stress while the reversible forms are dominating under mild oxidative stress (Jacob, 2011).

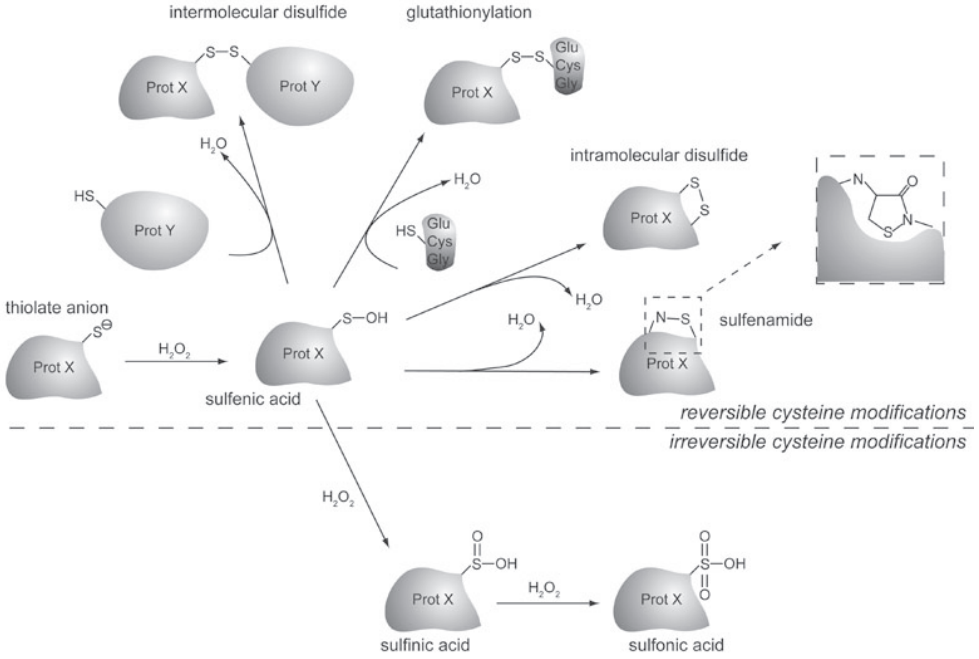

Figure 18: Schematic drawing of the main oxidative modifications of cysteine. The figure is adapted from http://groups.mcr.umcutrecht.nl/dansen/.

1.3.5 Detection techniques

Various methods are used within redox proteomics. The diversity in methods reflects the diversity of modifications and is in addition influenced by type of consequence examined (e.g. loss of function, identification, intermediates and end products). Methods to study oxidatively modified thiol proteins often involve labelling, separation

and identification. Common techniques are alkylation, labelling with a tag or antibody, gel electrophoresis, immune precipitation and mass spectrometry. The current limitation in the methods is sensitivity, which implies a high probability that important target proteins are lost due to low abundance. For these to be detected an alternative is to monitor the redox state of selected of proteins instead of all possibilities. Several techniques are well described by others in reviews and articles (Barelli et al., 2008; Baty et al., 2002; Bonini et al., 2006; Burgoyne & Eaton, 2011; Burkitt & Wardman, 2001; Camerini et al., 2005; Chouchani et al., 2011; Cuddihy et al., 2009; Dalle-Donne et al., 2006b; Fu et al., 2008; Gartner et al., 2007; Hawkins et al., 2009; Landar et al., 2006; Leichert & Jakob, 2004; Riederer, 2009; Rogers et al., 2006; Thamsen & Jakob, 2011; Tornvall, 2010; Wardman, 2007; Wardman, 2008) and will not be further described here.

1.3.6 Reversible thiol oxidation in cell signalling

Oxidants can both activate and inactivate transcription factors, membrane channels and enzymes, and regulate phosphorylation and calcium dependent signalling pathways. The controlled oxidation and reduction of cysteine residues constitutes a redox switch mechanism which is thought to be the major mechanism for reactive oxidants to regulate cell signalling (Dalle-Donne et al., 2007; Davies, 2005; Dickinson & Chang, 2011; Hogg, 2003; Janssen-Heininger et al., 2008; Winterbourn & Hampton, 2008). Signalling criteria would require the oxidation to be preferential for specific proteins and the process should be fast and reversible. Different models that fit signalling criteria are presented by Winterbourn and Hampton (Winterbourn & Hampton, 2008). The most important determining factors are probably the rate constant in the reaction between the oxidant and the thiol, the reduction potential of the thiol (E_{pa} or ORP) and the acid dissociation constant (pK_a) for each thiol species, as well as the conformation and the abundance of the actual thiol protein (Jacob, 2011). A low pK_a is a key property for enhancing the reactivity of a thiol protein (Poole, 2014). Almost all physiological oxidants can react with thiol proteins (Winterbourn & Hampton, 2008).

A number of mechanisms and enzymes are involved in the redox control of reversible thiol modifications. The ability to reverse an oxidative modification is a requisite for redox signalling, otherwise there would be no redox regulation. Cleavage of the disulphide bond has been reviewed (Hogg, 2003), but it is unclear whether this is a general mechanism for controlling protein function or if it is valid for a few selected proteins only. Some of the main redox controls for thiol proteins are briefly described below and more detailed elsewhere (Holmgren et al., 2005; Riederer, 2009).

Glutathione (GSH) is an antioxidant which can scavenge free radicals, reduce peroxides and bind electrophilic compounds. GSH is the major defence mechanism against oxidative and other forms of stress. Glutathione reduces disulphide bonds by electron donation, but this process transforms GSH into glutathione disulphide (GSSG). The GSH/GSSG ratio can be used as a measure of the oxidative stress level in cells. Glutathione disulphide is harmful for the cells and needs to be either transported out of the cell or converted by glutathione reductase. Addition of GSH to a protein is called glutathionylation and the mechanism is reviewed in (Dalle-Donne et al., 2011).

Glutaredoxins are small redox enzymes which are oxidized by substrates and reduced non-enzymatically by GSH. Hence, glutaredoxins are responsible for removing GSH from glutathionylated proteins (Holmgren et al., 2005).

Thioredoxins are a family of small redox enzymes which are present in nearly all organisms and are involved in many important biological processes. Their function is to reduce disulphide bonds in a variety of proteins by cysteine thiol-disulphide exchange reactions. Thioredoxins are kept in reduced state by thioredoxin reductase through a NADPH dependent reaction (Holmgren et al., 2005).

Thiol based signalling is found in plants, animals and single cell organisms (Wouters et al., 2011). Since oxidants act directly on the target, the response is fast. Furthermore, adjustment of the response can vary with the different thiol modifications and by modification of different thiol residues on the protein. The adjustment is illustrated by the triggering of different cellular pathways in response to an increasing level of oxidants, as shown in Figure 19.

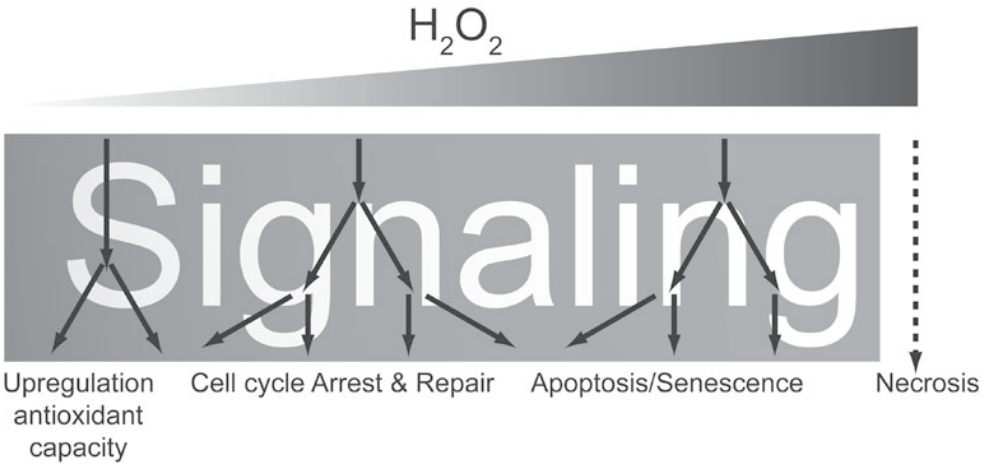

Figure 19: Cells responds to increasing oxidative stress. Different signal pathways are triggered at different stress level. H_2O_2 is often used as oxidant in model systems and here the increasing level of H_2O_2 illustrates increasing oxidative stress level. This figure is adapted from http://groups.mcr.umcutrecht.nl/dansen/.

Redox signalling is an important factor in e.g. inflammatory responses, stem cell biology, aging, cancer and cell signalling. The role of reversible oxidation is demonstrated on some central proteins. A few of them are listed below with relevant references while some redox-regulated proteins that are important in apoptosis will subsequently be discussed in more detail.

Several transcription factors are found to be regulated by redox switches. The most studied ones are NF-κB (Leonarduzzi et al., 2011; Oktyabrsky & Smirnova, 2007; Pineda-Molina et al., 2001) and AP-1 [(Leonarduzzi et al., 2011; Oktyabrsky & Smirnova, 2007) and references therein]. Other examples are; microbial Yap1p (Brandes et al., 2009; Georgiou, 2002; Paget & Buttner, 2003), microbial OxyR (Georgiou, 2002; Paget & Buttner, 2003), specificity protein-1 (Sp-1) (Leonarduzzi et al., 2011), Ets-1 (Leonarduzzi et al., 2011), hypoxia inducible factor-1 (HIF-1) (Leonarduzzi et al., 2011) and the mammalian family of fork head box proteins, class O, (FoxO) (Dansen et al., 2009; Leonarduzzi et al., 2011).

Protein kinases are known to regulate most of the cellular pathways and particularly signal transduction. The protein kinase family can be subdivided according to amino acid they act upon. Tyrosine specific kinases often function as growth factor

receptors and have a conserved cysteine residue in their catalytic domain that must be fully reduced for complete activity [(Gabbita et al., 2000) and references therein]. Redox regulation of phosphorylation is reviewed elsewhere (Brandes et al., 2009; Chiarugi & Buricchi, 2007; Gabbita et al., 2000; Janssen-Heininger et al., 2008; Leonarduzzi et al., 2011; Oktyabrsky & Smirnova, 2007).

Serine/threonine specific kinases are involved in the regulation of cell proliferation, differentiation, apoptosis and embryonic development. Their catalytic domain is highly conserved and contains a cysteine rich region. Studies has shown that several of these kinases are redox regulated e.g. protein kinase C (PKC) (Leonarduzzi et al., 2011), mitogen activated protein kinase (MAPK) family (Cross & Templeton, 2004; Gabbita et al., 2000; Giles, 2006; Leonarduzzi et al., 2011) and protein kinase B (PKB), also called Akt (Leonarduzzi et al., 2011).

Phosphatases are enzymes with a mechanism opposite of protein kinases, but similarly they contain a cysteine rich region in their catalytic domain. While protein kinases are activated by oxidants, phosphatases are transiently inhibited by oxidants [reviewed in (Chiarugi & Buricchi, 2007; Leonarduzzi et al., 2011)]. Specific examples are cell division cycle 25 (Cdc25) (Leonarduzzi et al., 2011) and PTP1B (Chiarugi & Buricchi, 2007; Cross & Templeton, 2004).

The redox regulation of thiol dependent pathways in cancer has been extensively reviewed (Giles, 2006). Often the cancer cells have altered redox homeostasis compared to normal cells. Many reviews state that the level of oxidants in cancer cells are elevated due to their high metabolism, but this is not definite (Choudhari et al., 2014; Kwee, 2014; Raninga et al., 2014). Cancer cells readily redox adapts to their environment and a tumour can have a range from well oxygenated to hypoxia, and there seems to be a difference between cancer stem cells and cancer cells (Acharya et al., 2010; Liou & Storz, 2010). However, central factors for cancer development are demonstrated to be redox regulated(Parri & Chiarugi, 2013); tumour suppressor protein p53 (Cross & Templeton, 2004; Leonarduzzi et al., 2011) and references therein] and nuclear factor (erythroid-derived 2)-like 2, also known as Nrf2 (Leonarduzzi et al., 2011; Na & Surh, 2006; Ray et al., 2012).

1.3.6.1 Redox regulation, a mechanism in the apoptotic pathway

Normal oxidant level in cells usually promotes cell proliferation, while a sub-toxic level induces apoptosis and toxic levels of oxidants can lead to necrosis and amplification of an inflammatory response, see Figure 19. In general, thiol oxidation activates pro-apoptotic signal pathways and inhibits pathways promoting cell survival.

Mitochondria are both a ROS-producing organelle and a sensitive oxidant target. Furthermore, mitochondria play an important role in apoptosis. The role of mitochondrial oxidative stress in apoptosis has been extensively reviewed by others (Circu & Aw, 2010; Orrenius et al., 2007). However, a few examples of redox regulation of apoptosis will be given below.

Mitochondrial permeability transition (MPT) occurs when a nonspecific pore (mitochondrial permeability transition pore, MPTP) in the inner mitochondrial membrane opens. There are several effects of MPT, including release of mitochondrial contents, depolarization of the mitochondrial membrane and thereby ATP depletion. MPT is a key event in apoptosis, by releasing cytochrome c. One model for pore formation is based on the conformational changes on the inner mitochondrial membrane transport protein adenine nucleotide translocase (Halestrap et al., 1997; Moran et al., 2001). The mitochondrial matrix protein cyclophilin-D appears to have a key role in this conformational change. Oxidative thiol modification on cyclophilin-D leads to increased binding of this protein to the inner mitochondrial membrane and increased sensitivity to MPT pore opening (Halestrap et al., 1997; Moran et al., 2001). Consequently, MPT seems to be subject to redox regulation, implicating cytochrome c release and subsequently apoptosis.

Apoptosis signal regulating kinase (ASK1) is a MAPK kinase which activates the JNK and p38 pathway in response to several stress factors, including oxidative stress. There are several layers of controlling ASK1 and a central contributor is thiol oxidation. ASK1 can bind directly to both thioredoxin and glutaredoxin. Both of them are part of the redox defence and are easily thiol oxidized. Upon thiol oxidation they detach from ASK1 and thereby induce apoptosis. The more detailed mechanism of this is reviewed in (Cross & Templeton, 2004).

Tumour suppressor PTEN (phosphatase and tensin homologue deleted from chromosome-10) directly counteracts the effect of PI3K. Many other phosphatases also regulate the PI3K/Akt/mTor pathway negatively. PTEN is redox regulated and is important for cellular proliferation. One study has shown that even in absence of growth factors, administration of exogenous peroxide is sufficient to oxidize PTEN which then activate the PI3K/Akt/mTor pathway (Giles, 2006; Leslie et al., 2003). The membrane-bound NADPH oxidase Nox 1 is an important source of oxidants for PTEN regulation. Furthermore, this oxidoreductase is coupled to PDGF receptor activation resulting in ROS activation of PI3K/Akt/mTor, increased proliferation rate and inhibited apoptosis. Since Nox 1 is upstream in the pathway, its activation is expected to increase the extracellular concentration of oxidants. This could imply that the extracellular environment exerts a paracrine regulatory role in cell signalling, as suggested in (Giles, 2006).

1.3.7 Summary of oxidative stress

PDT induces oxidants and cell death. These oxidants could both damage the cell intracellularly and induce reversible oxidation of thiol proteins. Some proteins are found to be redox-regulated by reversible oxidation of cysteine residues. Redox signalling is a growing field in science. Redox signalling is now recognized to be associated in important physiological events, such as apoptosis, cell cycle regulation, proliferation, aging, inflammation, cell migration and angiogenesis.

In redox signalling the oxidation and reduction of cysteine is the most studied mechanism and this thiol-based redox switch is also probably the principal mechanism. Thiol based signalling is proven to regulate important cellular mechanisms including apoptosis. It might turn out that redox signalling is just as important as protein phosphorylation is for regulating cellular responses.

Aims of the study

ALA-based PDT is in clinical use, but it has a potential for expansion as a clinical treatment mode. One of the obstacles of the treatment is the limited uptake of the prodrug ALA. HAL is an ester derivative of ALA that can diffuse through the cell membrane and it has thereby overcome the uptake obstacle. The thesis concentrates on HAL-PDT.

To further improve the PDT treatment it is important to learn as much as possible about the induced mechanisms and how the outcome of the treatment is affected when changing a treatment parameter. The irradiation parameters are in principle easy to alter and the treatment might be optimized by changing the light regimes, wavelength etc. The thesis concentrates on wavelength, fluence rate and fractionation of the delivered light.

Moreover, PDT generates photochemical reactions leading to oxidative damage in the cells. Subsequent cell death should occur after the treatment, preferably only in the cancerous cells/tissue. It is important to know details of these oxidative reactions and damages leading to cell death. The thesis concentrates on studies of oxidation of proteins, an important class of ROS damage.

With these aspects in mind, the main aims of the thesis have been identified and can be specified by the following hypotheses:

- Does fractionated light delivery give results different than continuous light delivery (paper I)
- Does wavelength or irradiation affect cell kill efficiency and which cell death pathway is triggered (paper II)
- Does HAL-PDT induce protein carbonylation, PTMs and altered protein expression (paper III)
- Does HAL-PDT induce reversible thiol protein oxidation and could some of these be a triggering signal for apoptosis (paper IV)

Summary of results

Paper I:

Photo induced hexylaminolevulinate destruction of rat bladder cells AY-27.

HAL-PDD is approved for diagnosis of bladder cancer by blue light cystoscopy. The rat bladder cancer cell line, AY-27, is well established as a useful *in vivo* animal model for bladder cancer. *In vitro* experiments using this cell line may therefore be of value in establishing basic photophysical parameters for future treatment of patients. For optimizing HAL-PDT in order to take the step from diagnosis to treatment, it is important to establish the best possible light protocol. In this study red light was used instead of blue light since red light is considered better for clinical treatment due to greater penetration depth of red light.

To establish a dose response curve for AY-27, mitochondrial metabolic activity was measured by MTT assay 24 hours after HAL-PDT (10 μM HAL, 3.5 hours, serum free, 36 mW/cm^2, 630 nm). There was no observable light toxicity and the curve was typical sigmoidal as PDT response curves mostly are. This dose response result shows that this bladder cancer cell line responds well to red light HAL-PDT.

To study the induction of apoptosis the Annexin V/PI assay and the YO-PRO-1/PI assay were used. Both assays were used at 1h and 24 h after HAL-PDT (same protocol as for the dose response, but irradiance at 20 mW/cm^2). Using these assays, we concluded that the main cell death pathway was necrosis. The maximum apoptotic fraction was 10 % measured for a low dose 1 h after PDT (total cell viability 30 %). The LD_{50} measured using the Annexin/PI assay at 1 h after HAL-PDT was substantially higher dose than the LD_{50} measured by MTT 24 h after HAL-PDT.

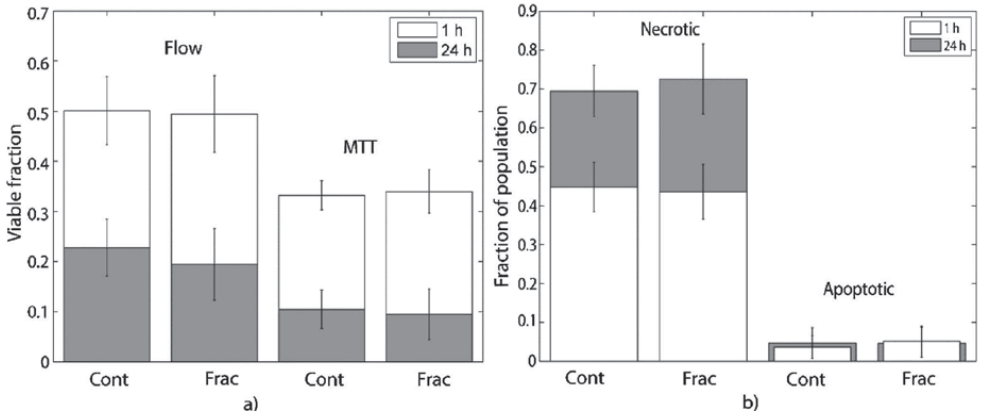

Figure 20: Viable fraction (at 1 h and 24 h) after red light (630 nm, 20 mW /cm^2, 5.4 J/cm^2) HAL-PDT (10mM, 3.5 h) measured by flow cytometry with annexin V/PI assay. MTT assay measurements (at 1 h and 24 h) after the same treatment are also shown (a). Apoptotic and necrotic fraction (at 1 h and 24 h) after red light HAL-PDT, measured by flow cytometry with annexin V/PI assay. The bars represent mean values±SD of 3 independent experiments, each done in duplicate (Ekroll et al., 2011).

To test whether fractionation of the light delivery influenced on the outcome, a light interval regime of light 45 s/darkness 60 s was used. The fractionation of the 5.4 J/cm^2 (20 mW/cm^2) dose gave the same results as continuous light delivery as measured both at 1 h and 24 h after the treatment and for both the MTT assay and the Annexin V/PI assay. This indicates that fractionation of light delivery with this light/dark interval does not influence the outcome.

Paper II:

Red versus blue light illumination in hexyl 5-aminolevulinate photodynamic therapy: the influence of light color and irradiance on the treatment outcome in vitro.

Without light there is no PDT. It is fundamental to optimize this treatment parameter for an optimal result. The in-house made lamps made it possible to study effects of the photophysical parameters wavelength and irradiance.

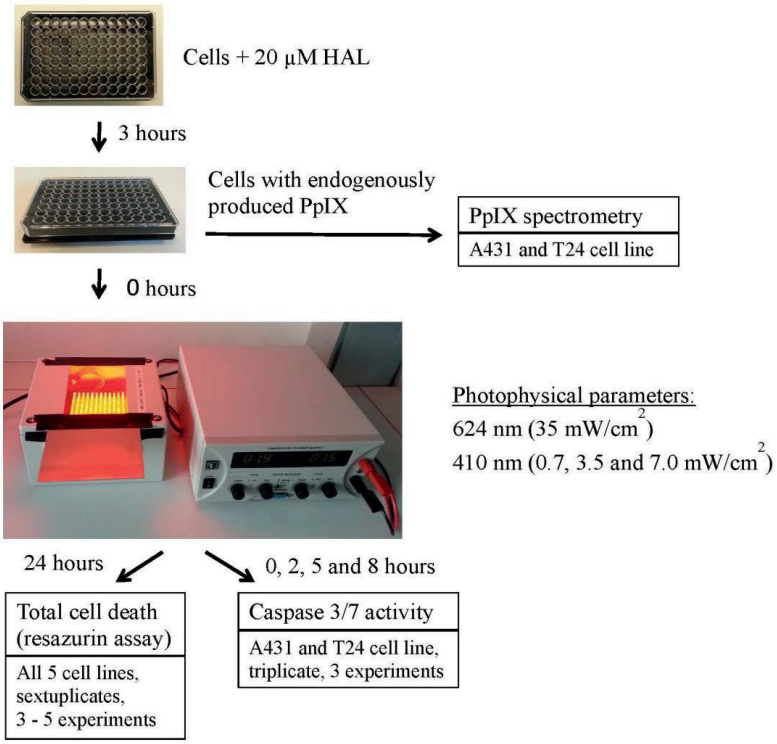

Figure 21: Flowchart of the experiments, the photophysical parameters tested and the cell lines used (Helander et al., 2014).

To study whether the irradiance had an effect on total cell death or whether total light dose was a determining factor, we measured cell viability for five human cancer cell lines at 24 hours after the treatment with different light doses and irradiances. Our results indicated that high irradiance is more efficient in killing cells compared to lower irradiance at the same total light doses. The efficacy difference between high and lower irradiance is cell line specific. For light doses resulting in close to complete cell death the difference between high and low irradiance is cannot be distinguished.

To improve the treatment it is important to know if the protocol in use generates only necrosis, only apoptosis or a mix of both cell death pathways. A mix of necrosis and apoptosis is favourable since this promotes activation of possible long-term immunity and immediate immune responses. One central measurable biochemical parameters in the apoptotic pathway is activation of caspase 3. We measured the caspase 3/7 activity for two of the cell lines, A431 and T24, for different light doses, two blue

light irradiances and one red light irradiance. Our results show that which pathway is triggered depends on both the cell line and on the photophysical parameters. Red light induces higher caspase 3/7 activity than blue light and elicits the highest caspase 3/7 activity at full doses resulting in complete cell kill. In contrast, blue light has highest caspase 3/7 activity at doses resulting in about 85 % cell kill. In addition, low irradiance activated visibly more caspase 3/7 activity than high irradiance at the same doses.

One important result from this study is the large difference between the five cell lines tested. Both the light doses required for cell killing and the shape of the dose response curves differ greatly.

Paper III:

Photodynamic therapy with hexyl aminolevulinate induces carbonylation, posttranslational modifications and changed expression of proteins in cell survival and cell death pathways.

PDT induces photochemical reactions and thereby oxidative stress. Cells have mechanisms to respond to oxidative stress and damage and these mechanisms depend on proteins. To examine if changes in protein modification could contribute to the effect of PDT, the AY-27 cell line was used as a model and HAL-PDT (10 μM HAL, 3.5 h, serum free, 12.9 mW/cm^2, 435 nm) as treatment. At 2 hours after illumination with 0.45 J/cm^2, which results in approximately 80 % cell kill, the cells were harvested and protein extracted for analyses.

2D-DIGE measurements of untreated control cells, HAL incubated cells and HAL-PDT treated cells demonstrated good reproducibility between experiments and that a large number of proteins were up or down regulated. In addition, we observed PI-shifts for some of the proteins, indicating an enzymatic modification of the protein. To be able to identify some of these altered proteins, a 2D-gel with much higher protein sample content was run and gel spots was picked based on the 2D-DIGE results. From this a total of 40 proteins were identified. Most of these proteins displayed an acidic PI-shift, indicating altered phosphorylation status or oxidative thiol modifications. Notably,

these proteins mostly belong to mitochondria/ER molecular chaperones and stress response proteins.

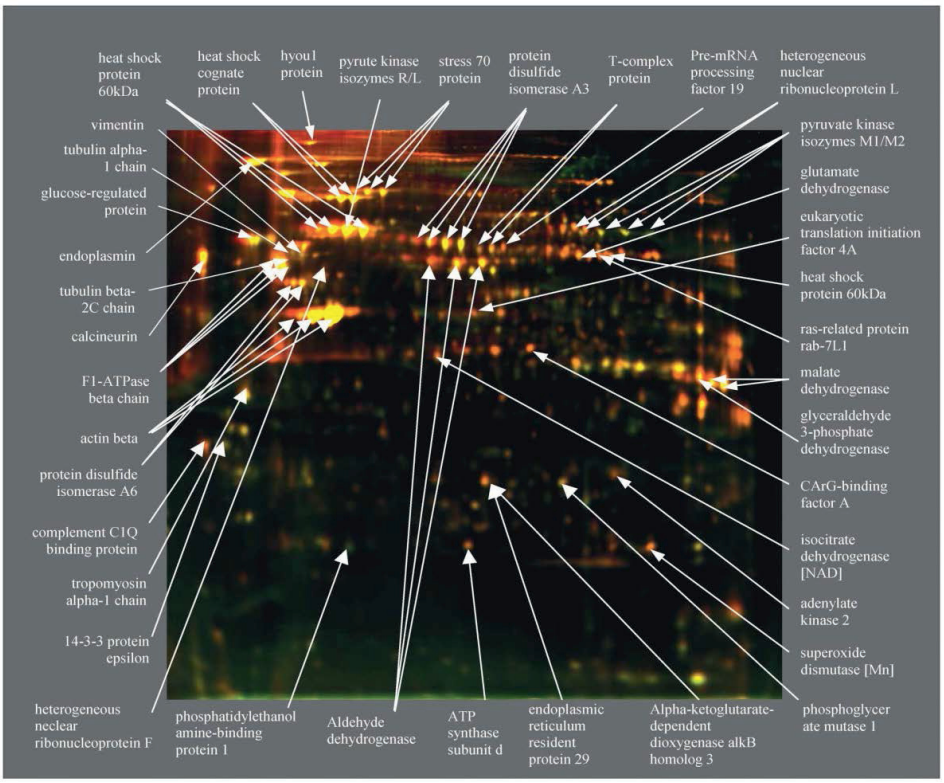

Figure 22: Mapping of 40 identified proteins in HAL-PDT treated AY-27 cells (Baglo et al., 2011).

Carbonylation is a permanent type of oxidative damage of proteins. Carbonylation does not induce PI-shift in 2D-DIGE gels so to identify carbonylated proteins, control cells and HAL-PDT treated cells were derivatized by DNPH, immunoprecipitated and separated by 2D-GE. From this experiment, 9 proteins were identified (by MS) to have increased carbonylation after HAL-PDT and one decreased.

The results from the 2D-DIGE and 2D-GE analyses were launched into PHANTER classification system to see if specific mechanisms were targeted by HAL-PDT. The majority of the identified proteins belonged to mitochondria, ER and

membranes, but the overall picture is that HAL-PDT induces changes in a large number of proteins involved in diverse functions.

Paper IV – manuscript

Reversible oxidation of thiol proteins after hexylaminolevulinate mediated photodynamic therapy.

The photochemical reactions generated from PDT will induce oxidants that can induce oxidative modifications and damage on cellular targets. Proteins are a major target due to their abundance and reactivity with oxidants. Most of the protein modifications are irreversible, although modifications on the thiol group on Cys residues are reversible. This is now recognized as a signalling mechanism and the knowledge about its significance is increasing (Poole, 2014; Popov, 2014; Reczek & Chandel, 2014; Sies, 2015). To examine if this type of modification was induced by HAL-PDT and possibly contributing to induced cell death, we used the human cancer cell line A431 as model system.

Red light HAL-PDT resulted in a sigmoidal dose response curve at 24 h after the treatment as expected, but the induction of apoptosis did not decrease as expected for the highest doses. At 12.5 J/cm^2 complete cell kill was measured at 24 h and the apoptotic fraction was 40 %. This dose was used for the proteomic study and the cells harvested 30 min post HAL-PDT.

The reversibly oxidized thiol proteins were enriched and then identified by LC-MS/MS. Over 1900 proteins were identified, about a third of them were also found in the untreated controls as well. The proteins that were found in at least two treated samples, but not in controls, and above an ID confidence threshold, were further analysed (283 proteins, HAL-PDT list). The proteins identified in this way were mapped to several cellular compartments, and mitochondria were not the major localization as expected. Their cellular function was compared to the 'normal percent' distribution (in IPA). Interestingly, the largest differences were observed within cellular homeostasis and cell cycle.

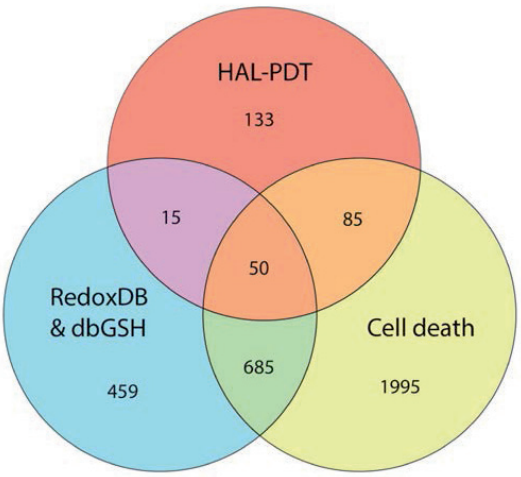

Figure 23: Venn diagram shows the overlap between our HAL-PDT list [blue], two databases for redox regulated proteins (dbGSH and RedoxDB) [yellow] and proteins known to be a part of cell death pathways (Cell Death Proteomics) [red].

Furthermore, 135 proteins from the HAL-PDT list are associated to programmed cell death according to the database Cell Death Proteomic. In the databases RedoxDB and dbGSH proteins with reported Cys residue oxidative modification (mostly S-gluthationylation) are manually assembled and 65 out of the HAL-PDT list proteins are found in these two databases. Out of these proteins, 50 were common in the HAL-PDT dataset, the redox databases and in the cell death database. We did a manual literature search to see if any of these were reported to be redox regulated. Two important redox regulated apoptosis proteins in this list were the 14-3-3 protein family (6 out of 7 isoforms in HAL-PDT dataset) and the kinase c-Src.

Further studies are needed to elucidate to what extent the identified proteins in HAL-PDT set are involved in redox-regulation of treatment-induced cell death signaling.

General discussion

The current status of PDT within oncology and its future perspectives have been well reviewed (Allison, 2014). A general discussion of the focus areas in this thesis follows in the subsequent text.

Photophysical parameters

Light is one out of three essential factors in PDT (light, PS and oxygen). It is easy to monitor the light, which is therefore amenable to optimization for PDT treatment. For optimizing this factor is it important to know how the different photophysical parameters affect the treatment outcome. A real improvement for PDT in general would be to monitor the bleaching/fluorescence from the applied light to do a real time actual dosimetry and thereby personalize the treatment. The development of improved light sources and sensors in combination with increased knowledge about the effect of photophysical parameters can make this a reality in the future. In two of the papers included in this thesis, Paper I and Paper II, photophysical parameters have been studied.

From paper I it looked like blue light HAL-PDT and red light HAL-PDT were about equally cytotoxic when taking into account the theoretical difference between PpIXs absorption capacity at those two wavelengths. In paper II the PpIX absorption spectrum was measured for T24 and A431 cells. The absorption ratio between the two wavelengths used in this study (410 nm: 624 nm) was 56 and this ratio correlated well with the cell killing efficiency for the two wavelengths, supporting the presumption from paper I. PSs based on porphyrin (including PpIX) can in principle be activated by blue, green and red light. In theory could the wavelength for clinical PDT application be chosen based on the wanted qualities, the assumption of wavelength independence for inducing cytotoxicity is supported by the results in paper I and II. This may be exploited by clinicians to administer light at different depths (although limited) to optimize the treatment, thus will information on cytotoxicity and mode of killing by

different wavelengths may be useful.

Cell cytotoxicity after PDT seemingly comprises apoptosis and necrosis as major death modes. To what extent the induction of the two pathways is influenced by applied wavelength and irradiance was studied in paper II. The results indicated that both wavelength and irradiance had an impact on which cell death pathways that was induced. It is important to have knowledge about which pathway that will be induced from the treatment, since they may trigger different additional responses. Necrosis alone can damage surrounding healthy tissue while tissue damage from apoptosis alone will be restricted. From this point of view apoptosis is preferable. However, due to the additional responses, PDT is not only a local treatment. Necrosis can release cell debris, immunogenic proteins and cytokines from the tumour cells. This causes up-regulation of the immune system and apoptosis and triggers the innate immune system to phagocytose. This combination can lead to a successful presentation of tumour associated antigens in the adaptive immune system, thus creating long term immunity in addition to the immediate immune response from necrosis, and that this has potential as "cancer vaccine"(Panzarini et al., 2013). Therefore, optimizing the photophysical parameters to achieve high cytotoxicity and inducing a mix of apoptosis and necrosis to achieve both immediate and long term immune response should be the goal.

The effect from fractionation of light delivery in ALA-based PDT has been studied by e.g. (Ascencio et al., 2008; Babilas et al., 2003; de Bruijn et al., 2013; de Bruijn et al., 2006; Iinuma et al., 1999; Middelburg et al., 2013; Oberdanner et al., 2005). In paper I we tested if an interval of 45s light/ 60 s darkness altered the cytotoxicity or percent apoptosis when applying blue light HAL-PDT on AY-27 cells. For a dose resulting in 50 % cell death there was no difference between the outcomes from fractionated light delivery compared to continuous light delivery in our study. Most other fractionation studies have been done *in vivo* and they either show improved PDT effect (Ascencio et al., 2008; Iinuma et al., 1999; Middelburg et al., 2013) or ambiguous effects (Babilas et al., 2003; de Bruijn et al., 2006). For other *in vitro* fractionation studies the effects of fractionation was not consistent, possibly due to different duration of the dark period. Oberdanner et al showed decreased cytotoxicity and decreased ROS induction with light

intervals similar to those used in paper I, while de Brujin et al found that a 2 h dark period increased the effect of PDT. If the dark period should be long or short remains unclear and requires further studies. Short repeated intervals of light may utilize the available oxygen in the surroundings by letting oxygen diffuse into the treatment area during the dark period and short fractionation reduces the fluence rate. While a longer dark period e.g. 2 h makes the cells sensitive to a second round of irradiation. The deoxygenation issue can probably be neglected in *in vitro* studies, so an effect of fractionation in these studies is likely to have another cause. The possible optimization of PDT by applying light in intervals is probably best studied *in vivo*.

Cell death pathways

In many PDT articles the subject cell death pathway, e.g. apoptosis, autophagy and necrosis, is a part of or is the main focus of the study. Paper I, paper II and paper IV in this thesis is no exception.

As mentioned in the previous paragraph the combination of apoptosis and necrosis could result in long time immunity against the treated cancer form (Korbelik & Sun, 2006). This prospect of PDT is an area of fast growing interest. The additional effect from activated immune system could constitute the difference between complete clinical regression and unsuccessful treatment.

By gaining knowledge about central mechanisms for effecting, or even better, to know the exact triggering mechanism for the cell death, makes it possible to enhance the effect by additional treatment [reviewed in (Agostinis et al., 2011), e.g. enhancing PpIX accumulation in tumours by adding vitamin D3 (Anand et al., 2011). Several apoptosis-modulating factors have been shown to enhance the PDT mediated cell death (Choi et al., 2014; Ferrario et al., 2005; Ferrario et al., 2007; Kessel, 2008; Kessel et al., 2012; Korbelik et al., 2011; Sarissky et al., 2005; Weyergang et al., 2009). When engineering apoptosis modulating factors it is important to keep in mind the complicating issue of cross talk between the different cell death pathways (Jain et al., 2013).

A possible enhancement factor for PpIX-PDT is the peripheral benzodiazepine

receptor (PBR), also called translocator protein (TSPO) [reviewed in (Buytaert et al., 2007)]. HAL-PDT is demonstrated to target PBR (Furre et al., 2005) and PBR is a putative component of the MPT pore amongst other roles in cell function (Kolodziejczyk, 2015). A strengthening of PBR mechanism/pathway could optimize PpIX-PDT.

Oxidative protein modifications

We have measured induction of ROS in AY-27 cells as a function of light dose in blue light HAL-PDT, unpublished results (Figure S1, Supplementary to paper IV). This result clearly shows that the amount of induced ROS increases with increased light dose. And, pilot studies done in Salzburg shows that the same applies for red light HAL-PDT on A431 cells. Proteins are major target for the induced oxidants and two types of oxidative modifications has been studied in this thesis, carbonylation in paper III and reversible thiol modification in paper IV.

Carbonylation of proteins is irreversible and frequently results in loss of protein function. It is regarded a major hallmark of oxidative damage and is central in aging and age related diseases (Cabiscol et al., 2014; Dalle-Donne et al., 2006a; Dalle-Donne et al., 2006b; Dalle-Donne et al., 2003; Fedorova et al., 2014). Whether carbonylation is involved in signalling pathways, such as antioxidant biology and cellular homeostasis, is debated and there exist few studies on the subject (Curtis et al., 2012). The role of carbonylation might change during the life cycle of an organism. Presently, carbonylation is mostly used within PDT research as an indirect measure of oxidative stress.

The research field of redox proteomics and its role in signalling is gaining interest (Sies, 2015). A PubMed search (24.01.2015) on the terms “redox proteomics” resulted in 1633 entries and by adding the term “photodynamic” the number of entries decreased to 2. These numbers illustrate the novelty of redox proteomics within PDT. The role of redox signalling is briefly described in 1.3.6, but the overall comprehension is that redox signalling is a mechanism that is neither only harmful nor only protective (Holmstrom & Finkel, 2014). It seems likely redox signalling has an important role in

redox homeostasis (Groitl & Jakob, 2014; Ray et al., 2012; Schieber & Chandel, 2014) and that its extent in cell death increases (Allen & Mieyal, 2012; Chiu & Dawes, 2012; Circu & Aw, 2010; Lee et al., 2012; Navarro-Yepes et al., 2014; Trachootham et al., 2008; Wang et al., 2012). The role of redox signalling in PDT efficacy is quite unexplored. Paper IV in this thesis is a contribution to this topic and will hopefully evoke curiosity of other researchers to follow up the topic. To identify a likely trigger mechanism and point of no return mechanisms in cell death require more studies. Available state-of-the-art technology makes the required studies possible (Ckless, 2014; Couvertier et al., 2014; Huang et al., 2014; Panis, 2014; Paulech et al., 2013).

The clinical future for HAL-PDT

The discussion above applies to PDT in general, including HAL-PDT. In this section the focus will be on HAL-PDT and its possibilities as clinical treatment. Only the application areas and improvements that seem most likely according literature search are discussed below.

HAL-PDD is already approved for blue light cystoscopy diagnosis of non-muscle invasive bladder cancer under the name Cysview (US) and Hexvix (Europe) (Babjuk et al., 2013; Oosterlinck et al., 2004; van der Meijden et al., 2005). The use of HAL-PDD as diagnostic tool may improve the diagnosis and treatment of other superficial cancer forms as well, e.g. intestinal cancer. Since HAL-PDD gives immediate diagnostic outcome, thus anxiety during the waiting period for outcome of the biopsy may be avoided. Furthermore, fluorescence-guided resection of tumour tissue will minimize normal tissue loss, improving the functional and cosmetic outcome. This may be especially important in head and neck surgery. In addition, further irradiation after tumour tissue removal could improve eradication of potential remaining tumour cells.

The World Health Organization has pointed out drug resistant microbes as major threat to human health (Cars et al., 2008). ALA-based PDT was found to inactivate a broad range of microbes, including drug resistant strains [reviewed in (Harris & Pierpoint,

2011)]. ALA uptake is energy dependent, while HAL can diffuse through membranes, this is one thing making HAL an interesting alternative for inactivation of microbes (Yung et al., 2007). Two highly relevant applications are wound healing and inactivation of multidrug resistant bacteria. ALA-PDT shows promising results against multiresistant *staphylococcus aureus* (Fu et al., 2013; Li et al., 2013).

The technical development of new light sources enlarges the possible clinical use of PDT. A new and interesting light source for PDT are the organic light emitting diodes (OLED) (Minaev et al., 2014). These can be used as a light emitting patch and thereby as an ambulatory treatment diminishing the clinic time. Attili and co-workers carried out an open pilot study treating Bowens disease and superficial basal cell carcinoma (BCC) patients with good curing rate and less pain compared to routine PDT (Attili et al., 2009). Another relevant light source for minimal clinic time is daylight (Enk et al., 2014; Fai et al., 2014; Kellner et al., 2014; Neittaanmaki-Perttu et al., 2014; Perez-Perez et al., 2014; Rubel et al., 2014; Togsverd-Bo et al., 2014; Togsverd-Bo et al., 2013; Wiegell et al., 2012a; Wiegell et al., 2013a; Wiegell et al., 2013b; Wiegell et al., 2012b). HAL-PDT cannot easily be overdosed due to the photobleaching of PpIX. This makes HAL-PDT especially well-suited for daylight PDT.

HAL-PDT is closer to being an approved clinical treatment within some medical fields. Some studies, including clinical trials, show promising results for HAL-PDT on cervical cancer (Guyon et al., 2014; Hillemanns et al., 2015; Hillemanns et al., 2014a; Hillemanns et al., 2014b) and on bladder cancer (Bader et al., 2012; Bader et al., 2013; Lee et al., 2013). ALA and MAL-PDT is already in clinical use within dermatology with good results (Christensen, 2013; Ericson et al., 2008; Rkein & Ozog, 2014; Wang et al., 2015). A few studies indicate that HAL-PDT is at least well suited within dermatology as MAL and ALA (Togsverd-Bo et al., 2012a; Togsverd-Bo et al., 2012b; Togsverd-Bo et al., 2010).

The perhaps biggest challenge for HAL-PDT on patients is their sensation of pain during irradiance and shortly after. This challenge applies to MAL- and ALA-PDT patients as well, as described in some studies e.g. (Attili et al., 2011; Chaves et al.,

2012; Halldin et al., 2011; Halldin et al., 2013; Steinbauer et al., 2009; Warren et al., 2009). In one study, incubation with HAL induced less pain during illumination than incubation with MAL(Yung et al., 2007). Reducing the fluence rate, cooling the treated area or using an anaesthetic is actions that can reduce the pain, but for some patients the pain is so severe that the treatment must be aborted. The pain inducing mechanism is undefined. If the pain challenge is solved successfully, the implementation of HAL-PDT on patients will be much easier.

The last and perhaps most important factor for PDT (including HAL-PDT) to achieve more clinical use are to increase the number of phase 3 trials. To speed up this process it is important that research at the cellular level is carried out with the patients in mind. This could pave the way from cells, to animal models, to clinical trials and make studies, hopefully, better and time saving.

References

ABELS, C., HEIL, P., DELLIAN, M., KUHNLE, G. E., BAUMGARTNER, R. & GOETZ, A. E. (1994). In vivo kinetics and spectra of 5-aminolaevulinic acid-induced fluorescence in an amelanotic melanoma of the hamster. British Journal of Cancer, 70(5), 826-833.

ACHARYA, A., DAS, I., CHANDHOK, D. & SAHA, T. (2010). Redox regulation in cancer: a double-edged sword with therapeutic potential. Oxid Med Cell Longev, 3(1), 23-34.

ADIGBLI, D. K. & MACROBERT, A. J. (2012). Photochemical internalisation: the journey from basic scientific concept to the threshold of clinical application. Curr Opin Pharmacol, 12(4), 434-438.

AGOSTINIS, P., BERG, K., CENGEL, K. A., FOSTER, T. H., GIROTTI, A. W., GOLLNICK, S. O., HAHN, S. M., HAMBLIN, M. R., JUZENIENE, A., KESSEL, D., KORBELIK, M., MOAN, J., MROZ, P., NOWIS, D., PIETTE, J., WILSON, B. C. & GOLAB, J. (2011). Photodynamic therapy of cancer: An update. CA: A Cancer Journal for Clinicians.

AGOSTINIS, P., BUYTAERT, E., BREYSSENS, H. & HENDRICKX, N. (2004). Regulatory pathways in photodynamic therapy induced apoptosis. Photochem Photobiol Sci, 3(8), 721-729.

ALBERTS, B., JOHNSON, A., LEWIS, J., RAFF, M., ROBERTS, K. & WALTER, P. (2008). Molecular biology of the cell. Fifth edition.

ALLEN, E. M. & MIEYAL, J. J. (2012). Protein-thiol oxidation and cell death: regulatory role of glutaredoxins. Antioxid Redox Signal, 17(12), 1748-1763.

ALLISON, R. R. (2014). Photodynamic therapy: oncologic horizons. Future Oncol, 10(1), 123-124.

ANAND, S., WILSON, C., HASAN, T. & MAYTIN, E. V. (2011). Vitamin D3 enhances the apoptotic response of epithelial tumors to aminolevulinate-based photodynamic therapy. Cancer Research, 71(18), 6040-6050.

ASCENCIO, M., ESTEVEZ, J. P., DELEMER, M., FARINE, M. O., COLLINET, P. & MORDON, S. (2008). Comparison of continuous and fractionated illumination during hexaminolaevulinate-photodynamic therapy. Photodiagnosis Photodyn Ther, 5(3), 210-216.

ATTILI, S. K., DAWE, R. & IBBOTSON, S. (2011). A review of pain experienced during topical photodynamic therapy--our experience in Dundee. Photodiagnosis Photodyn Ther, 8(1), 53-57.

ATTILI, S. K., LESAR, A., MCNEILL, A., CAMACHO-LOPEZ, M., MOSELEY, H., IBBOTSON, S., SAMUEL, I. D. & FERGUSON, J. (2009). An open pilot study of ambulatory photodynamic therapy using a wearable low-irradiance organic light-emitting diode light source in the treatment of nonmelanoma skin cancer. British Journal of Dermatology, 161(1), 170-173.

AZUMA, M., KABE, Y., KURAMORI, C., KONDO, M., YAMAGUCHI, Y. & HANDA, H. (2008). Adenine nucleotide translocator transports haem precursors into mitochondria. PLoS One, 3(8), e3070.

BABILAS, P., SCHACHT, V., LIEBSCH, G., WOLFBEIS, O. S., LANDTHALER, M.,

SZEIMIES, R. M. & ABELS, C. (2003). Effects of light fractionation and different fluence rates on photodynamic therapy with 5-aminolaevulinic acid in vivo. British Journal of Cancer, 88(9), 1462-1469.
BABJUK, M., BURGER, M., ZIGEUNER, R., SHARIAT, S. F., VAN RHIJN, B. W., COMPERAT, E., SYLVESTER, R. J., KAASINEN, E., BOHLE, A., PALOU REDORTA, J. & ROUPRET, M. (2013). EAU guidelines on non-muscle-invasive urothelial carcinoma of the bladder: update 2013. European Urology, 64(4), 639-653.
BADER, M. J., STEPP, H., BEYER, W., PONGRATZ, T., SROKA, R., KRIEGMAIR, M., ZAAK, D., WELSCHOF, M., TILKI, D., STIEF, C. G. & WAIDELICH, R. (2012). Photodynamic Therapy of Bladder Cancer - A Phase I Study Using Hexaminolevulinate (HAL). Urol Oncol.
BADER, M. J., STEPP, H., BEYER, W., PONGRATZ, T., SROKA, R., KRIEGMAIR, M., ZAAK, D., WELSCHOF, M., TILKI, D., STIEF, C. G. & WAIDELICH, R. (2013). Photodynamic therapy of bladder cancer - a phase I study using hexaminolevulinate (HAL). Urol Oncol, 31(7), 1178-1183.
BAGLO, Y., SOUSA, M. M., SLUPPHAUG, G., HAGEN, L., HAVAG, S., HELANDER, L., ZUB, K. A., KROKAN, H. E. & GEDERAAS, O. A. (2011). Photodynamic therapy with hexyl aminolevulinate induces carbonylation, posttranslational modifications and changed expression of proteins in cell survival and cell death pathways. Photochem Photobiol Sci, 10(7), 1137-1145.
BALDEA, I. & FILIP, A. G. (2012). Photodynamic therapy in melanoma--an update. Journal of Physiology and Pharmacology, 63(2), 109-118.
BARELLI, S., CANELLINI, G., THADIKKARAN, L., CRETTAZ, D., QUADRONI, M., ROSSIER, J. S., TISSOT, J. D. & LION, N. (2008). Oxidation of proteins: Basic principles and perspectives for blood proteomics. Proteomics Clin Appl, 2(2), 142-157.
BATY, J. W., HAMPTON, M. B. & WINTERBOURN, C. C. (2002). Detection of oxidant sensitive thiol proteins by fluorescence labeling and two-dimensional electrophoresis. Proteomics, 2(9), 1261-1266.
BAUMANN, K. (2012). Cell death: multitasking p53 promotes necrosis. Nat Rev Mol Cell Biol, 13(8), 480-481.
BERLETT, B. S. & STADTMAN, E. R. (1997). Protein oxidation in aging, disease, and oxidative stress. Journal of Biological Chemistry, 272(33), 20313-20316.
BESUR, S., HOU, W., SCHMELTZER, P. & BONKOVSKY, H. L. (2014). Clinically important features of porphyrin and heme metabolism and the porphyrias. Metabolites, 4(4), 977-1006.
BHUVANESWARI, R., GAN, Y. Y., SOO, K. C. & OLIVO, M. (2009). The effect of photodynamic therapy on tumor angiogenesis. Cellular and Molecular Life Sciences, 66(14), 2275-2283.
BIRGISDOTTIR, A. B., LAMARK, T. & JOHANSEN, T. (2013). The LIR motif - crucial for selective autophagy. Journal of Cell Science, 126(Pt 15), 3237-3247.
BISSONNETTE, R. (2011). Treatment of acne with photodynamic therapy. Giornale Italiano di Dermatologia e Venereologia, 146(6), 445-456.
BLOOMER, J. R. (1998). Liver metabolism of porphyrins and haem. Journal of Gastroenterology and Hepatology, 13(3), 324-329.
BONINI, M. G., ROTA, C., TOMASI, A. & MASON, R. P. (2006). The oxidation of

2',7'-dichlorofluorescin to reactive oxygen species: a self-fulfilling prophesy? Free Radical Biology and Medicine, 40(6), 968-975.
BOOTH, L. A., TAVALLAI, S., HAMED, H. A., CRUICKSHANKS, N. & DENT, P. (2014). The role of cell signalling in the crosstalk between autophagy and apoptosis. Cellular Signalling, 26(3), 549-555.
BOZZINI, G., COLIN, P., BETROUNI, N., NEVOUX, P., OUZZANE, A., PUECH, P., VILLERS, A. & MORDON, S. (2012). Photodynamic therapy in urology: what can we do now and where are we heading? Photodiagnosis Photodyn Ther, 9(3), 261-273.
BRANCALEON, L. & MOSELEY, H. (2002). Laser and non-laser light sources for photodynamic therapy. Lasers Med Sci, 17(3), 173-186.
BRANDES, N., SCHMITT, S. & JAKOB, U. (2009). Thiol-based redox switches in eukaryotic proteins. Antioxid Redox Signal, 11(5), 997-1014.
BURGOYNE, J. R. & EATON, P. (2011). Contemporary techniques for detecting and identifying proteins susceptible to reversible thiol oxidation. Biochemical Society Transactions, 39(5), 1260-1267.
BURKITT, M. J. & WARDMAN, P. (2001). Cytochrome C is a potent catalyst of dichlorofluorescin oxidation: implications for the role of reactive oxygen species in apoptosis. Biochemical and Biophysical Research Communications, 282(1), 329-333.
BUYTAERT, E., DEWAELE, M. & AGOSTINIS, P. (2007). Molecular effectors of multiple cell death pathways initiated by photodynamic therapy. Biochimica et Biophysica Acta, 1776(1), 86-107.
CABISCOL, E., TAMARIT, J. & ROS, J. (2014). Protein carbonylation: proteomics, specificity and relevance to aging. Mass Spectrometry Reviews, 33(1), 21-48.
CALIN, M. A., DIACONEASA, A., SAVASTRU, D. & TAUTAN, M. (2011). Photosensitizers and light sources for photodynamic therapy of the Bowen's disease. Archives for Dermatological Research. Archiv fur Dermatologische Forschung, 303(3), 145-151.
CAMERINI, S., POLCI, M. L. & BACHI, A. (2005). Proteomics approaches to study the redox state of cysteine-containing proteins. Annali dell Istituto Superiore di Sanita, 41(4), 451-457.
CARS, O., HOGBERG, L. D., MURRAY, M., NORDBERG, O., SIVARAMAN, S., LUNDBORG, C. S., SO, A. D. & TOMSON, G. (2008). Meeting the challenge of antibiotic resistance. BMJ, 337, a1438.
CASTANO, A. P., DEMIDOVA, T. N. & HAMBLIN, M. R. (2005). Mechanisms in photodynamic therapy: part two-cellular signaling, cell metabolism and modes of cell death. Photodiagnosis and Photodynamic Therapy, 2(1), 1-23.
CASTANO, A. P., MROZ, P. & HAMBLIN, M. R. (2006). Photodynamic therapy and anti-tumour immunity. Nat Rev Cancer, 6(7), 535-545.
CHAN, W. H., YU, J. S. & YANG, S. D. (2000). Apoptotic signalling cascade in photosensitized human epidermal carcinoma A431 cells: involvement of singlet oxygen, c-Jun N-terminal kinase, caspase-3 and p21-activated kinase 2. Biochemical Journal, 351(Pt 1), 221-232.
CHANG, T. C., CHOU, W. Y. & CHANG, G. G. (2000). Protein oxidation and turnover. Journal of Biomedical Science, 7(5), 357-363.
CHAVAN, H., KHAN, M. M., TEGOS, G. & KRISHNAMURTHY, P. (2013). Efficient

purification and reconstitution of ATP binding cassette transporter B6 (ABCB6) for functional and structural studies. Journal of Biological Chemistry, 288(31), 22658-22669.
CHAVES, Y. N., TOREZAN, L. A., MAUTARI NIWA, A. B., SANCHES JUNIOR, J. A. & NETO, C. F. (2012). Pain in photodynamic therapy: mechanism of action and management strategies. Anais Brasileiros de Dermatologia, 87(4), 521-529.
CHEESEMAN, K. H. & SLATER, T. F. (1993). AN INTRODUCTION TO FREE-RADICAL BIOCHEMISTRY. British Medical Bulletin, 49(3), 481-493.
CHEN, B., POGUE, B. W., HOOPES, P. J. & HASAN, T. (2006). Vascular and cellular targeting for photodynamic therapy. Critical Reviews in Eukaryotic Gene Expression, 16(4), 279-305.
CHIARUGI, P. & BURICCHI, F. (2007). Protein tyrosine phosphorylation and reversible oxidation: two cross-talking posttranslation modifications. Antioxid Redox Signal, 9(1), 1-24.
CHIU, J. & DAWES, I. W. (2012). Redox control of cell proliferation. Trends in Cell Biology, 22(11), 592-601.
CHOI, B. H., RYOO, I. G., KANG, H. C. & KWAK, M. K. (2014). The sensitivity of cancer cells to pheophorbide a-based photodynamic therapy is enhanced by Nrf2 silencing. PLoS One, 9(9), e107158.
CHOI, M. S., YUN, S. J., BEOM, H. J., PARK, H. R. & LEE, J. B. (2010). Comparative study of the bactericidal effects of 5-aminolevulinic acid with blue and red light on Propionibacterium acnes. Journal of Dermatology.
CHOI, Y. J., PARK, J. W., WOO, J. H., KIM, Y. H., LEE, S. H., LEE, J. M. & KWON, T. K. (2002). Failure to activate caspase 3 in phorbol ester-resistant leukemia cells is associated with resistance to apoptotic cell death. Cancer Letters, 182(2), 183-191.
CHOUCHANI, E. T., JAMES, A. M., FEARNLEY, I. M., LILLEY, K. S. & MURPHY, M. P. (2011). Proteomic approaches to the characterization of protein thiol modification. Current Opinion in Chemical Biology, 15(1), 120-128.
CHOUDHARI, S. K., CHAUDHARY, M., GADBAIL, A. R., SHARMA, A. & TEKADE, S. (2014). Oxidative and antioxidative mechanisms in oral cancer and precancer: a review. Oral Oncology, 50(1), 10-18.
CHRISTENSEN, E. (2013). 5-Aminolevulinic acid based photodynamic therapy for basal cell carcinoma: a 10-years follow-up study. Stomatologija, 15(3), ii.
CIOLINO, H. P. & LEVINE, R. L. (1997). Modification of proteins in endothelial cell death during oxidative stress. Free Radical Biology and Medicine, 22(7), 1277-1282.
CIRCU, M. L. & AW, T. Y. (2010). Reactive oxygen species, cellular redox systems, and apoptosis. Free Radical Biology and Medicine, 48(6), 749-762.
CKLESS, K. (2014). Redox proteomics: from bench to bedside. Advances in Experimental Medicine and Biology, 806, 301-317.
COHEN, G. M. (1997). Caspases: the executioners of apoptosis. Biochemical Journal, 326, 1-16.
COUVERTIER, S. M., ZHOU, Y. & WEERAPANA, E. (2014). Chemical-proteomic strategies to investigate cysteine posttranslational modifications. Biochimica et Biophysica Acta, 1844(12), 2315-2330.
COX, G. S., BOBILLIER, C. & WHITTEN, D. G. (1982). PHOTO-OXIDATION AND

SINGLET OXYGEN SENSITIZATION BY PROTOPORPHYRIN-IX AND ITS PHOTO-OXIDATION PRODUCTS. Photochemistry and Photobiology, 36(4), 401-407.
COX, G. S. & WHITTEN, D. G. (1982). MECHANISMS FOR THE PHOTO-OXIDATION OF PROTOPORPHYRIN-IX IN SOLUTION. Journal of the American Chemical Society, 104(2), 516-521.
CROSS, J. V. & TEMPLETON, D. J. (2004). Thiol oxidation of cell signaling proteins: Controlling an apoptotic equilibrium. Journal of Cellular Biochemistry, 93(1), 104-111.
CUDDIHY, S. L., BATY, J. W., BROWN, K. K., WINTERBOURN, C. C. & HAMPTON, M. B. (2009). Proteomic detection of oxidized and reduced thiol proteins in cultured cells. Methods in Molecular Biology, 519, 363-375.
CURTIS, J. M., HAHN, W. S., LONG, E. K., BURRILL, J. S., ARRIAGA, E. A. & BERNLOHR, D. A. (2012). Protein carbonylation and metabolic control systems. Trends Endocrinol Metab, 23(8), 399-406.
DAI, T., FUCHS, B. B., COLEMAN, J. J., PRATES, R. A., ASTRAKAS, C., ST DENIS, T. G., RIBEIRO, M. S., MYLONAKIS, E., HAMBLIN, M. R. & TEGOS, G. P. (2012). Concepts and principles of photodynamic therapy as an alternative antifungal discovery platform. Front Microbiol, 3, 120.
DALLE-DONNE, I., ALDINI, G., CARINI, M., COLOMBO, R., ROSSI, R. & MILZANI, A. (2006a). Protein carbonylation, cellular dysfunction, and disease progression. J Cell Mol Med, 10(2), 389-406.
DALLE-DONNE, I., COLOMBO, G., GAGLIANO, N., COLOMBO, R., GIUSTARINI, D., ROSSI, R. & MILZANI, A. (2011). S-glutathiolation in life and death decisions of the cell. Free Radical Research, 45(1), 3-15.
DALLE-DONNE, I., ROSSI, R., COLOMBO, R., GIUSTARINI, D. & MILZANI, A. (2006b). Biomarkers of oxidative damage in human disease. Clinical Chemistry, 52(4), 601-623.
DALLE-DONNE, I., ROSSI, R., GIUSTARINI, D., COLOMBO, R. & MILZANI, A. (2007). S-glutathionylation in protein redox regulation. Free Radical Biology and Medicine, 43(6), 883-898.
DALLE-DONNE, I., ROSSI, R., GIUSTARINI, D., MILZANI, A. & COLOMBO, R. (2003). Protein carbonyl groups as biomarkers of oxidative stress. Clinica Chimica Acta, 329(1-2), 23-38.
DANIAL, N. N. & KORSMEYER, S. J. (2004). Cell death: critical control points. Cell, 116(2), 205-219.
DANSEN, T. B., SMITS, L. M., VAN TRIEST, M. H., DE KEIZER, P. L., VAN LEENEN, D., KOERKAMP, M. G., SZYPOWSKA, A., MEPPELINK, A., BRENKMAN, A. B., YODOI, J., HOLSTEGE, F. C. & BURGERING, B. M. (2009). Redox-sensitive cysteines bridge p300/CBP-mediated acetylation and FoxO4 activity. Nat Chem Biol, 5(9), 664-672.
DAVIES, M. J. (2003). Singlet oxygen-mediated damage to proteins and its consequences. Biochemical and Biophysical Research Communications, 305(3), 761-770.
DAVIES, M. J. (2005). The oxidative environment and protein damage. Biochimica et Biophysica Acta, 1703(2), 93-109.
DAVIES, M. J. & TRUSCOTT, R. J. (2001). Photo-oxidation of proteins and its role in

cataractogenesis. Journal of Photochemistry and Photobiology. B, Biology, 63(1-3), 114-125.
DE BRUIJN, H. S., CASAS, A. G., DI VENOSA, G., GANDARA, L., STERENBORG, H. J., BATLLE, A. & ROBINSON, D. J. (2013). Light fractionated ALA-PDT enhances therapeutic efficacy in vitro; the influence of PpIX concentration and illumination parameters. Photochem Photobiol Sci, 12(2), 241-245.
DE BRUIJN, H. S., VAN DER PLOEG - VAN DEN HEUVEL, A., STERENBORG, H. & ROBINSON, D. J. (2006). Fractionated illumination after topical application of 5-aminolevulinic acid on normal skin of hairless mice: The influence of the dark interval. Journal of Photochemistry and Photobiology B-Biology, 85(3), 184-190.
DI VENOSA, G., FUKUDA, H., BATLLE, A., MACROBERT, A. & CASAS, A. (2006). Photodynamic therapy: regulation of porphyrin synthesis and hydrolysis from ALA esters. Journal of Photochemistry and Photobiology. B, Biology, 83(2), 129-136.
DICKINSON, B. C. & CHANG, C. J. (2011). Chemistry and biology of reactive oxygen species in signaling or stress responses. Nat Chem Biol, 7(8), 504-511.
DOLMANS, D. E., FUKUMURA, D. & JAIN, R. K. (2003). Photodynamic therapy for cancer. Nat Rev Cancer, 3(5), 380-387.
DOUGHERTY, T. J., GRINDEY, G. B., FIEL, R., WEISHAUPT, K. R. & BOYLE, D. G. (1975). PHOTORADIATION THERAPY .2. CURE OF ANIMAL TUMORS WITH HEMATOPORPHYRIN AND LIGHT. Journal of the National Cancer Institute, 55(1), 115-121.
EKROLL, I. K., GEDERAAS, O. A., HELANDER, L., HJELDE, A., MELO, T. B. & JOHNSSON, A. (2011). Photo induced hexylaminolevulinate destruction of rat bladder cells AY-27. Photochem Photobiol Sci, 10(6), 1072-1079.
ELMORE, S. (2007). Apoptosis: a review of programmed cell death. Toxicologic Pathology, 35(4), 495-516.
ENK, C. D., NASEREDDIN, A., ALPER, R., DAN-GOOR, M., JAFFE, C. L. & WULF, H. C. (2014). Cutaneous leishmaniasis responds to daylight-activated photodynamic therapy: Proof-of-concept for a novel self-administered therapeutic modality. British Journal of Dermatology.
ERICSON, M. B., GRAPENGIESSER, S., GUDMUNDSON, F., WENNBERG, A. M., LARKO, O., MOAN, J. & ROSEN, A. (2003). A spectroscopic study of the photobleaching of protoporphyrin IX in solution. Lasers in Medical Science, 18(1), 56-62.
ERICSON, M. B., WENNBERG, A. M. & LARKO, O. (2008). Review of photodynamic therapy in actinic keratosis and basal cell carcinoma. Ther Clin Risk Manag, 4(1), 1-9.
FAI, D., ROMANO, I., FAI, C., CASSANO, N. & VENA, G. A. (2014). Daylight photodynamic therapy with methyl aminolaevulinate in patients with actinic keratoses: A preliminary experience in southern Italy. Giornale Italiano di Dermatologia e Venereologia.
FEDOROVA, M., BOLLINENI, R. C. & HOFFMANN, R. (2014). Protein carbonylation as a major hallmark of oxidative damage: update of analytical strategies. Mass Spectrometry Reviews, 33(2), 79-97.

FERRARIO, A., FISHER, A. M., RUCKER, N. & GOMER, C. J. (2005). Celecoxib and NS-398 enhance photodynamic therapy by increasing in vitro apoptosis and decreasing in vivo inflammatory and angiogenic factors. Cancer Research, 65(20), 9473-9478.
FERRARIO, A., RUCKER, N., WONG, S., LUNA, M. & GOMER, C. J. (2007). Survivin, a member of the inhibitor of apoptosis family, is induced by photodynamic therapy and is a target for improving treatment response. Cancer Research, 67(10), 4989-4995.
FESTJENS, N., VANDEN BERGHE, T. & VANDENABEELE, P. (2006). Necrosis, a well-orchestrated form of cell demise: signalling cascades, important mediators and concomitant immune response. Biochimica et Biophysica Acta, 1757(9-10), 1371-1387.
FOOTE, C. S. (1991). Definition of type I and type II photosensitized oxidation. Photochemistry and Photobiology, 54(5), 659.
FOTINOS, N., CAMPO, M. A., POPOWYCZ, F., GURNY, R. & LANGE, N. (2006). 5-Aminolevulinic acid derivatives in photomedicine: Characteristics, application and perspectives. Photochemistry and Photobiology, 82(4), 994-1015.
FROST, G. A., HALLIDAY, G. M. & DAMIAN, D. L. (2011). Photodynamic therapy-induced immunosuppression in humans is prevented by reducing the rate of light delivery. Journal of Investigative Dermatology, 131(4), 962-968.
FU, C., HU, J., LIU, T., AGO, T., SADOSHIMA, J. & LI, H. (2008). Quantitative analysis of redox-sensitive proteome with DIGE and ICAT. J Proteome Res, 7(9), 3789-3802.
FU, X. J., FANG, Y. & YAO, M. (2013). Antimicrobial photodynamic therapy for methicillin-resistant Staphylococcus aureus infection. Biomed Res Int, 2013, 159157.
FUENTES-PRIOR, P. & SALVESEN, G. S. (2004). The protein structures that shape caspase activity, specificity, activation and inhibition. Biochemical Journal, 384(Pt 2), 201-232.
FULDA, S. & KOGEL, D. (2015). Cell death by autophagy: emerging molecular mechanisms and implications for cancer therapy. Oncogene.
FURRE, I. E., MOLLER, M. T., SHAHZIDI, S., NESLAND, J. M. & PENG, Q. (2006). Involvement of both caspase-dependent and -independent pathways in apoptotic induction by hexaminolevulinate-mediated photodynamic therapy in human lymphoma cells. Apoptosis, 11(11), 2031-2042.
FURRE, I. E., SHAHZIDI, S., LUKSIENE, Z., MOLLER, M. T., BORGEN, E., MORGAN, J., TKACZ-STACHOWSKA, K., NESLAND, J. M. & PENG, Q. (2005). Targeting PBR by hexaminolevulinate-mediated photodynamic therapy induces apoptosis through translocation of apoptosis-inducing factor in human leukemia cells. Cancer Research, 65(23), 11051-11060.
GABBITA, S. P., ROBINSON, K. A., STEWART, C. A., FLOYD, R. A. & HENSLEY, K. (2000). Redox regulatory mechanisms of cellular signal transduction. Archives of Biochemistry and Biophysics, 376(1), 1-13.
GALLUZZI, L., BRAVO-SAN PEDRO, J. M., VITALE, I., AARONSON, S. A., ABRAMS, J. M., ADAM, D., ALNEMRI, E. S., ALTUCCI, L., ANDREWS, D., ANNICCHIARICO-PETRUZZELLI, M., BAEHRECKE, E. H., BAZAN, N. G., BERTRAND, M. J., BIANCHI, K., BLAGOSKLONNY, M. V.,

BLOMGREN, K., BORNER, C., BREDESEN, D. E., BRENNER, C., CAMPANELLA, M., CANDI, E., CECCONI, F., CHAN, F. K., CHANDEL, N. S., CHENG, E. H., CHIPUK, J. E., CIDLOWSKI, J. A., CIECHANOVER, A., DAWSON, T. M., DAWSON, V. L., DE LAURENZI, V., DE MARIA, R., DEBATIN, K. M., DI DANIELE, N., DIXIT, V. M., DYNLACHT, B. D., EL-DEIRY, W. S., FIMIA, G. M., FLAVELL, R. A., FULDA, S., GARRIDO, C., GOUGEON, M. L., GREEN, D. R., GRONEMEYER, H., HAJNOCZKY, G., HARDWICK, J. M., HENGARTNER, M. O., ICHIJO, H., JOSEPH, B., JOST, P. J., KAUFMANN, T., KEPP, O., KLIONSKY, D. J., KNIGHT, R. A., KUMAR, S., LEMASTERS, J. J., LEVINE, B., LINKERMANN, A., LIPTON, S. A., LOCKSHIN, R. A., LOPEZ-OTIN, C., LUGLI, E., MADEO, F., MALORNI, W., MARINE, J. C., MARTIN, S. J., MARTINOU, J. C., MEDEMA, J. P., MEIER, P., MELINO, S., MIZUSHIMA, N., MOLL, U., MUNOZ-PINEDO, C., NUNEZ, G., OBERST, A., PANARETAKIS, T., PENNINGER, J. M., PETER, M. E., PIACENTINI, M., PINTON, P., PREHN, J. H., PUTHALAKATH, H., RABINOVICH, G. A., RAVICHANDRAN, K. S., RIZZUTO, R., RODRIGUES, C. M., RUBINSZTEIN, D. C., RUDEL, T., SHI, Y., SIMON, H. U., STOCKWELL, B. R., SZABADKAI, G., TAIT, S. W., TANG, H. L., TAVERNARAKIS, N., TSUJIMOTO, Y., VANDEN BERGHE, T., VANDENABEELE, P., VILLUNGER, A., WAGNER, E. F., WALCZAK, H., WHITE, E., WOOD, W. G., YUAN, J., ZAKERI, Z., ZHIVOTOVSKY, B., MELINO, G. & KROEMER, G. (2014). Essential versus accessory aspects of cell death: recommendations of the NCCD 2015. Cell Death and Differentiation.

GARG, A. D., DUDEK, A. M., FERREIRA, G. B., VERFAILLIE, T., VANDENABEELE, P., KRYSKO, D. V., MATHIEU, C. & AGOSTINIS, P. (2013). ROS-induced autophagy in cancer cells assists in evasion from determinants of immunogenic cell death. Autophagy, 9(9), 1292-1307.

GARG, A. D., KRYSKO, D. V., VANDENABEELE, P. & AGOSTINIS, P. (2011). DAMPs and PDT-mediated photo-oxidative stress: exploring the unknown. Photochem Photobiol Sci, 10(5), 670-680.

GARG, A. D., NOWIS, D., GOLAB, J. & AGOSTINIS, P. (2010). Photodynamic therapy: illuminating the road from cell death towards anti-tumour immunity. Apoptosis, 15(9), 1050-1071.

GARTNER, C. A., ELIAS, J. E., BAKALARSKI, C. E. & GYGI, S. P. (2007). Catch-and-release reagents for broadscale quantitative proteomics analyses. J Proteome Res, 6(4), 1482-1491.

GEORGIOU, G. (2002). How to flip the (redox) switch. Cell, 111(5), 607-610.

GILES, G. I. (2006). The redox regulation of thiol dependent signaling pathways in cancer. Current Pharmaceutical Design, 12(34), 4427-4443.

GRANVILLE, D. J., CARTHY, C. M., JIANG, H., SHORE, G. C., MCMANUS, B. M. & HUNT, D. W. (1998). Rapid cytochrome c release, activation of caspases 3, 6, 7 and 8 followed by Bap31 cleavage in HeLa cells treated with photodynamic therapy. FEBS Letters, 437(1-2), 5-10.

GREEN, D. R. & REED, J. C. (1998). Mitochondria and apoptosis. Science, 281(5381), 1309-1312.

GROITL, B. & JAKOB, U. (2014). Thiol-based redox switches. Biochimica Et Biophysica Acta-Proteins and Proteomics, 1844(8), 1335-1343.

GUYON, L., FARINE, M. O., LESAGE, J. C., GEVAERT, A. M., SIMONIN, S., SCHMITT, C., COLLINET, P. & MORDON, S. (2014). Photodynamic therapy of ovarian cancer peritoneal metastasis with hexaminolevulinate: a toxicity study. Photodiagnosis Photodyn Ther, 11(3), 265-274.
HALESTRAP, A. P., WOODFIELD, K. Y. & CONNERN, C. P. (1997). Oxidative stress, thiol reagents, and membrane potential modulate the mitochondrial permeability transition by affecting nucleotide binding to the adenine nucleotide translocase. Journal of Biological Chemistry, 272(6), 3346-3354.
HALLDIN, C. B., GILLSTEDT, M., PAOLI, J., WENNBERG, A. M. & GONZALEZ, H. (2011). Predictors of pain associated with photodynamic therapy: a retrospective study of 658 treatments. Acta Dermato-Venereologica, 91(5), 545-551.
HALLDIN, C. B., GONZALEZ, H., WENNBERG, A. M. & LEPP, M. (2013). Patients' experiences of pain and pain relief during photodynamic therapy on actinic keratoses: an interview study. Acta Dermato-Venereologica, 93(4), 433-437.
HAMZA, I. & DAILEY, H. A. (2012). One ring to rule them all: trafficking of heme and heme synthesis intermediates in the metazoans. Biochimica et Biophysica Acta, 1823(9), 1617-1632.
HARRIS, F. & PIERPOINT, L. (2011). Photodynamic therapy based on 5-aminolevulinic acid and its use as an antimicrobial agent. Medicinal Research Reviews.
HAWKINS, C. L. & DAVIES, M. J. (2001). Generation and propagation of radical reactions on proteins. Biochimica et Biophysica Acta, 1504(2-3), 196-219.
HAWKINS, C. L., MORGAN, P. E. & DAVIES, M. J. (2009). Quantification of protein modification by oxidants. Free Radical Biology and Medicine, 46(8), 965-988.
HEINEMANN, I. U., JAHN, M. & JAHN, D. (2008). The biochemistry of heme biosynthesis. Archives of Biochemistry and Biophysics, 474(2), 238-251.
HELANDER, L., KROKAN, H. E., JOHNSSON, A., GEDERAAS, O. A. & PLAETZER, K. (2014). Red versus blue light illumination in hexyl 5-aminolevulinate photodynamic therapy: the influence of light color and irradiance on the treatment outcome in vitro. J Biomed Opt, 19(8), 088002.
HENGARTNER, M. O. (2000). The biochemistry of apoptosis. Nature, 407(6805), 770-776.
HENRIQUEZ, M., ARMISEN, R., STUTZIN, A. & QUEST, A. F. (2008). Cell death by necrosis, a regulated way to go. Curr Mol Med, 8(3), 187-206.
HERMAN, M. A., WEBBER, J., FROMM, D. & KESSEL, D. (1998). Hemodynamic effects of 5-aminolevulinic acid in humans. Journal of Photochemistry and Photobiology. B, Biology, 43(1), 61-65.
HILLEMANNS, P., EINSTEIN, M. H. & IVERSEN, O. E. (2015). Topical hexaminolevulinate photodynamic therapy for the treatment of persistent human papilloma virus infections and cervical intraepithelial neoplasia. Expert Opin Investig Drugs, 24(2), 273-281.
HILLEMANNS, P., GARCIA, F., PETRY, K. U., DVORAK, V., SADOVSKY, O., IVERSEN, O. E. & EINSTEIN, M. H. (2014a). A randomized study of hexaminolevulinate photodynamic therapy in patients with cervical intraepithelial neoplasia 1/2. American Journal of Obstetrics and Gynecology.
HILLEMANNS, P., PETRY, K. U., SOERGEL, P., COLLINET, P., ARDAENS, K.,

GALLWAS, J., LUYTEN, A. & DANNECKER, C. (2014b). Efficacy and safety of hexaminolevulinate photodynamic therapy in patients with low-grade cervical intraepithelial neoplasia. Lasers in Surgery and Medicine, 46(6), 456-461.
HOGG, P. J. (2003). Disulfide bonds as switches for protein function. Trends in Biochemical Sciences, 28(4), 210-214.
HOLMGREN, A., JOHANSSON, C., BERNDT, C., LONN, M. E., HUDEMANN, C. & LILLIG, C. H. (2005). Thiol redox control via thioredoxin and glutaredoxin systems. Biochemical Society Transactions, 33(Pt 6), 1375-1377.
HOLMSTROM, K. M. & FINKEL, T. (2014). Cellular mechanisms and physiological consequences of redox-dependent signalling. Nature Reviews Molecular Cell Biology, 15(6), 411-421.
HONIGSMANN, H. (2013). History of phototherapy in dermatology. Photochem Photobiol Sci, 12(1), 16-21.
HUANG, J., WANG, F., YE, M. & ZOU, H. (2014). Enrichment and separation techniques for large-scale proteomics analysis of the protein post-translational modifications. Journal of Chromatography A, 1372c, 1-17.
IINUMA, S., SCHOMACKER, K. T., WAGNIERES, G., RAJADHYAKSHA, M., BAMBERG, M., MOMMA, T. & HASAN, T. (1999). In vivo fluence rate and fractionation effects on tumor response and photobleaching: photodynamic therapy with two photosensitizers in an orthotopic rat tumor model. Cancer Research, 59(24), 6164-6170.
IKEDA, N., USUDA, J., KATO, H., ISHIZUMI, T., ICHINOSE, S., OTANI, K., HONDA, H., FURUKAWA, K., OKUNAKA, T. & TSUTSUI, H. (2011). New aspects of photodynamic therapy for central type early stage lung cancer. Lasers in Surgery and Medicine, 43(7), 749-754.
JACOB, C. (2011). Redox signalling via the cellular thiolstat. Biochemical Society Transactions, 39(5), 1247-1253.
JAIN, M. V., PACZULLA, A. M., KLONISCH, T., DIMGBA, F. N., RAO, S. B., ROBERG, K., SCHWEIZER, F., LENGERKE, C., DAVOODPOUR, P., PALICHARLA, V. R., MADDIKA, S. & LOS, M. (2013). Interconnections between apoptotic, autophagic and necrotic pathways: implications for cancer therapy development. J Cell Mol Med, 17(1), 12-29.
JANICKE, R. U., SPRENGART, M. L., WATI, M. R. & PORTER, A. G. (1998). Caspase-3 is required for DNA fragmentation and morphological changes associated with apoptosis. Journal of Biological Chemistry, 273(16), 9357-9360.
JANSSEN-HEININGER, Y. M., MOSSMAN, B. T., HEINTZ, N. H., FORMAN, H. J., KALYANARAMAN, B., FINKEL, T., STAMLER, J. S., RHEE, S. G. & VAN DER VLIET, A. (2008). Redox-based regulation of signal transduction: principles, pitfalls, and promises. Free Radical Biology and Medicine, 45(1), 1-17.
JUZENAS, P., JUZENIENE, A., IANI, V. & MOAN, J. (2009). Depth profile of protoporphyrin IX fluorescence in an amelanotic mouse melanoma model. Photochemistry and Photobiology, 85(3), 760-764.
JUZENIENE, A., NIELSEN, K. P. & MOAN, J. (2006). Biophysical aspects of photodynamic therapy. Journal of Environmental Pathology Toxicology and Oncology, 25(1-2), 7-28.
KARRER, S., KOHL, E., FEISE, K., HIEPE-WEGENER, D., LISCHNER, S.,

PHILIPP-DORMSTON, W., PODDA, M., PRAGER, W., WALKER, T. & SZEIMIES, R. M. (2013). Photodynamic therapy for skin rejuvenation: review and summary of the literature--results of a consensus conference of an expert group for aesthetic photodynamic therapy. J Dtsch Dermatol Ges, 11(2), 137-148.

KELLNER, C., BAURIEDL, S., HOLLSTEIN, S. & REINHOLD, U. (2014). Simulated daylight photodynamic therapy with BF-200 ALA for actinic keratosis: assessment of the efficacy and tolerability in a retrospective study. British Journal of Dermatology.

KELLY, J. F. (1975). Haematoporphyrins in the diagnosis and treatment of carcinoma of the bladder. Proceedings of the Royal Society of Medicine, 68(8), 527-528.

KELLY, J. F., SNELL, M. E. & BERENBAUM, M. C. (1975). Photodynamic destruction of human bladder carcinoma. British Journal of Cancer, 31(2), 237-244.

KENNEDY, J. C. & POTTIER, R. H. (1992). Endogenous protoporphyrin IX, a clinically useful photosensitizer for photodynamic therapy. Journal of Photochemistry and Photobiology. B, Biology, 14(4), 275-292.

KENNEDY, J. C., POTTIER, R. H. & PROSS, D. C. (1990). Photodynamic therapy with endogenous protoporphyrin IX: basic principles and present clinical experience. Journal of Photochemistry and Photobiology. B, Biology, 6(1-2), 143-148.

KERR, J. F., WYLLIE, A. H. & CURRIE, A. R. (1972). Apoptosis: a basic biological phenomenon with wide-ranging implications in tissue kinetics. British Journal of Cancer, 26(4), 239-257.

KESSEL, D. (2008). Promotion of PDT efficacy by a Bcl-2 antagonist. Photochemistry and Photobiology, 84(3), 809-814.

KESSEL, D., ANTOLOVICH, M. & SMITH, K. M. (2001). The role of the peripheral benzodiazepine receptor in the apoptotic response to photodynamic therapy. Photochemistry and Photobiology, 74(2), 346-349.

KESSEL, D. & LUO, Y. (1998). Mitochondrial photodamage and PDT-induced apoptosis. Journal of Photochemistry and Photobiology. B, Biology, 42(2), 89-95.

KESSEL, D. & REINERS, J. J., JR. (2007). Apoptosis and autophagy after mitochondrial or endoplasmic reticulum photodamage. Photochemistry and Photobiology, 83(5), 1024-1028.

KESSEL, D., VICENTE, M. G. & REINERS, J. J., JR. (2006). Initiation of apoptosis and autophagy by photodynamic therapy. Autophagy, 2(4), 289-290.

KESSEL, D. H., PRICE, M. & REINERS, J. J., JR. (2012). ATG7 deficiency suppresses apoptosis and cell death induced by lysosomal photodamage. Autophagy, 8(9), 1333-1341.

KHARKWAL, G. B., SHARMA, S. K., HUANG, Y. Y., DAI, T. & HAMBLIN, M. R. (2011). Photodynamic therapy for infections: clinical applications. Lasers in Surgery and Medicine, 43(7), 755-767.

KIESSLICH, T., HELANDER, L., ILLIG, R., OBERDANNER, C., WAGNER, A., LETTNER, H., JAKAB, M. & PLAETZER, K. (2014). Real-time analysis of endogenous protoporphyrin IX fluorescence from delta-aminolevulinic acid and its derivatives reveals distinct time- and dose-dependent characteristics in vitro.

J Biomed Opt, 19(8), 085007.
KIESSLICH, T., TORTIK, N., PICHLER, M., NEUREITER, D. & PLAETZER, K. (2013). Apoptosis in cancer cells induced by photodynamic treatment - a methodological approach. Journal of Porphyrins and Phthalocyanines, 17(3), 197-209.
KITAZUMI, I. & TSUKAHARA, M. (2011). Regulation of DNA fragmentation: the role of caspases and phosphorylation. FEBS J, 278(3), 427-441.
KJELDSTAD, B. & JOHNSSON, A. (1986). AN ACTION SPECTRUM FOR BLUE AND NEAR ULTRAVIOLET INACTIVATION OF PROPIONIBACTERIUM-ACNES - WITH EMPHASIS ON A POSSIBLE PORPHYRIN PHOTOSENSITIZATION. Photochemistry and Photobiology, 43(1), 67-70.
KOLODZIEJCZYK, A. (2015). 18 kDa translocator protein - implications in cell's functions. Postepy Hig Med Dosw (Online), 69(0), 34-50.
KORBELIK, M. & SUN, J. (2006). Photodynamic therapy-generated vaccine for cancer therapy. Cancer Immunology, Immunotherapy, 55(8), 900-909.
KORBELIK, M., ZHANG, W. & SEPAROVIC, D. (2011). Amplification of cancer cell apoptosis in photodynamic therapy-treated tumors by adjuvant ceramide analog LCL29. Lasers in Surgery and Medicine, 43(7), 614-620.
KRAMMER, B. (2001). Vascular effects of photodynamic therapy. Anticancer Research, 21(6b), 4271-4277.
KRAMMER, B. & PLAETZER, K. (2008). ALA and its clinical impact, from bench to bedside. Photochem Photobiol Sci, 7(3), 283-289.
KRAMMER, B. & UBERRIEGLER, K. (1996). In-vitro investigation of ALA-induced protoporphyrin IX. Journal of Photochemistry and Photobiology. B, Biology, 36(2), 121-126.
KRIEG, M. & WHITTEN, D. G. (1984). SELF-SENSITIZED PHOTO-OXIDATION OF PROTOPORPHYRIN-IX AND RELATED PORPHYRINS IN ERYTHROCYTE-GHOSTS AND MICROEMULSIONS - A NOVEL PHOTO-OXIDATION PATHWAY INVOLVING SINGLET OXYGEN. Journal of Photochemistry, 25(2-4), 235-252.
KROEMER, G., GALLUZZI, L. & BRENNER, C. (2007). Mitochondrial membrane permeabilization in cell death. Physiological Reviews, 87(1), 99-163.
KROEMER, G., GALLUZZI, L., VANDENABEELE, P., ABRAMS, J., ALNEMRI, E. S., BAEHRECKE, E. H., BLAGOSKLONNY, M. V., EL-DEIRY, W. S., GOLSTEIN, P., GREEN, D. R., HENGARTNER, M., KNIGHT, R. A., KUMAR, S., LIPTON, S. A., MALORNI, W., NUNEZ, G., PETER, M. E., TSCHOPP, J., YUAN, J., PIACENTINI, M., ZHIVOTOVSKY, B., MELINO, G. & NOMENCLATURE COMMITTEE ON CELL, D. (2009). Classification of cell death: recommendations of the Nomenclature Committee on Cell Death 2009. Cell Death and Differentiation, 16(1), 3-11.
KUROKAWA, M. & KORNBLUTH, S. (2009). Caspases and kinases in a death grip. Cell, 138(5), 838-854.
KUSHIBIKI, T., HIRASAWA, T., OKAWA, S. & ISHIHARA, M. (2013). Responses of cancer cells induced by photodynamic therapy. J Healthc Eng, 4(1), 87-108.
KWEE, J. K. (2014). A paradoxical chemoresistance and tumor suppressive role of antioxidant in solid cancer cells: a strange case of Dr. Jekyll and Mr. Hyde. Biomed Res Int, 2014, 209845.

KWITNIEWSKI, M., JUZENIENE, A., GLOSNICKA, R. & MOAN, J. (2008). Immunotherapy: a way to improve the therapeutic outcome of photodynamic therapy? Photochem Photobiol Sci, 7(9), 1011-1017.
LANDAR, A., OH, J. Y., GILES, N. M., ISOM, A., KIRK, M., BARNES, S. & DARLEY-USMAR, V. M. (2006). A sensitive method for the quantitative measurement of protein thiol modification in response to oxidative stress. Free Radical Biology and Medicine, 40(3), 459-468.
LANGE, N., JICHLINSKI, P., ZELLWEGER, M., FORRER, M., MARTI, A., GUILLOU, L., KUCERA, P., WAGNIERES, G. & VAN DEN BERGH, H. (1999). Photodetection of early human bladder cancer based on the fluorescence of 5-aminolaevulinic acid hexylester-induced protoporphyrin IX: a pilot study. British Journal of Cancer, 80(1-2), 185-193.
LAYER, G., REICHELT, J., JAHN, D. & HEINZ, D. W. (2010). Structure and function of enzymes in heme biosynthesis. Protein Science, 19(6), 1137-1161.
LEE, J., GIORDANO, S. & ZHANG, J. (2012). Autophagy, mitochondria and oxidative stress: cross-talk and redox signalling. Biochemical Journal, 441(2), 523-540.
LEE, J. Y., DIAZ, R. R., CHO, K. S., LIM, M. S., CHUNG, J. S., KIM, W. T., HAM, W. S. & CHOI, Y. D. (2013). Efficacy and safety of photodynamic therapy for recurrent, high grade nonmuscle invasive bladder cancer refractory or intolerant to bacille Calmette-Guerin immunotherapy. Journal of Urology, 190(4), 1192-1199.
LEE, S. Y., YOU, C. E. & PARK, M. Y. (2007). Blue and red light combination LED phototherapy for acne vulgaris in patients with skin phototype IV. Lasers in Surgery and Medicine, 39(2), 180-188.
LEE, Y. & BARON, E. D. (2011). Photodynamic therapy: current evidence and applications in dermatology. Seminars in Cutaneous Medicine and Surgery, 30(4), 199-209.
LEICHERT, L. I. & JAKOB, U. (2004). Protein thiol modifications visualized in vivo. PLoS Biol, 2(11), e333.
LENNON, S. V., MARTIN, S. J. & COTTER, T. G. (1991). Dose-dependent induction of apoptosis in human tumour cell lines by widely diverging stimuli. Cell Proliferation, 24(2), 203-214.
LEONARDUZZI, G., SOTTERO, B., TESTA, G., BIASI, F. & POLI, G. (2011). New insights into redox-modulated cell signaling. Current Pharmaceutical Design, 17(36), 3994-4006.
LESLIE, N. R., BENNETT, D., LINDSAY, Y. E., STEWART, H., GRAY, A. & DOWNES, C. P. (2003). Redox regulation of PI 3-kinase signalling via inactivation of PTEN. EMBO Journal, 22(20), 5501-5510.
LEVINE, R. L. (2002). Carbonyl modified proteins in cellular regulation, aging, and disease. Free Radical Biology and Medicine, 32(9), 790-796.
LEVINE, R. L. & STADTMAN, E. R. (2001). Oxidative modification of proteins during aging. Experimental Gerontology, 36(9), 1495-1502.
LI, X., GUO, H., TIAN, Q., ZHENG, G., HU, Y., FU, Y. & TAN, H. (2013). Effects of 5-aminolevulinic acid-mediated photodynamic therapy on antibiotic-resistant staphylococcal biofilm: an in vitro study. Journal of Surgical Research, 184(2), 1013-1021.
LIOU, G. Y. & STORZ, P. (2010). Reactive oxygen species in cancer. Free Radical

Research, 44(5), 479-496.
LOCKSHIN, R. A. & WILLIAMS, C. M. (1965). PROGRAMMED CELL DEATH--I. CYTOLOGY OF DEGENERATION IN THE INTERSEGMENTAL MUSCLES OF THE PERNYI SILKMOTH. Journal of Insect Physiology, 11, 123-133.
LOO, D. T. (2011). In situ detection of apoptosis by the TUNEL assay: an overview of techniques. Methods in Molecular Biology, 682, 3-13.
MALIK, Z. & DJALDETTI, M. (1979). 5-AMINOLEVULINIC ACID STIMULATION OF PORPHYRIN AND HEMOGLOBIN-SYNTHESIS BY UNINDUCED FRIEND-ERYTHROLEUKEMIC CELLS. Cell Differentiation, 8(3), 223-233.
MALIK, Z., HALBRECHT, I. & DJALDETTI, M. (1979). REGULATION OF HEMOGLOBIN-SYNTHESIS, IRON-METABOLISM, AND MATURATION OF FRIEND LEUKEMIC-CELLS BY 5-AMINO LEVULINIC ACID AND HEMIN. Differentiation, 13(2), 71-79.
MARINO, G., NISO-SANTANO, M., BAEHRECKE, E. H. & KROEMER, G. (2014). Self-consumption: the interplay of autophagy and apoptosis. Nature Reviews Molecular Cell Biology, 15(2), 81-94.
MARTI, A., JICHLINSKI, P., LANGE, N., BALLINI, J. P., GUILLOU, L., LEISINGER, H. J. & KUCERA, P. (2003). Comparison of aminolevulinic acid and hexylester aminolevulinate induced protoporphyrin IX distribution in human bladder cancer. Journal of Urology, 170(2 Pt 1), 428-432.
MAZIERE, J. C., SANTUS, R., MORLIERE, P., REYFTMANN, J. P., CANDIDE, C., MORA, L., SALMON, S., MAZIERE, C., GATT, S. & DUBERTRET, L. (1990). Cellular uptake and photosensitizing properties of anticancer porphyrins in cell membranes and low and high density lipoproteins. Journal of Photochemistry and Photobiology. B, Biology, 6(1-2), 61-68.
MESENHOLLER, M. & MATTHEWS, E. K. (2000). A key role for the mitochondrial benzodiazepine receptor in cellular photosensitisation with delta-aminolaevulinic acid. European Journal of Pharmacology, 406(2), 171-180.
MICHAEL R. HAMBLIN, P. M. (2008). Advances in photodynamic therapy. Basic, translational, and clinical., 1 edition.
MIDDELBURG, T. A., DE BRUIJN, H. S., VAN DER PLOEG-VAN DEN HEUVEL, A., NEUMANN, H. A. & ROBINSON, D. J. (2013). The effect of light fractionation with a 2-h dark interval on the efficacy of topical hexyl-aminolevulinate photodynamic therapy in normal mouse skin. Photodiagnosis Photodyn Ther, 10(4), 703-709.
MIDDELBURG, T. A., DE VIJLDER, H. C., DE BRUIJN, H. S., VAN DER PLOEG-VAN DEN HEUVEL, A., NEUMANN, H. A., DE HAAS, E. R. & ROBINSON, D. J. (2014). Topical photodynamic therapy using different porphyrin precursors leads to differences in vascular photosensitization and vascular damage in normal mouse skin. Photochemistry and Photobiology, 90(4), 896-902.
MINAEV, B., BARYSHNIKOV, G. & AGREN, H. (2014). Principles of phosphorescent organic light emitting devices. Phys Chem Chem Phys, 16(5), 1719-1758.
MOAN, J. (1990). ON THE DIFFUSION LENGTH OF SINGLET OXYGEN IN CELLS AND TISSUES. Journal of Photochemistry and Photobiology B-Biology, 6(3), 343-347.

MOAN, J. & BERG, K. (1991). The photodegradation of porphyrins in cells can be used to estimate the lifetime of singlet oxygen. Photochemistry and Photobiology, 53(4), 549-553.
MOAN, J. & JUZENAS, P. (2006). Singlet oxygen in photosensitization. Journal of Environmental Pathology, Toxicology and Oncology, 25(1-2), 29-50.
MOAN, J. & PENG, Q. (2003). An outline of the hundred-year history of PDT. Anticancer Research, 23(5A), 3591-3600.
MOAN, J., STRECKYTE, G., BAGDONAS, S., BECH, O. & BERG, K. (1997). Photobleaching of protoporphyrin IX in cells incubated with 5-aminolevulinic acid. International Journal of Cancer, 70(1), 90-97.
MORAN, L. K., GUTTERIDGE, J. M. & QUINLAN, G. J. (2001). Thiols in cellular redox signalling and control. Current Medicinal Chemistry, 8(7), 763-772.
MOVASSAGH, M. & FOO, R. S. (2008). Simplified apoptotic cascades. Heart Fail Rev, 13(2), 111-119.
MROZ, P. & HAMBLIN, M. R. (2011). The immunosuppressive side of PDT. Photochem Photobiol Sci.
MROZ, P., HUANG, Y.-Y. & HAMBLIN, M. R. (2010). Photodynamic Therapy for Cancer and Activation of Immune Response. In Biophotonics and Immune Responses V, vol. 7565 (ed. W. R. Chen).
MROZ, P., YAROSLAVSKY, A., KHARKWAL, G. B. & HAMBLIN, M. R. (2011). Cell Death Pathways in Photodynamic Therapy of Cancer. Cancers, 3(2), 2516-2539.
NA, H. K. & SURH, Y. J. (2006). Transcriptional regulation via cysteine thiol modification: a novel molecular strategy for chemoprevention and cytoprotection. Molecular Carcinogenesis, 45(6), 368-380.
NAGATA, S. (1997). Apoptosis by death factor. Cell, 88(3), 355-365.
NAVARRO-YEPES, J., BURNS, M., ANANDHAN, A., KHALIMONCHUK, O., DEL RAZO, L. M., QUINTANILLA-VEGA, B., PAPPA, A., PANAYIOTIDIS, M. I. & FRANCO, R. (2014). Oxidative Stress, Redox Signaling, and Autophagy: Cell Death Versus Survival. Antioxidants & Redox Signaling, 21(1), 66-85.
NEITTAANMAKI-PERTTU, N., KARPPINEN, T. T., GRONROOS, M., TANI, T. T. & SNELLMAN, E. (2014). Daylight photodynamic therapy for actinic keratoses: a randomized double-blinded nonsponsored prospective study comparing 5-aminolaevulinic acid nanoemulsion (BF-200) with methyl-5-aminolaevulinate. British Journal of Dermatology, 171(5), 1172-1180.
NIKOLETOPOULOU, V., MARKAKI, M., PALIKARAS, K. & TAVERNARAKIS, N. (2013). Crosstalk between apoptosis, necrosis and autophagy. Biochimica et Biophysica Acta, 1833(12), 3448-3459.
NOOTHETI, P. K. & GOLDMAN, M. P. (2007). Aminolevulinic acid-photodynamic therapy for photorejuvenation. Dermatologic Clinics, 25(1), 35-45.
NYSTROM, T. (2005). Role of oxidative carbonylation in protein quality control and senescence. EMBO Journal, 24(7), 1311-1317.
OBERDANNER, C. B., PLAETZER, K., KIESSLICH, T. & KRAMMER, B. (2005). Photodynamic treatment with fractionated light decreases production of reactive oxygen species and cytotoxicity in vitro via regeneration of glutathione. Photochemistry and Photobiology, 81(3), 609-613.
OCHSNER, M. (1997). Photophysical and photobiological processes in the

photodynamic therapy of tumours. Journal of Photochemistry and Photobiology. B, Biology, 39(1), 1-18.
OKTYABRSKY, O. N. & SMIRNOVA, G. V. (2007). Redox regulation of cellular functions. Biochemistry, 72(2), 132-145.
OLEINICK, N. L., MORRIS, R. L. & BELICHENKO, I. (2002). The role of apoptosis in response to photodynamic therapy: what, where, why, and how. Photochem Photobiol Sci, 1(1), 1-21.
OOSTERLINCK, W., SOLSONA, E., VAN DER MEIJDEN, A. P., SYLVESTER, R., BOHLE, A., RINTALA, E. & LOBEL, B. (2004). EAU guidelines on diagnosis and treatment of upper urinary tract transitional cell carcinoma. European Urology, 46(2), 147-154.
ORRENIUS, S., GOGVADZE, V. & ZHIVOTOVSKY, B. (2007). Mitochondrial oxidative stress: implications for cell death. Annual Review of Pharmacology and Toxicology, 47, 143-183.
OTT, M., GOGVADZE, V., ORRENIUS, S. & ZHIVOTOVSKY, B. (2007). Mitochondria, oxidative stress and cell death. Apoptosis, 12(5), 913-922.
PAGET, M. S. & BUTTNER, M. J. (2003). Thiol-based regulatory switches. Annual Review of Genetics, 37, 91-121.
PANIS, C. (2014). Unraveling Oxidation-Induced Modifications in Proteins by Proteomics. In Advances in Protein Chemistry and Structural Biology, Vol 94, vol. 94 (ed. R. Donev), pp. 19-38. San Diego: Elsevier Academic Press Inc.
PANZARINI, E., INGUSCIO, V. & DINI, L. (2013). Immunogenic cell death: can it be exploited in PhotoDynamic Therapy for cancer? Biomed Res Int, 2013, 482160.
PARRI, M. & CHIARUGI, P. (2013). Redox molecular machines involved in tumor progression. Antioxid Redox Signal, 19(15), 1828-1845.
PAULECH, J., SOLIS, N., EDWARDS, A. V., PUCKERIDGE, M., WHITE, M. Y. & CORDWELL, S. J. (2013). Large-scale capture of peptides containing reversibly oxidized cysteines by thiol-disulfide exchange applied to the myocardial redox proteome. Analytical Chemistry, 85(7), 3774-3780.
PEREZ-PEREZ, L., GARCIA-GAVIN, J. & GILABERTE, Y. (2014). Daylight-mediated photodynamic therapy in Spain: advantages and disadvantages. Actas Dermo-Sifiliograficas, 105(7), 663-674.
PEROTTI, C., FUKUDA, H., DIVENOSA, G., MACROBERT, A. J., BATLLE, A. & CASAS, A. (2004). Porphyrin synthesis from ALA derivatives for photodynamic therapy. In vitro and in vivo studies. British Journal of Cancer, 90(8), 1660-1665.
PINEDA-MOLINA, E., KLATT, P., VAZQUEZ, J., MARINA, A., GARCIA DE LACOBA, M., PEREZ-SALA, D. & LAMAS, S. (2001). Glutathionylation of the p50 subunit of NF-kappaB: a mechanism for redox-induced inhibition of DNA binding. Biochemistry, 40(47), 14134-14142.
PIZOVA, K., TOMANKOVA, K., DASKOVA, A., BINDER, S., BAJGAR, R. & KOLAROVA, H. (2012). Photodynamic therapy for enhancing antitumour immunity. Biomed Pap Med Fac Univ Palacky Olomouc Czech Repub, 156(2), 93-102.
PLAETZER, K., KIESSLICH, T., KRAMMER, B. & HAMMERL, P. (2002). Characterization of the cell death modes and the associated changes in cellular energy supply in response to AlPcS4-PDT. Photochem Photobiol Sci, 1(3), 172-

177.
PLAETZER, K., KIESSLICH, T., OBERDANNER, C. B. & KRAMMER, B. (2005). Apoptosis following photodynamic tumor therapy: induction, mechanisms and detection. Current Pharmaceutical Design, 11(9), 1151-1165.
PLAETZER, K., KRAMMER, B., BERLANDA, J., BERR, F. & KIESSLICH, T. (2008). Photophysics and photochemistry of photodynamic therapy: fundamental aspects. Lasers Med Sci.
PLAETZER, K., KRAMMER, B., BERLANDA, J., BERR, F. & KIESSLICH, T. (2009). Photophysics and photochemistry of photodynamic therapy: fundamental aspects. Lasers Med Sci, 24(2), 259-268.
POOLE, L. B. (2014). The basics of thiols and cysteines in redox biology and chemistry. Free Radical Biology and Medicine.
POPOV, D. (2014). Protein S-glutathionylation: from current basics to targeted modifications. Archives of Physiology and Biochemistry, 120(4), 123-130.
PORTER, A. G. & JANICKE, R. U. (1999). Emerging roles of caspase-3 in apoptosis. Cell Death and Differentiation, 6(2), 99-104.
POTTIER, R. H., CHOW, Y. F., LAPLANTE, J. P., TRUSCOTT, T. G., KENNEDY, J. C. & BEINER, L. A. (1986). Non-invasive technique for obtaining fluorescence excitation and emission spectra in vivo. Photochemistry and Photobiology, 44(5), 679-687.
RAHAL, A., KUMAR, A., SINGH, V., YADAV, B., TIWARI, R., CHAKRABORTY, S. & DHAMA, K. (2014). Oxidative Stress, Prooxidants, and Antioxidants: The Interplay. Biomed Research International, 19.
RANINGA, P. V., TRAPANI, G. D. & TONISSEN, K. F. (2014). Cross Talk between Two Antioxidant Systems, Thioredoxin and DJ-1: Consequences for Cancer. Oncoscience, 1(1), 95-110.
RAVIKUMAR, B., FUTTER, M., JAHREISS, L., KOROLCHUK, V. I., LICHTENBERG, M., LUO, S., MASSEY, D. C., MENZIES, F. M., NARAYANAN, U., RENNA, M., JIMENEZ-SANCHEZ, M., SARKAR, S., UNDERWOOD, B., WINSLOW, A. & RUBINSZTEIN, D. C. (2009). Mammalian macroautophagy at a glance. Journal of Cell Science, 122(Pt 11), 1707-1711.
RAY, P. D., HUANG, B. W. & TSUJI, Y. (2012). Reactive oxygen species (ROS) homeostasis and redox regulation in cellular signaling. Cellular Signalling.
RECZEK, C. R. & CHANDEL, N. S. (2014). ROS-dependent signal transduction. Current Opinion in Cell Biology, 33c, 8-13.
REDMOND, R. W. & GAMLIN, J. N. (1999). A compilation of singlet oxygen yields from biologically relevant molecules. Photochemistry and Photobiology, 70(4), 391-475.
REINERS, J. J., JR., AGOSTINIS, P., BERG, K., OLEINICK, N. L. & KESSEL, D. (2010). Assessing autophagy in the context of photodynamic therapy. Autophagy, 6(1), 7-18.
RIEDERER, B. M. (2009). Oxidation Proteomics: The Role of Thiol Modifications. Current Proteomics, 6(1), 51-62.
RKEIN, A. M. & OZOG, D. M. (2014). Photodynamic therapy. Dermatologic Clinics, 32(3), 415-425, x.
ROCK, K. L. & KONO, H. (2008). The inflammatory response to cell death. Annu Rev

Pathol, 3, 99-126.
ROGERS, L. K., LEINWEBER, B. L. & SMITH, C. V. (2006). Detection of reversible protein thiol modifications in tissues. Analytical Biochemistry, 358(2), 171-184.
RUBEL, D. M., SPELMAN, L., MURRELL, D. F., SEE, J. A., HEWITT, D., FOLEY, P., BOSC, C., KEROB, D., KERROUCHE, N., WULF, H. C. & SHUMACK, S. (2014). Daylight photodynamic therapy with methyl aminolevulinate cream as a convenient, similarly effective, nearly painless alternative to conventional photodynamic therapy in actinic keratosis treatment: a randomized controlled trial. British Journal of Dermatology, 171(5), 1164-1171.
SALVESEN, G. S. & RIEDL, S. J. (2008). Caspase mechanisms. Advances in Experimental Medicine and Biology, 615, 13-23.
SANOVIC, R., KRAMMER, B., GRUMBOECK, S. & VERWANGER, T. (2009). Time-resolved gene expression profiling of human squamous cell carcinoma cells during the apoptosis process induced by photodynamic treatment with hypericin. International Journal of Oncology, 35(4), 921-939.
SARISSKY, M., LAVICKA, J., KOCANOVA, S., SULLA, I., MIROSSAY, A., MISKOVSKY, P., GAJDOS, M., MOJZIS, J. & MIROSSAY, L. (2005). Diazepam enhances hypericin-induced photocytotoxicity and apoptosis in human glioblastoma cells. Neoplasma, 52(4), 352-359.
SARKAR, S., FLOTO, R. A., BERGER, Z., IMARISIO, S., CORDENIER, A., PASCO, M., COOK, L. J. & RUBINSZTEIN, D. C. (2005). Lithium induces autophagy by inhibiting inositol monophosphatase. Journal of Cell Biology, 170(7), 1101-1111.
SCHIEBER, M. & CHANDEL, N. S. (2014). ROS Function in Redox Signaling and Oxidative Stress. Current Biology, 24(10), R453-R462.
SCOLARO, L. M., CASTRICIANO, M., ROMEO, A., PATANE, S., CEFALI, E. & ALLEGRINI, M. (2002). Aggregation behavior of protoporphyrin IX in aqueous solutions: Clear evidence of vesicle formation. Journal of Physical Chemistry B, 106(10), 2453-2459.
SENGE, M. O. & RADOMSKI, M. W. (2013). Platelets, photosensitizers, and PDT. Photodiagnosis Photodyn Ther, 10(1), 1-16.
SHALINI, S., DORSTYN, L., DAWAR, S. & KUMAR, S. (2014). Old, new and emerging functions of caspases. Cell Death and Differentiation.
SHIMIZU, S., KANASEKI, T., MIZUSHIMA, N., MIZUTA, T., ARAKAWA-KOBAYASHI, S., THOMPSON, C. B. & TSUJIMOTO, Y. (2004). Role of Bcl-2 family proteins in a non-apoptotic programmed cell death dependent on autophagy genes. Nat Cell Biol, 6(12), 1221-1228.
SIES, H. (1993). Strategies of antioxidant defense. European Journal of Biochemistry, 215(2), 213-219.
SIES, H. (2015). Oxidative stress: a concept in redox biology and medicine. Redox Biol, 4c, 180-183.
SINHA, K., DAS, J., PAL, P. B. & SIL, P. C. (2013). Oxidative stress: the mitochondria-dependent and mitochondria-independent pathways of apoptosis. Archives of Toxicology, 87(7), 1157-1180.
STADTMAN, E. R. & LEVINE, R. L. (2000). Protein oxidation. Annals of the New York Academy of Sciences, 899, 191-208.
STADTMAN, E. R. & LEVINE, R. L. (2002). Why have cells selected reactive oxygen

species to regulate cell signaling events? Human and Experimental Toxicology, 21(2), 83.
STEINBAUER, J. M., SCHREML, S., BABILAS, P., ZEMAN, F., KARRER, S., LANDTHALER, M. & SZEIMIES, R. M. (2009). Topical photodynamic therapy with porphyrin precursors-assessment of treatment-associated pain in a retrospective study. Photochem Photobiol Sci, 8(8), 1111-1116.
TAUB, A. F. (2004). Photodynamic therapy for the treatment of acne: a pilot study. J Drugs Dermatol, 3(6 Suppl), S10-14.
THAMSEN, M. & JAKOB, U. (2011). The redoxome: Proteomic analysis of cellular redox networks. Current Opinion in Chemical Biology, 15(1), 113-119.
THOMPSON, C. B. (1995). APOPTOSIS IN THE PATHOGENESIS AND TREATMENT OF DISEASE. Science, 267(5203), 1456-1462.
THORNBERRY, N. A. & LAZEBNIK, Y. (1998). Caspases: Enemies within. Science, 281(5381), 1312-1316.
TOGSVERD-BO, K., IDORN, L. W., PHILIPSEN, P. A., WULF, H. C. & HAEDERSDAL, M. (2012a). Protoporphyrin IX formation and photobleaching in different layers of normal human skin: methyl- and hexylaminolevulinate and different light sources. Experimental Dermatology, 21(10), 745-750.
TOGSVERD-BO, K., LEI, U., ERLENDSSON, A. M., TAUDORF, E. H., PHILIPSEN, P. A., WULF, H. C., SKOV, L. & HAEDERSDAL, M. (2014). Combination of ablative fractional laser and daylight-mediated photodynamic therapy for actinic keratosis in organ transplant recipients - a randomized controlled trial. British Journal of Dermatology.
TOGSVERD-BO, K., LERCHE, C. M., PHILIPSEN, P. A., HAEDERSDAL, M. & WULF, H. C. (2013). Artificial daylight photodynamic therapy with "non-inflammatory" doses of hexyl aminolevulinate only marginally delays SCC development in UV-exposed hairless mice. Photochem Photobiol Sci, 12(12), 2130-2136.
TOGSVERD-BO, K., LERCHE, C. M., PHILIPSEN, P. A., POULSEN, T., WULF, H. C. & HAEDERSDAL, M. (2012b). Porphyrin biodistribution in UV-exposed murine skin after methyl- and hexyl-aminolevulinate incubation. Experimental Dermatology, 21(4), 260-264.
TOGSVERD-BO, K., LERCHE, C. M., POULSEN, T., WULF, H. C. & HAEDERSDAL, M. (2010). Photodynamic therapy with topical methyl- and hexylaminolevulinate for prophylaxis and treatment of UV-induced SCC in hairless mice. Experimental Dermatology, 19(8), e166-172.
TORNVALL, U. (2010). Pinpointing oxidative modifications in proteins-recent advances in analytical methods. Analytical Methods, 2(11), 1638-1650.
TRACHOOTHAM, D., LU, W., OGASAWARA, M. A., NILSA, R. D. & HUANG, P. (2008). Redox regulation of cell survival. Antioxid Redox Signal, 10(8), 1343-1374.
TSUJIMOTO, Y. & SHIMIZU, S. (2005a). Another way to die: autophagic programmed cell death. Cell Death and Differentiation, 12 Suppl 2, 1528-1534.
TSUJIMOTO, Y. & SHIMIZU, S. (2005b). Another way to die: autophagic programmed cell death. Cell Death and Differentiation, 12 Suppl 2, 1528-1534.
TUNSTALL, R. G., BARNETT, A. A., SCHOFIELD, J., GRIFFITHS, J., VERNON, D. I., BROWN, S. B. & ROBERTS, D. J. (2002). Porphyrin accumulation induced

by 5-aminolaevulinic acid esters in tumour cells growing in vitro and in vivo. British Journal of Cancer, 87(2), 246-250.
VALENTINE, R. M., IBBOTSON, S. H., WOOD, K., BROWN, C. T. & MOSELEY, H. (2013). Modelling fluorescence in clinical photodynamic therapy. Photochem Photobiol Sci, 12(1), 203-213.
VAN DER MEIJDEN, A. P., SYLVESTER, R., OOSTERLINCK, W., SOLSONA, E., BOEHLE, A., LOBEL, B. & RINTALA, E. (2005). EAU guidelines on the diagnosis and treatment of urothelial carcinoma in situ. European Urology, 48(3), 363-371.
VANDEN BERGHE, T., LINKERMANN, A., JOUAN-LANHOUET, S., WALCZAK, H. & VANDENABEELE, P. (2014). Regulated necrosis: the expanding network of non-apoptotic cell death pathways. Nature Reviews Molecular Cell Biology, 15(2), 134-146.
VERWANGER, T., SANOVIC, R., ABERGER, F., FRISCHAUF, A. M. & KRAMMER, B. (2002). Gene expression pattern following photodynamic treatment of the carcinoma cell line A-431 analysed by cDNA arrays. International Journal of Oncology, 21(6), 1353-1359.
WANG, H., XU, Y., SHI, J., GAO, X. & GENG, L. (2015). Photodynamic therapy in the treatment of basal cell carcinoma: a systematic review and meta-analysis. Photodermatology, Photoimmunology and Photomedicine, 31(1), 44-53.
WANG, X., RYTER, S. W., DAI, C., TANG, Z. L., WATKINS, S. C., YIN, X. M., SONG, R. & CHOI, A. M. (2003). Necrotic cell death in response to oxidant stress involves the activation of the apoptogenic caspase-8/bid pathway. Journal of Biological Chemistry, 278(31), 29184-29191.
WANG, Y., YANG, J. & YI, J. (2012). Redox sensing by proteins: oxidative modifications on cysteines and the consequent events. Antioxid Redox Signal, 16(7), 649-657.
WARDMAN, P. (2007). Fluorescent and luminescent probes for measurement of oxidative and nitrosative species in cells and tissues: progress, pitfalls, and prospects. Free Radical Biology and Medicine, 43(7), 995-1022.
WARDMAN, P. (2008). Use of the dichlorofluorescein assay to measure "reactive oxygen species". Radiation Research, 170(3), 406-407.
WARREN, C. B., KARAI, L. J., VIDIMOS, A. & MAYTIN, E. V. (2009). Pain associated with aminolevulinic acid-photodynamic therapy of skin disease. Journal of the American Academy of Dermatology, 61(6), 1033-1043.
WEBBER, J., KESSEL, D. & FROMM, D. (1997a). Plasma levels of protoporphyrin IX in humans after oral administration of 5-aminolevulinic acid. Journal of Photochemistry and Photobiology. B, Biology, 37(1-2), 151-153.
WEBBER, J., KESSEL, D. & FROMM, D. (1997b). Side effects and photosensitization of human tissues after aminolevulinic acid. Journal of Surgical Research, 68(1), 31-37.
WEI, Y., PATTINGRE, S., SINHA, S., BASSIK, M. & LEVINE, B. (2008). JNK1-mediated phosphorylation of Bcl-2 regulates starvation-induced autophagy. Molecular Cell, 30(6), 678-688.
WEISHAUPT, K. R., GOMER, C. J. & DOUGHERTY, T. J. (1976). Identification of singlet oxygen as the cytotoxic agent in photoinactivation of a murine tumor. Cancer Research, 36(7 PT 1), 2326-2329.

WEYERGANG, A., BERG, K., KAALHUS, O., PENG, Q. & SELBO, P. K. (2009). Photodynamic therapy targets the mTOR signaling network in vitro and in vivo. Mol Pharm, 6(1), 255-264.
WIEGELL, S. R., FABRICIUS, S., GNIADECKA, M., STENDER, I. M., BERNE, B., KROON, S., ANDERSEN, B. L., MORK, C., SANDBERG, C., IBLER, K. S., JEMEC, G. B., BROCKS, K. M., PHILIPSEN, P. A., HEYDENREICH, J., HAEDERSDAL, M. & WULF, H. C. (2012a). Daylight-mediated photodynamic therapy of moderate to thick actinic keratoses of the face and scalp: a randomized multicentre study. British Journal of Dermatology, 166(6), 1327-1332.
WIEGELL, S. R., FABRICIUS, S., HEYDENREICH, J., ENK, C. D., ROSSO, S., BAUMLER, W., BALDURSSON, B. T. & WULF, H. C. (2013a). Weather conditions and daylight-mediated photodynamic therapy: protoporphyrin IX-weighted daylight doses measured in six geographical locations. British Journal of Dermatology, 168(1), 186-191.
WIEGELL, S. R., SKODT, V. & WULF, H. C. (2013b). Daylight-mediated photodynamic therapy of basal cell carcinomas - an explorative study. Journal of the European Academy of Dermatology and Venereology.
WIEGELL, S. R., WULF, H. C., SZEIMIES, R. M., BASSET-SEGUIN, N., BISSONNETTE, R., GERRITSEN, M. J., GILABERTE, Y., CALZAVARA-PINTON, P., MORTON, C. A., SIDOROFF, A. & BRAATHEN, L. R. (2012b). Daylight photodynamic therapy for actinic keratosis: an international consensus: International Society for Photodynamic Therapy in Dermatology. Journal of the European Academy of Dermatology and Venereology, 26(6), 673-679.
WINTERBOURN, C. C. & HAMPTON, M. B. (2008). Thiol chemistry and specificity in redox signaling. Free Radical Biology and Medicine, 45(5), 549-561.
WOUTERS, M. A., IISMAA, S., FAN, S. W. & HAWORTH, N. L. (2011). Thiol-based redox signalling: rust never sleeps. International Journal of Biochemistry and Cell Biology, 43(8), 1079-1085.
YING-YING HUANG, P. M., AND MICHAEL R. HAMBLIN. (2009). Basic Photomedicine. In Photobiological Sciences Online (KC Smith, ed.). American Society for Photobiology, http://www.photobiology.info/
YOO, J. O. & HA, K. S. (2012). New insights into the mechanisms for photodynamic therapy-induced cancer cell death. Int Rev Cell Mol Biol, 295, 139-174.
YU, L., ALVA, A., SU, H., DUTT, P., FREUNDT, E., WELSH, S., BAEHRECKE, E. H. & LENARDO, M. J. (2004). Regulation of an ATG7-beclin 1 program of autophagic cell death by caspase-8. Science, 304(5676), 1500-1502.
YUNG, A., STABLES, G. I., FERNANDEZ, C., WILLIAMS, J., BOJAR, R. A. & GOULDEN, V. (2007). Microbiological effect of photodynamic therapy (PDT) in healthy volunteers: a comparative study using methyl aminolaevulinate and hexyl aminolaevulinate cream. Clinical and Experimental Dermatology, 32(6), 716-721.
ZHANG, J. (2015). Teaching the basics of autophagy and mitophagy to redox biologists-Mechanisms and experimental approaches. Redox Biol, 4c, 242-259.
ZHAO, B. Z. & HE, Y. Y. (2010). Recent advances in the prevention and treatment of skin cancer using photodynamic therapy. Expert Review of Anticancer Therapy, 10(11), 1797-1809.

ZIMMERMANN, K. C. & GREEN, D. R. (2001). How cells die: apoptosis pathways. Journal of Allergy and Clinical Immunology, 108(4 Suppl), S99-103.

Papers I-IV

Paper I

Photochemical & Photobiological Sciences

Dynamic Article Links

Cite this: *Photochem. Photobiol. Sci.*, 2011, **10**, 1072

www.rsc.org/pps

PAPER

Photo induced hexylaminolevulinate destruction of rat bladder cells AY-27

Ingvild Kinn Ekroll,[a,c] Odrun Arna Gederaas,[b] Linda Helander,[b] Astrid Hjelde,[a] Thor Bernt Melø[c] and Anders Johnsson[c]

Received 30th December 2010, Accepted 21st February 2011
DOI: 10.1039/c0pp00393j

Photodynamic therapy (PDT) is of increasing interest as a relevant treatment for human urinary bladder cancer. In the present experiments, the rat bladder transitional carcinoma cell line AY-27 was used as a model to study cell destruction mechanisms induced by PDT. Red LED light (630 nm) PDT with hexylaminolevulinate (HAL) as precursor for the photosensitizer protoporphyrin IX (PpIX) was used in treatment of the cells. Flow cytometry with fluorescent markers annexin V, propidium iodide and YO-PRO-1, as well as MTT assay and confocal microscopy, were used to map cell inactivation after PDT. Dark toxicity of HAL alone was low in these procedures and LD_{50} (24 h, MTT assay) was approximately 1.6 J cm^{-2} for standard red light (LED) irradiation (36 mW cm^{-2}). Measurements done 1 h after HAL-PDT showed a maximum apoptotic level of about 10% at 6 J cm^{-2}, however the dominating mode of cell death was necrosis. Forward light scattering indicated an increase in cell size at low doses, possibly due to necrosis. Survival curves had a dual-slope shape, a fit to single hit, multi-target approximation gave a parameter estimate of $n = 10$ and D_0 about 2.6 J cm^{-2}. Replacing continuous light with fractionated light delivery (45 s light/60 s darkness) did not affect the treatment outcome.

Introduction

Urinary bladder cancer causes more than 130 000 deaths every year worldwide[1] and 90% of these are caused by transitional cell carcinomas (TCC).[2] The strongest known risk factor for bladder cancer is smoking, probably due to the high content of carcinogenic acrylamides in cigarette smoke.[2] Treatment of bladder cancer depends on the stage of the disease, the type of cancer, and the patient's age and general health condition. So far, treatment options have included surgery, endoscopic resection, chemotherapy and immunotherapy.

Photodynamic therapy (PDT) is a potential treatment modality. This therapy is based on photochemical reactions between a photosensitizer and light, where the photosensitizer accumulated in cancerous tissue is activated by light of an appropriate wavelength.[3–5] This can in turn induce cell death by the production of singlet oxygen and other reactive oxygen species.[6–8] Since cancer cells have higher accumulation of photosensitizer than normal cells, PDT is a selective treatment modality.[9–12] In order to achieve curative treatment with PDT, it is crucial to find the correct balance between the drug and light doses to destroy cancerous tissue and avoid irreparable damage to surrounding tissues.[13]

[a]*Department of Circulation and Medical Imaging, Norwegian University of Science and Technology (NTNU), MTFS Pb 8909, 7489, Trondheim, Norway. E-mail: ingvild.k.ekroll@ntnu.no*
[b]*Department of Cancer Research and Molecular Medicine, NTNU, Laboratory Center, N-7006, Trondheim, Norway*
[c]*Department of Physics, NTNU, N-7491, Trondheim, Norway*

Optical spectroscopy is commonly used for both detection and diagnosis in medicine,[14] including the case of superficial urinary bladder cancer. In a recently published paper by Larsen *et al.*,[13] *in vivo* reflectance and fluorescence spectroscopy were used on a rat bladder cancer model. The combined methods can, for example, predict the therapeutic efficacy of PDT. In the present report, different spectroscopy techniques and fluorescent markers will, likewise, be used to study cancer cell destruction mechanisms.

Superficial urinary bladder cancer is potentially well suited for effective treatment by PDT because the bladder is easily accessible for both intravesical instillation and illumination. Intravesical instillation, *i.e.* direct injection of a photosensitizer into the bladder, has been shown to cause less damage to normal tissue than intravenous injection, while still giving the same PDT efficacy.[15] A number of photosensitizers are currently available for PDT, among which 5-aminolevulinic acid (ALA) is often preferred. ALA derivates such as hexylaminolevulinate (HAL) can increase the efficacy of PDT due to higher lipophilicity, which leads to better penetration into cells and ultimately a higher concentration of the acting photosensitizer protoporphyrin IX (PpIX).[16–18] Moreover, HAL is approved for bladder cancer diagnosis in the EU, EEA countries and the US.[19]

PDT can induce apoptotic and necrotic cell death both *in vivo* and *in vitro*. The balance between apoptosis and necrosis following different doses of ALA-based PDT is not fully understood, but may be important in a clinical setting. The aim of this work is to study the modes of cell death following hexylaminolevulinate mediated photodynamic therapy (HAL-PDT) of rat bladder

transitional cell carcinoma cells (AY-27), a cell type of clinical interest and relevance. The cell destruction processes are investigated using flow cytometry, confocal microscopy and measurements of mitochondrial activity. These techniques are also used to study effects of fractionated or pulsed light delivery *versus* continuous light delivery in the PDT process.

Materials and methods

Chemicals

RPMI-1640 medium, L-glutamine, foetal bovine serum (FBS), phosphate buffered saline (PBS), Accutase, Hepes and 3-(4,5 dimethylthiazol-2-yl)-2,5-diphenyl-tetrazoliumbromide (MTT) were obtained from Sigma Chemicals Co. (St. Louis, MO, USA). Annexin V Fluos (annexin V) was purchased from Roche Applied Science (Basel, Switzerland). Quinolinium, 4-(3-methyl-2[^{3}H]-benzoxazolylidene)methyl)-1–1(3-(triethylammonio)propyl) diiodide (YO-PRO-1) were from Invitrogen (Carlsbad, CA, USA). Propidium iodide (PI) was obtained from Fluka (Sigma Aldrich Schweiz, Buchs SG, Switzerland) when used with annexin V and from Invitrogen when used with YO-PRO-1. Hexylaminolevulinate (HAL) was kindly provided by Photocure ASA (Oslo, Norway).

Cell culture

The AY-27 cell line, generously supplied by Professor Steven H. Selman (Medical College of Ohio, Toledo, USA), was grown in RPMI-1640 medium supplemented with 10% v/v FBS and L-glutamine (for a total of 0.7 mM), referred to as regular cultivation medium. The cells were kept in a Binder incubator at 37 °C with a humidified atmosphere containing 5% CO_2 and subcultured twice a week.

Light conditions

An Aktilite lamp, model CL-128 from Photocure ASA, Oslo, Norway, (peak intensity at 630 nm) was used as red light (LED) source in the photodynamic experiments. The lamp was situated in a room holding a temperature of 37 °C. A housing with a diffuser plate (white glass) on top gave a constant irradiance over an area larger that two Petri dishes. When establishing the first survival curve the irradiance was 36 ± 1 mW cm^{-2}, in the subsequent experiments the irradiance was lowered to 20 ± 1 mW cm^{-2} (LI-COR quantum detector, type LI-190SA, LI-COR Corporate Offices, Lincoln, Nebraska, USA). Photosensitized cells and light sensitive solutions were shielded from light with aluminium foil and the experiments were performed with minimum of ambient light.

Photodynamic experiments

Cells were seeded in Petri dishes (r = 3 cm, Nunc) two days prior to PDT at a density of 1.5 × 10^4 per ml, giving a total of 6 × 10^5 cells ideally, using regular cultivation medium. On the day of the PDT experiment, a sterile stock solution of HAL (10 mM) was made by dissolving HAL powder in PBS (pH 6.0) before sterile filtration (22 μM). The cells were washed once with PBS and incubated (37 °C) in medium containing HAL (10 μM, 3.5 h) but without FBS. Serum free medium was used during HAL-incubation to avoid porphyrin excretion to the culture medium.[20] The cells were washed twice with PBS, before red light exposure (630 nm, 20 mW cm^{-2}). After irradiation, cells were incubated (1 h or 24) in regular cultivation medium before further measurements. Samples receiving neither HAL nor light served as controls. Samples receiving only HAL constituted dark toxicity controls. Controls were otherwise handled as treated samples.

Mitochondrial dehydrogenase assay (MTT assay)

The MTT assay measures mitochondrial activity, and is commonly used to make dose-response curves when cell survival is studied.[21] Cells were washed with PBS 1 h or 24 h after PDT and further incubated (1 h, 37 °C) in freshly prepared MTT-solution (2 ml, 0.5 mg ml^{-1} MTT in regular cultivation medium, 37 °C). The MTT-solution was carefully removed before isopropanol (2 ml) was added, and the dishes were placed on a plate shaker (500 rpm, 30 min) for solubilization of the formazan crystals. The colored solution was transferred to tubes and centrifuged (1500 rpm, 5 min). The absorbance of the crystal free supernatant at 588 nm was measured immediately using a Shimadzu UV-160 IPC spectrophotometer for deciding the cell survival after treatment.

Flow cytometry using the fluorescence markers annexin V and propidium iodide

Cells were detached using accutase (3.3 ml, 15-20 min, 37 °C) 1 h or 24 h after PDT. Accutase was used for cell detachment since trypsin has been reported to be inefficient after PDT.[22–23] The detached cells were centrifuged (3 min, 1300 rpm) and incubated in Hepes buffer (12 min, 20 °C) containing annexin V and PI according to the manufacturer's instructions. The samples were immediately analyzed in a flow cytometer (LSR-1, Becton Dickinson) with a 488 nm excitation laser line. Fluorescence emission was evaluated by a 530 ± 28 nm band pass filter for annexin V and a 660 ± 13 nm band pass filter for PI. The resulting data was exported to the software MATLAB (The MathWorks Inc.) for processing.

Flow cytometry using the fluorescent markers YO-PRO-1 and propidium iodide

Cells were detached using accutase (3.3 ml, 15–20 min, 37 °C) 1 h or 24 h after PDT and centrifuged (3 min, 1300 rpm). Further handling was performed on ice. Cell pellets were resuspended in PBS (1 ml, 4 °C) containing YO-PRO-1 (1 μl) and PI (1 μl) and incubated on ice (25 min). The samples were immediately analyzed in a flow cytometer as described in the previous subsection.

Confocal microscopy

Both pairs of fluorochromes were also used in confocal microscopy studies (Leica TCS SP5, with objective Universal 50.0 × 0.80) of the AY-27 cells after HAL-PDT. A 458 nm laser line was used for excitation, and fluorescence emission was evaluated by band pass filters of 500–550 nm and 650–720 nm for annexin V/YO-PRO-1 and PI respectively.

Comparison of continuous and fractionated light delivery

The LD_{50} dose determined 1 h post PDT (5.4 J cm^{-2}, 270 s) was used in the comparative studies. Fractionated light (630 nm,

20 mW cm^{-2}) was delivered in intervals of 45 s separated by 60 s of darkness. Both the MTT assay and flow cytometry with the Annexin V/PI assay were used to analyze the treatment outcome.

Hit theory

The experimental survival curve was fitted (least square method) to a single hit, multi-target model.[24] The following expression was thus applied:

$$S_f = 1 - (1 - \exp(-D/D_0))^n,$$

where S_f is the fraction of surviving cells when the dose D is administered. The calculated dose D_0 and the exponent n give estimates related to the shoulder width of the survival curve and the number of targets necessary to hit before killing a cell, respectively.

Statistical analysis

Data are presented as the mean value from all experiments ± standard deviation (SD).

Results

Cell survival

Exposing cells incubated with HAL (10 μM, 3.5 h) to red light (630 nm, 36 mW cm^{-2}) produced the survival curve in Fig. 1. Incubation with HAL but with no irradiation resulted only in about 5% reduction of the cell survival, thus showing that the dark toxicity of HAL was small in the applied procedure. Cell survival without HAL incubation was measured in separate experiments and was not influenced by illumination alone. The LD_{50} value was approximately 1.6 J cm^{-2} in the applied procedure and was achieved after 45 s of irradiation. An irradiation period of 2.5 min equals the LD_{70}. During relatively high light doses (10–32 J cm^{-2}) approximately 99% of the cells were killed. There were no further changes in survival values when the dose was increased up to 64 J cm^{-2} (data not shown).

The images in Fig. 2 are results from confocal microscopy experiments 1 h post HAL-PDT where the fluorescent markers annexin V (green color) and PI (red color) were used on controls (a) and PDT treated cells (b). The density plots (Fig. 2c and 2d) from flow cytometry clearly show a distinctly different pattern for the two situations. Cells classified as viable are in the lower left corner showing little fluorescence from neither annexin V nor PI, indicating an intact cell membrane with no display of phosphatidyl serine (PS) on the outer membrane surface. Apoptotic cells are clustered in lower right corner displaying high annexin V fluorescence and little PI fluorescence, indicating an intact cell membrane with PS present on the outer surface which is an early hallmark of apoptosis. Necrotic and late apoptotic cells are in the upper right corner displaying high fluorescence of both annexin V and PI, indicating a permeable outer membrane.

The fraction of viable cells was determined for different treatment doses, seen in Fig. 3a. The determinations were done 1 h after treatment with HAL (10 μM, 3.5 h) and light (630 nm, 20 mW cm^{-2}). The shape of the survival curve allowed a comparison with PDT survival curves reported for other cell types. Using hit theory, we could get an estimate of the number of targets in the cells. The parameters in the model were found by fitting the single hit, multi target equation to the data points obtained, using a nonlinear least squares approach. When all data points were considered to have equal weight, the estimated parameter values were (with 95% confidence intervals) n = 10 (0, 21) and D_0 = 2 (1.1, 2.6) J cm^{-2}. The result is depicted in Fig. 3b.

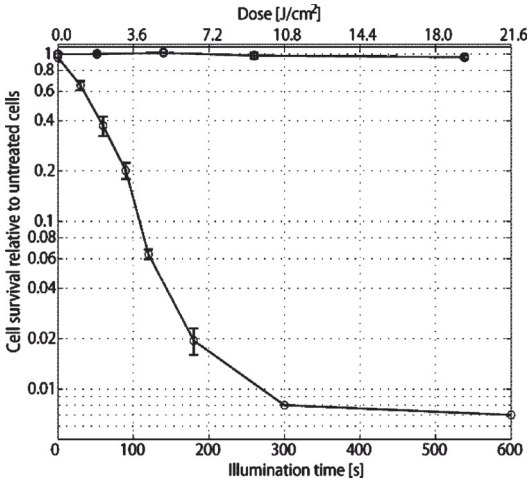

Fig. 1 Cell survival as measured by MTT 24 h after red light (630 nm, 36 mW cm^{-2}) HAL-PDT (10 μM, 3.5 h). Without incubation with HAL, the cells show no response to illumination.

Modes of cell death

The apoptotic fraction (green curve in Fig. 3a) is nearly constant (4%) in dose range between 0–4 J cm^{-2} and settles at its maximum level (10%) already at 6 J cm^{-2}. The necrotic fraction (blue curve) rises rapidly with increasing dose, reaching 10% at 2.4 J cm^{-2}, 50% at about 6 J cm^{-2}. In samples having received doses higher than 12 J cm^{-2}, necrosis dominates, as more than 80% of the cell population is classified as necrotic. In this dose range, the viable fraction is decreased below 5%.

The curves seen in Fig. 3 were based on flow cytometry experiments performed with annexin V/PI assay. HAL-PDT outcome studied by an alternative fluorochrome pair, YO-PRO-1 and PI, gave similar results in the tested dose range (data not shown).

Forward light scattering

The forward light scattering (FSC) was also recorded during all flow cytometry experiments. Averaged FSC signals are plotted in Fig. 4 as a function of light dose. For small doses the FSC signal increases with increasing dose until it passes its maximum at 2.5 J cm^{-2} after which the signal strongly decreases. The FSC signal is usually interpreted as a coarse measure of the size of the cells, and will be discussed later.

Continuous *vs.* fractionated light delivery.

The LD_{50} dose determined by flow cytometry 1 h after treatment was 5.4 J cm^{-2} with continuous light delivery, corresponding to 270 s of light exposure (630 nm, 20 mW cm^{-2}). As seen in

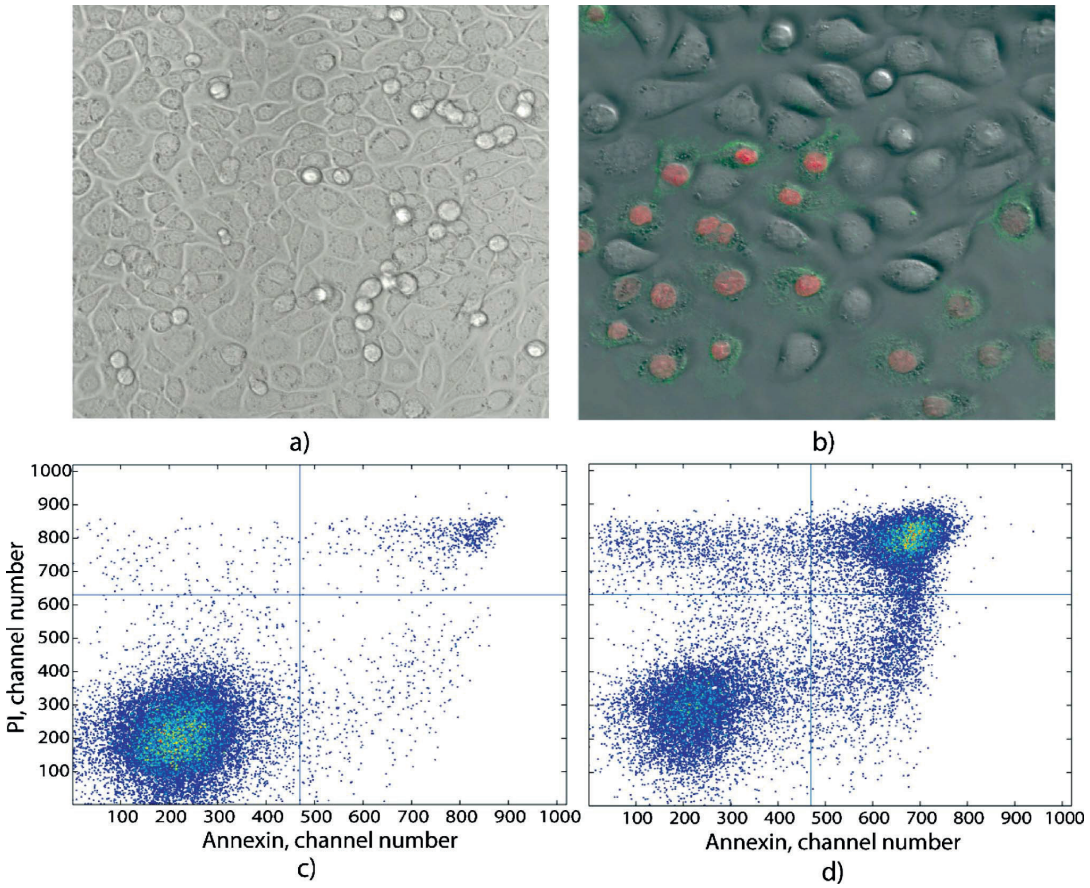

Fig. 2 Confocal microscopy image of untreated AY-27 cells (a). Confocal microscopy image 1 h after red light (630 nm, 20 mW cm^{-2}) HAL-PDT (10 μM, 3.5 h), using a light dose of 1.8 J cm^{-2} (b). Density plot from flow cytometry of untreated cells (c). Density plot from flow cytometry 1 h post red light HAL-PDT, using a light dose of 6 J cm^{-2} (d). The colours in density plots range from blue (lower density) towards red (higher density).

Fig. 5a, exposing the cells to the same dose, but in light/dark intervals of 45/60 s produced the same amount of cell death as the continuous light delivery. The MTT assay confirmed the results from flow cytometry; there was no difference between fractionated and continuous light delivery. Measurements of cell survival 24 h after treatment also produced identical results for continuous and fractionated light delivery in both experimental methods (MTT assay giving lower survival fractions in both cases). No changes in the amount of apoptosis or necrosis were observed when the two modes of light delivery were compared (Fig. 5b).

Discussion

Cell survival

Specific studies on bladder cancer cells are scarce and for the AY-27 cells only a limited amount of PDT data is reported. But the LD_{50} (24 h, MTT assay) value of 1.6 J cm^{-2} obtained in this study using red light at 630 nm with 36 mW cm^{-2} can be compared to experiments using 435 nm blue light at 13 mW cm^{-2} (unpublished data). An LD_{50} value of 0.4 J cm^{-2} was obtained after blue light HAL-PDT of AY-27 cells. Since absorption by PpIX is about 3 times more efficient at 435 nm than 630 nm (in ethanol solution) these two LD_{50} values seem to correspond well. Both LD_{50} values are found using the MTT assay 24 h after identical treatment protocols. This indicates that the difference in dose response curves for blue and red light HAL-PDT on AY-27 cells is accounted for by the difference in PpIX absorption of red and blue light alone.

Two survival curves are presented in this work (Fig. 1 and red curve in Fig. 3a). While the curve obtained from flow cytometry one hour after treatment clearly have a shoulder region, this is not as evident in the curve obtained from MTT measurements 24 h after treatment. The survival curve established with the MTT assay using an irradiance of 36 mW cm^{-2} was very steep, and it was therefore chosen to operate with a lower irradiance (20 mW cm^{-2}) in the subsequent flow cytometry experiments.

The flow cytometry procedure requires suitable detachment of cells after treatment with PDT, ideally not influencing the outcome.

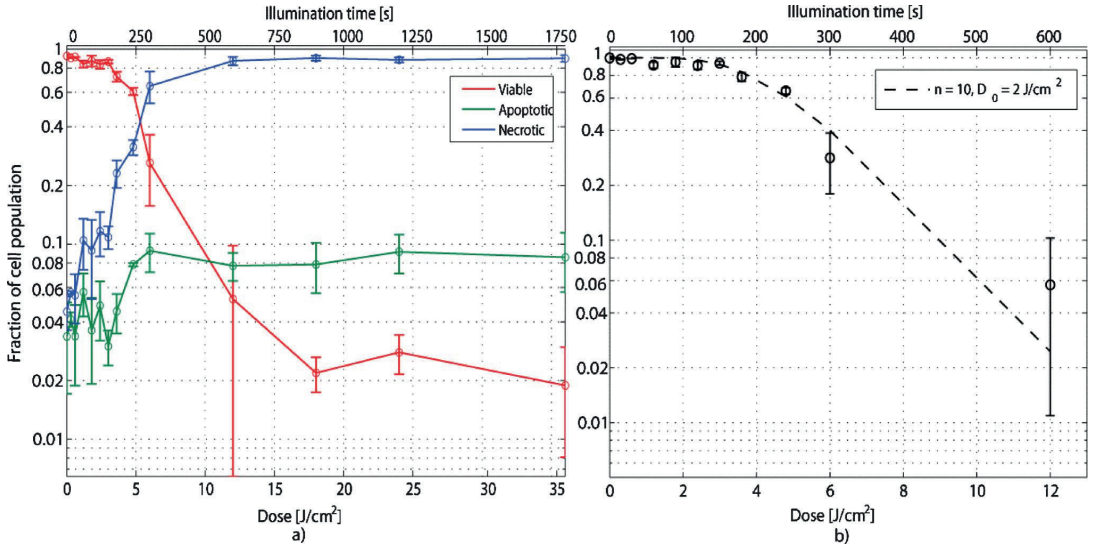

Fig. 3 Cell death 1 h post red light (630 nm, 20 mW cm^{-2}) HAL-PDT (10 μM, 3.5 h), measured by flow cytometry with annexin V/PI assay (a). Fitted survival curve (b). Circles represent mean values ± SD from four separate experiments, each with two parallels.

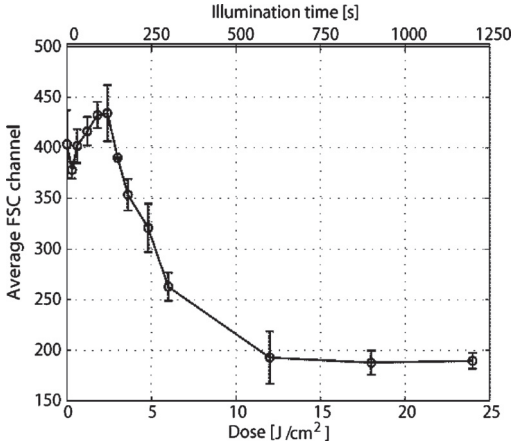

Fig. 4 Average FSC signal from flow cytometry measurements as a function of light dose, 1 h post red light (630 nm, 20 mW cm^{-2}) HAL-PDT (10 μM, 3.5 h).

Accutase was used in this step, as trypsin has been reported to be inefficient after PDT[22–23] (confirmed in our experiments, data not shown). By using accutase, problems with inhomogeneous cell suspension were avoided, as were membrane damages resulting from the detachment process. As depicted in Fig. 2c, as much as 90% of the untreated cell population displayed low annexin V and PI fluorescence after detachment using accutase, indicating that the experimental technique resulted in a low level of falsely fluorescing cells.

From these latter experiments, it is seen that the cells' response to HAL-PDT consisted of two dose regions, below and above 3.5 J cm^{-2}, where doses higher than the threshold gave an increased treatment response. Doses higher than 15 J cm^{-2} did not further increase cell destruction. By using the lower irradiance in the studies of apoptosis and necrosis, a larger accuracy in the measurements was achieved. Still, in the areas of rapid decrease in the survival curve (region around 300 s of light exposure), the experimental error is larger than in other areas where the response to HAL-PDT is slower. This may influence the parameter estimation used with the single hit, multi target equation, and could be the reason why the estimated values of n and D_0 have such large confidence intervals.

The number of hits needed for inactivation of a cell was estimated in a straight forward calculation to be to $n = 10$. This value might seem high but it is in accordance with values obtained by Juzeniene *et al.*,[25] who found a value of $n = 11$ for ALA-PDT (0.5 mM, 22 h, 420 nm, 10 ± 0.5 mW cm^{-2}) performed on WiDr cells. However, the detailed PDT mechanisms might well be different in different cell lines and under all circumstances the fitting of a survival curve is strongly dependent on the weight ascribed to the data points.

The results must therefore be regarded as indicative and only pointing at a multi-target process during ALA based PDT.

Modes of cell death

The flow cytometry results using the annexin V/PI assay indicate that necrosis is the most important mode of cell death following our HAL-PDT protocol. The outcome of photodynamic therapy on cells does, however, depend on experimental factors,[26] such as photosensitizer concentration, and on internal factors, such as cellular metabolic state.[8] It also differs markedly between cell lines. For example, Noodt *et al.*[27] found that V79 Chinese hamster fibroblasts went into apoptosis after PDT while WiDr cells were killed *via* necrosis. It is therefore difficult to compare the amount of apoptosis and necrosis after treatment *between* different cell lines.

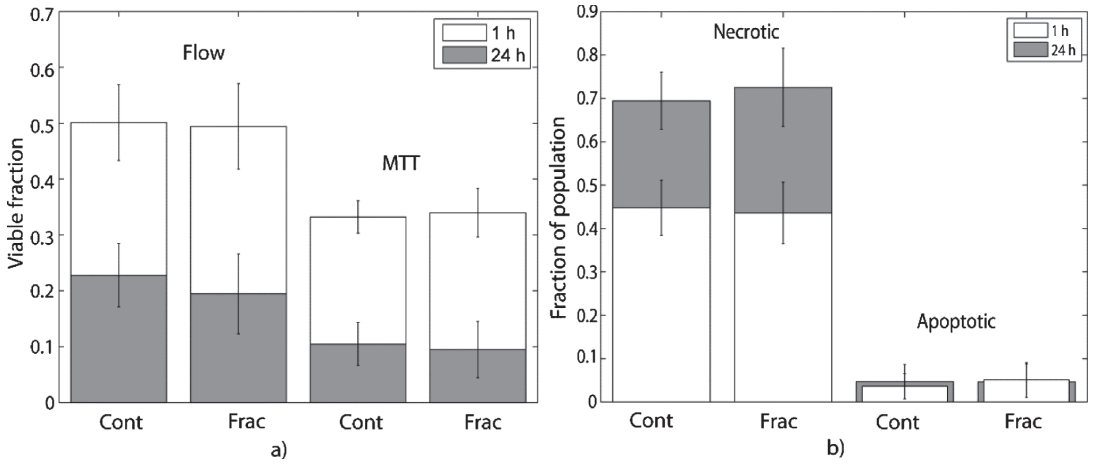

Fig. 5 Viable fraction (1 h and 24 h) after red light (630 nm, 20 mW cm^{-2}, 5.4 J cm^{-2}) HAL-PDT (10 μM, 3.5 h) measured by flow cytometry with annexin V/PI assay. MTT assay measurements (1 h and 24 h) after the same treatment are also shown (a). Apoptotic and necrotic fraction (1 h and 24 h) after red light HAL-PDT, measured by flow cytometry with annexin V/PI assay. The bars represent mean values ± SD of 3 independent and identical experiments, each done in duplicates.

As PpIX is usually assumed to be formed in the mitochondria of eukaryotic cells,[28] it seems reasonable that HAL-PDT could lead to mitochondria-mediated apoptosis.[29–30] This was, however, not reflected in the present experiments. One reason could be diffusion of the produced PpIX to other intracellular membrane sites such as lysosomes or the plasma membrane. Fluorescence microscopy studies of AY-27 cells incubated with HAL (1 μM) for 3 h and 4 h showed an accumulation of the lipophilic photosensitizer PpIX in the plasma membrane.[31] In our experiments an incubation time of 3.5 h was used, which could accordingly lead to a sensitized plasma membrane. Sufficient oxidative damage to molecules in the plasma membrane will induce necrosis by loss of the membrane integrity.[32] Also, the apparent increase in cell size at low doses, as indicated by the increased forward scattering in flow cytometry experiments (Fig. 5), points at necrosis as the dominant path after HAL-PDT under our conditions.

Experimental techniques may lead to hasty conclusions though. The results presented in Fig. 5 clearly indicate some uncertainties in the measurements of apoptotic levels. There is a discrepancy between the apoptotic level and the mitochondrial activity measured 1 h and 24 h after treatment. In Fig. 5a, between 1 h and 24 h after treatment, the mitochondrial activity is dramatically reduced. According to Plaetzer *et al.*[33] the temporal dynamics of the mitochondrial activity reflects the apoptotic fraction of cells after $AlPcS_4$-PDT on A431 cells when measured 3 and 24 h after treatment. If we assume this to hold also in our case, a large fraction of the cell population was apoptotic 1 h after treatment and had entered necrosis 24 h after treatment. Inspecting Fig. 5b, we also see that the necrotic fraction as measured by flow cytometry is strongly increased (25%) between 1 and 24 h. Still, the increase in the necrotic fraction is *not* reflected in a decrease of the apoptotic fraction, which would be expected as cells progress from early to late apoptosis. These observations indicate that the flow cytometry method may have underestimated the level of apoptosis after treatment, and that more robust methods should be used to further investigate the modes of cell death after HAL-PDT. The measurement point of 1 h after treatment was chosen to avoid confusing late apoptotic cells with necrotic cells, assuming late apoptosis does not occur within 1 h of HAL-PDT, while necrosis does. The latter seemed to be justified as 50% of the cell population was classified as necrotic 1 h after incubation with HAL and illumination equivalent to 5.4 J cm^{-2}. Still, estimates of the time from cell damage to death by necrosis vary, and according to Kramer *et al.*[34] necrosis may not occur before 2–4 h after the triggering injury.

The effects of fractionated radiation

We found *no* difference in PDT efficacy between fractionated and continuous light delivery. The surviving fractions measured by MTT and flow cytometry after identical PDT protocols were different, the MTT always providing a lower estimate of cell survival. However, since the two techniques use different mechanisms to measure cell viability, the difference in cell survival between the two light regimes is more important than the exact values of cell survival measured by a single technique.

The usefulness of fractionated exposure is debated in the literature. The different light protocols used, the different cell types tested *etc.*, provide reasons for discrepancies. It has been reported that fractionation is *not* successful in clinical ALA-PDT of hamster melanoma.[35] On the other hand, Curnow *et al.*[36–37] reported more necrosis when light treatment was interrupted by a single dark period in rat colon cells. De Bruijn *et al.*[38] also report improvement of nodular tumor response when interrupting light delivery with a substantial dark period.

The treatment regime used in the present experiments consisted of light/dark/light intervals of 45 s/60 s/45 s until the LD_{50} (1 h, flow cytometry) dose of 5.4 J cm^{-2} was reached and the procedure was adapted from Oberdanner *et al.*.[39] They reported a decrease in the PDT efficacy with this light regime, using the lipophilic

photosensitizer hypericin on the adherent A431 cell line. Their experimental conditions resemble those in our system, where the lipophilic photosensitizer PpIX is used in photodynamic therapy of the adherent AY-27 cell line. Oberdanner *et al.* suggested that fractionated photodynamic therapy *in vitro* is influenced by recycling of the ROS quenching GSH (reduced glutathione) by glutathione reductase during the dark intervals, which could explain the increase in survival levels when fractionated irradiation was used. Although we did not see a similar difference between the different modes of light delivery, it would be of interest to test for possible effect on survival rate from addition of BCNU, an inhibitor of glutathione reductase, to the cultivation medium before irradiation. Decreased survival would then support a participation of the GSH system.

Conclusion

The present data on AY-27 cells facilitate the choice of HAL-PDT parameters to be chosen on further study and treatment of bladder cancer. HAL-PDT seems to be as efficient in the blue as in the red light regime (dose properly adjusted) as expected since protoporphyrin IX acts as the photosensitizer. It should, therefore, be possible to optimize the PDT protocol with respect to tissue penetration of different wavelengths. Our survival curves indicate practical doses for HAL-PDT and the experiments with fractionated exposure do not indicate further efficacy of HAL-PDT by this technique. We could not find apoptosis to be a dominant pathway to cell destruction, but this could be influenced by our experimental techniques. As apoptosis may be desirable from clinical point of view, the optimum treatment deserves further studies.

Acknowledgements

We are thankful to Photocure ASA, Oslo, Norway, for providing us with hexylaminolevulinate for the experiments. Comments on the manuscript were gratefully received from Kristian Berg. Kristin Sæterbø is warmly thanked for all assistance – she was of utmost importance for the technical performance of the equipment and the successful treatment of the AY-27 cells.

Notes and references

1 D. M. Parkin, Estimating the world cancer burden, Globocan 2000, *Int. J. Cancer*, 2001, **94**, 153–156.
2 D. Shackley, C. Whitehurst, J. Moore, N. George, C. Betts and N. Clarke, Light penetration in bladder tissue: implications for the intravesical photodynamic therapy of bladder tumours, *BJU Int.*, 2001, **86**, 638–643.
3 H. Fukuda, A. Batlle and P. Riley, Kinetics of porphyrin accumulation in cultured epithelial cells exposed to ALA, *Int. J. Biochem.*, 1993, **25**, 1407.
4 J. Gaullier, M. Geze, R. Santus, M. Sa, J. Maziere, M. Bazin, P. Morliere and L. Dubertret, Subcellular localization of and photosensitization by protoporphyrin IX in human keratinocytes and fibroblasts cultivated with 5-aminolevulinic acid, *Photochem. Photobiol.*, 1995, **62**, 114.
5 R. Pottier, Y. Chow, J. LaPlante, T. Truscott, J. Kennedy and L. Beiner, Non-invasive technique for obtaining fluorescence excitation and emission spectra in vivo, *Photochem. Photobiol.*, 1986, **44**, 679–687.
6 H. Fisher, H. Hilmer, F. Lindner and B. Putzer, Chemische befunde bei einem fall von porphyrie (Petry), *Hoppe-Seyler's Z. Physiol. Chem.*, 1925, **150**, 44–101.
7 M. Moore, K. McColl, C. Rimington and A. Goldberg, *Disorders of porphyrin metabolism*, Plenum Medical New York, 1987.
8 K. Plaetzer, T. Kiesslich, T. Verwanger and B. Krammer, The modes of cell death induced by PDT: an overview, *Med. Laser Appl.*, 2003, **18**, 7–19.
9 T. Dougherty, Photosensitization of malignant tumors, *J. Surg. Oncol.*, 1986, **2**, 24–37.
10 J. Moan and K. Berg, The photodegradation of porphyrins in cells can be used to estimate the lifetime of singlet oxygen, *Photochem. Photobiol.*, 1991, **53**, 549–553.
11 Q. Peng, T. Warloe, K. Berg, J. Moan, M. Kongshaug, K. Giercksky and J. Nesland, 5-Aminolevulinic acid-based photodynamic therapy, *Cancer J. Clin.*, 1997, **79**, 2282–2308.
12 N. Schoenfeld, O. Epstein, M. Lahav, R. Mamet, M. Shaklai and A. Atsmon, The heme biosynthetic pathway in lymphocytes of patients with malignant lymphoproliferative disorders, *Cancer Lett.*, 1988, **43**, 43.
13 E. Larsen, L. Randeberg, O. Gederaas, C. Arum, A. Hjelde, C. Zhao, D. Chen, H. Krokan and L. Svaasand, Monitoring of hexyl 5-aminolevulinate-induced photodynamic therapy in rat bladder cancer by optical spectroscopy, *J. Biomed. Opt.*, 2008, **13**, 044031.
14 N. Lange, P. Jichlinski, M. Zellweger, M. Forrer, A. Marti, L. Guillou, P. Kucera, G. Wagnieres and H. Van Den Bergh, Photodetection of early human bladder cancer based on the fluorescence of 5-aminolaevulinic acid hexylester-induced protoporphyrin IX: a pilot study, *Br. J. Cancer*, 1999, **80**, 185.
15 Z. Xiao, K. Brown, J. Tulip and R. Moore, Whole bladder photodynamic therapy for orthotopic superficial bladder cancer in rats: a study of intravenous and intravesical administration of photosensitizers, *J. Urol.*, 2003, **169**, 352–356.
16 N. J. Berlin, A. Neuberger and J. J. Scott, The metabolism of 5-aminolevulinic acid, *Biochem. J.*, 1956, **64**, 80–90.
17 O. Gederaas, A. Holroyd, S. Brown, D. Vernon, J. Moan and K. Berg, 5-Aminolaevulinic acid methyl ester transport on amino acid carriers in a human colon adenocarcinoma cell line, *Photochem. Photobiol.*, 2001, **73**, 164–169.
18 A. Marti, P. Jichlinski, N. Lange, J. Ballini, L. Guillou, H. Leisinger and P. Kucera, Comparison of aminolevulinic acid and hexylester aminolevulinate induced protoporphyrin IX distribution in human bladder cancer, *J. Urol.*, 2003, **170**, 428–432.
19 http://www.photocure.com/RD/, 2010.
20 J. Moan, Ø. Bech, J. M. Gaullier, T. Stokke, H. Steen, L. Ma and K. Berg, Protoporphyrin IX accumulation in cells treated with 5-aminolevulinic acid: dependence on cell density, cell size and cell cycle, *Int. J. Cancer*, 1998, **75**, 134–139.
21 J. Carmichael, W. G. DeGraff, A. F. Gazdar, J. D. Minna and J. B. Mitchell, Evaluation of a tetrazolium-based, semiautomated colorimetric assay:assessment of chemosensitivity testing, *Cancer Res.*, 1987, **47**, 936–942.
22 D. Ball, S. Mayhew, D. Vernon, M. Griffin and S. Brown, Decreased efficiency of trypsinization of cells following photodynamic therapy: Evaluation of a role for tissue transglutaminase, *Photochem. Photobiol.*, 2001, **73**, 47–53.
23 K. Plaetzer, T. Kiesslich, B. Krammer and P. Hammerl, Characterization of the cell death modes and the associated changes in cellular energy supply in response to AlPcS 4-PDT, *Photochem. Photobiol. Sci.*, 2002, **1**, 172–177.
24 H. Dertinger and H. Jung, *Molecular Radiation Biology*, Springer Verlag, 1969.
25 A. Juzeniene, P. Juzenas, I. Bronshtein, A. Vorobey and J. Moan, The influence of temperature on photodynamic cell killing in vitro with 5-aminolevulinic acid, *J. Photochem. Photobiol., B*, 2006, **84**, 161–166.
26 L. Wyld, M. Reed and N. Brown, Differential cell death response to photodynamic therapy is dependent on dose and cell type, *Br. J. Cancer*, 2001, **84**, 1384–1386.
27 B. B. Noodt, K. Berg, Q. Peng and J. M. Nesland, Apoptosis and necrosis induced with light and 5-aminolaevulinic acid-derived protoporphyrin IX, *Br. J. Cancer*, 1996, **74**, 22–29.
28 A. H. Jackson, D. E. Games, P. Couch, J. R. Jackson, R. B. Belcher and S. G. Smith, Conversion of coproporphyrinogen III to protoporphyrin IX, *Enzyme*, 1974, **17**, 81–87.
29 R. D. Almeida, B. J. Manadas, A. P. Carvalho and C. B. Duarte, Intracellular signaling mechanisms in photodynamic therapy, *Biochim. Biophys. Acta, Rev. Cancer*, 2004, **1704**, 59–86.

30 T. Amo, N. Kawanishi, M. Uchida, H. Fujita, E. Oyanagi, T. Utsumi, T. Ogino, K. Inoue, T. Shuin, K. Utsumi and J. Sasaki, Mechanism of cell death by 5-aminolevulinic acid-based photodynamic action and its enhancement by ferrochelatase inhibitors in human histiocytic lymphoma cell line U937, *Cell Biochem. Funct.*, 2009, **27**, 503–515.
31 B. Kuitert, *Investigations of photoreactions in the cancer cell line AY-27, with special emphasis on reactive oxygen species*, Master's Thesis, NTNU, Norway, 2007.
32 W. Zong and C. Thompson, Necrotic death as a cell fate, *Genes Dev.*, 2006, **20**, 1.
33 K. Plaetzer, T. Kiesslich, C. Oberdanner and B. Krammer, Apoptosis following photodynamic tumor therapy: induction, mechanisms and detection, *Curr. Pharm. Des.*, 2005, **11**, 1151–1165.
34 G. Kroemer, L. Galluzzi and C. Brenner, Mitochondrial membrane permeabilization in cell death, *Physiol. Rev.*, 2007, **87**, 99–163.
35 P. Babilas, V. Schacht, G. Liebsch, O. S. Wolfbeis, M. Landthaler, R.-M. Szeimies and C. Abels, Effects of light fractionating an different fluence rates on photodynamic therapy with 5-aminolevulinic acid in vivo, *Br. J. Cancer*, 2003, **88**, 1462–1469.
36 A. Curnow, J. C. Haller and S. G. Brown, Oxygen monitoring during 5-aminolevulinic acid induced photodynamic therapy in normal rat colon. Comparison of continuous and fractionated light regimes, *J. Photochem. Photobiol., B*, 2000, **58**, 149–155.
37 A. Curnow, B. W. McIlroy, M. J. Postle-Hacon, A. J. MacRobert and S. G. Bown, Light dose fractionation to enhance photodynamic therapy using 5-aminolevulinic acid in the normal rat colon, *Photochem. Photobiol.*, 1999, **69**, 71–76.
38 H. S. De Bruijn, N. Van der Veen, D. J. Robinson and W. M. Star, Improvement of systemic 5-Aminolevulinic acid-based photodynamic therapy in vivo using light fractionation with a 75-minute interval, *Cancer Res.*, 1999, **59**, 901–904.
39 C. Oberdanner, K. Plaetzer, T. Kiesslich and B. Krammer, Photodynamic treatment with fractionated light decreases production of reactive oxygen species and cytotoxicity *in vitro via* regeneration of glutathione, *Photochem. Photobiol.*, 2005, **81**, 609–613.

Paper II

Journal of Biomedical Optics

BiomedicalOptics.SPIEDigitalLibrary.org

Red versus blue light illumination in hexyl 5-aminolevulinate photodynamic therapy: the influence of light color and irradiance on the treatment outcome *in vitro*

Linda Helander
Hans E. Krokan
Anders Johnsson
Odrun A. Gederaas
Kristjan Plaetzer

SPIE.

Journal of Biomedical Optics 19(8), 088002 (August 2014)

Red versus blue light illumination in hexyl 5-aminolevulinate photodynamic therapy: the influence of light color and irradiance on the treatment outcome *in vitro*

Linda Helander,[a,*] Hans E. Krokan,[a] Anders Johnsson,[b] Odrun A. Gederaas,[a] and Kristjan Plaetzer[c]
[a]Norwegian University of Science and Technology, Faculty of Medicine, Department of Cancer Research and Molecular Medicine, Erling Skjalgssons gate 1, Trondheim 7491, Norway
[b]Norwegian University of Science and Technology, Faculty of Natural Sciences and Technology, Department of Physics, Høgskoleringen 5, Trondheim 7491, Norway
[c]University of Salzburg, Division of Physics and Biophysics, Department of Materials Science and Physics, Laboratory of Photodynamic Inactivation of Microorganisms, Hellbrunnerstraße 34, Salzburg 5020, Austria

Abstract. Hexyl 5-aminolevulinate (HAL) is a lipophilic derivative of 5-aminolevulinate, a key intermediate in biosynthesis of the photosensitizer protoporphyrin IX (PpIX). The photodynamic efficacy and cell death mode after red versus blue light illumination of HAL-induced PpIX have been examined and compared using five different cancer cell lines. LED arrays emitting at 410 and 624 nm served as homogenous and adjustable light sources. Our results show that the response after HAL-PDT is cell line specific, both regarding the shape of the dose-survival curve, the overall dose required for efficient cell killing, and the relative amount of apoptosis. The ratio between 410 and 624 nm in absorption coefficient correlates well with the difference in cell killing at the same wavelengths. In general, the PDT efficacy was several folds higher for blue light as compared with red light, as expected. However, HAL-PDT_{624} induced more apoptosis than HAL-PDT_{410} and illumination with low irradiance resulted in more apoptosis than high irradiance at the same lethal dose. This indicates differences in death modes after low and high irradiance after similar total light doses. From a treatment perspective, these differences may be important. [DOI: 10.1117/1.JBO.19.8.088002]

Keywords: photodynamic therapy; hexyl 5-aminolevulinate; protoporphyrin IX; irradiation; light dosimetry; apoptosis.

Paper 140217RR received Apr. 4, 2014; revised manuscript received Jul. 4, 2014; accepted for publication Jul. 8, 2014; published online Aug. 8, 2014.

1 Introduction

Presently, 5-aminolevulinate (ALA) and two of its derivatives [methyl 5-aminolevulinate and hexyl 5-aminolevulinate (HAL)] are in routine clinical use as photosensitizer precursors in photodynamic therapy (PDT) and photodiagnosis.[1,2] HAL shows improved tissue penetration[3–5] and cellular uptake[6–8] compared to ALA. Following conversion of HAL to ALA by cellular esterases, the molecule enters the heme synthesis pathway and induces increased intracellular levels of the photosensitizer protoporphyrin IX (PpIX), the direct precursor of heme. PpIX features a typical absorption spectrum for porphyrins with a high Soret peak around 410 nm and Q-bands in the green and red wavelength ranges.[9] For PDT or photodiagnosis based on ALA or its esters, both blue and red light lamps are used. Red light offers the advantage of deeper penetration into tissue (about 6 mm).[2,10–12] By contrast, blue light penetrates only about 1 mm into tissue,[13] but has much higher efficiency for PpIX activation.

Protocols for PDT treatment in research and in the clinic vary widely, probably at least in part because there is no strong scientific basis for choosing one protocol over another. A solution to this problem will require comparative analyses of biological effects of different photophysical parameters, such as light wavelength, irradiance, and total dose. In addition, general conclusions can only be made by analyzing the effects of the same protocol applied to different tissues and cancer cells.

While treatment by chemotherapy and radiation largely kill cells by apoptosis, apparently PDT may work through apoptosis, necrosis, autophagy, and even mitotic catastrophe.[2,14–18] In general, the death mode may depend on several factors, including cell-specific properties, type of photosensitizer, light wavelength, total light dose, and irradiance.[17,19–21] Interestingly, the irradiance also modulates immunological responses which are likely to affect treatment outcome. Thus, high irradiance was found to be immunosuppressive, whereas a similar total dose administered using lower irradiance was not immunosuppressive.[22] In the present study, we have used five different human cancer cell lines and compared the overall PDT efficiency when using HAL-induced PpIX as photosensitizer activated by light of either 410 or 624 nm. We observed substantial differences among the cell types in their sensitivities to light. More importantly, the death mode, here measured as apoptosis, was not only influenced by the light source and total light dose but also by irradiance. From a perspective of treatment efficacy, our results may contribute to a better fundament for understanding the biological effects of the photophysical parameters in PDT.

*Address all correspondence to: Linda Helander, E-mail: linda.helander@ntnu.no

2 Materials and Methods

2.1 *Cell Lines*

Five human cancer cell lines were used in this study, all of them representative of a cancer type suitable for clinical HAL-PDT. The cell line A431 (ATCC CRL-1555) is an epidermoid carcinoma and serves as a model system for skin cancer. The A549 cell line (ATCC CCL-185) is a lung carcinoma and HeLa S3 (ATCC CCL-2.2) is a cervical adenocarcinoma. WiDr (ATCC CCL-218) is a colorectal adenocarcinoma and T24 (ATCC HTB-4) is a transitional cell carcinoma from urinary bladder.

2.2 *Light Sources*

To obtain a homogenous light field at appropriate wavelengths and within a range of irradiance values, light sources based on a light emitting diode (LED) array were used for this study.[23] Each lamp consists of an array containing 247 (13×19 diodes, 624 nm, illumination field 9×14 cm) or 260 (13×20 diodes, 410 nm, illumination field 9×15 cm) LEDs (Roithner LaserTechnik, Vienna, Austria) connected in parallel. The irradiance of these LEDs is adjusted by the current applied as described by Pieslinger et al.[23] The assembly of the LEDs and the distance from the LEDs to the illumination field are optimized to achieve a homogenous light field (maximal variation 10%). The LED light source for blue light illumination (LED type VL410-5-15, dominant wavelength 410 nm, spectral half-wave width 18 nm) allows for irradiance values up to 7.0 mW/cm^2, and the red light illumination source (LED type R5CA5111P, dominant wavelength 624 nm, spectral half-wave width 20 nm) delivers up to 35.0 mW/cm^2. The emittance spectra can be found in Ref. 24 and the light viewing angle is 15 deg. Irradiance was measured in a grid pattern (covering the whole light field) by an LI-189 light meter equipped with a PY pyranometer detector (LI-COR, Lincoln, Nebraska, diameter 7.5 mm) and a LabMaster Ultima laser measurement system with a vis-sensor (Coherent Inc., Wilsonville, California, diameter 8 mm). Both light meters had a typical accuracy of $\pm 3\%$ for the total system. The light transmission of the microplates used is reported to be close to 100% at wavelengths >350 nm according to information from the manufacturer. The transmission spectrum should, therefore, be close to that of the lamp itself.

2.3 *Cell Culture*

All growth media were supplemented with 10% (v/v) fetal bovine serum, 2 mM L-glutamine, 100 U ml^{-1} penicillin/0.1 mg ml^{-1} streptomycin, amphothericin B (2.5 μg/ml), and 10 mM 4-(2-hydroxyethyl)-1-piperazineethanesulfonic acid (HEPES), all obtained from Sigma (Oslo, Norway). For culture of T24 and A431, 1-mM Na pyruvate (BioWhittaker, Lonza, Belgium) was also added to the media. All cell lines used Dulbecco's modified eagle medium (DMEM) as a basic medium except for WiDr cells which were cultured in RPMI 1640 medium. Subcultivation was done by rinsing the cells twice with phosphate buffered saline (PBS) (37°C) before detachment by trypsinization. For all experiments, cells were seeded in appropriate cell culture dishes the day before treatment. Cell numbers (total, live, and dead) were determined by using the Countess™ system (Invitrogen™, Oslo, Norway) and the number of live cells was used for calculating the seeding.

2.4 *Hexyl 5-Aminolevulinate Photodynamic Therapy*

A stock solution of 10 mM HAL dissolved in PBS (adjusted to pH 6.0) was freshly prepared on the day of the experiment and sterilized by filtration (0.2-μm filter). The growth medium was carefully removed from the dishes and replaced by medium without serum containing 20 μM HAL. After 3 h of incubation (dark conditions, 37°C, 5% CO_2, humidified atmosphere), the HAL medium was replaced by growth medium without HAL (with serum). The samples were illuminated from below using either of the LED arrays described above immediately after HAL removal and were subsequently placed in the incubator until further processing. All experimental steps after adding of HAL to the cells were done under subdued light conditions.

2.5 *Dose-Response*

Cells were seeded (1 day before treatment) in 96-well cell culture microplates (black walls, clear bottom, Optilux, Falcon, VWR, Norway, see picture in Fig. 1) at the following densities, resulting in 50% to 60% confluency at the day of treatment: A431: 10,000 cells/well, A549: 10,000 cells/well, HeLa S3: 11,000 cells/well, T24: 9000 cells/well and WiDr: 11,000 cells/well. The standard filling volume was 100 μl/well. Six wells in each row contained cells while the outer ones only contained medium to minimize evaporation. Every experiment was accompanied by a "control" [no Photosensitizer (PS), no light], a "light-only" sample (no PS, maximal light dose), and a "HAL-only" sample (PS, kept in the dark). Please notice that all doses and controls necessary for the one dose–response curve were on the same microplate to ensure identical conditions except those of the varied photophysical parameters.

2.6 *Resazurin Assay*

The resazurin assay is based on the conversion of the non-fluorescent resazurin to the fluorescing resorufin in viable cells. Approximately 22 h after illumination, 20-μl resazurin (2.5 mM, Sigma) was added into each well and incubated for

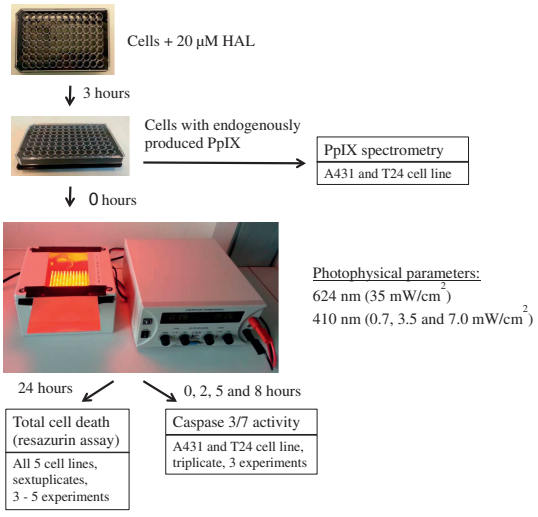

Fig. 1 A flow chart of the experimental design including the number of parallels and experiments is presented.

2 h in the dark incubator. Subsequently, resorufin fluorescence was determined using a microplate reader (BMG Labtech FluoStar Omega, Oslo, Norway, excitation wavelength 544 nm, emission wavelength 590 nm).

2.7 *PpIX Absorbance and Emission*

Approximately 95% confluent 75 cm^2 cell culture bottles of T24 and A431 cells were incubated with 20 μM HAL for 3 h. Cells were then rinsed once with PBS (37°C) and 5 ml of accutase (Sigma) was added. After a few minutes in the incubator, the detached cells were transferred into tubes. From each cell suspension, 10 μl were taken for cell counting by Bürker chamber. The suspensions were then centrifuged at 450 g (4°C, 5 min). The supernatants were removed and the pellets were resuspended in PBS to a final concentration of 4.0×10^6 cells/ml. All samples were kept on ice until spectra were read using a Fluorolog III fluorometer (Jobin Yvon-Spex, Horiba Group, Kjeller, Norway). For the fluorescence-excitation spectra, an LP700 filter was placed in front of the detector, the excitation slit was 3 nm, and the emission slit was 4 nm. Fluorescence emission was measured at 710 nm and excitation was performed in 1-nm steps from 350 to 700 nm in a signal/reference mode to make it comparable to absorption spectra. Emission spectra (550 to 750 nm, 1-nm step width) were excited at 405 nm with an excitation slit at 4 nm and an emission slit at 3 nm.

2.8 *Caspase 3/7 Activity*

The lethal dose (LD) values as determined from the dose–response curves for A431 and T24 cells in Figs. 2 and 3 were used for this part of the study. For determination of the caspase activity, cells were seeded the day before treatment in Optilux-microplates (cell density: 9000/well for T24 10,000/well for A431). HAL-PDT was done as described above, but the cells were covered with only 30 μl medium (with serum) per well after illumination. At 0, 2, 5, and 8 h post illumination, a microplate was allowed to equilibrate to room temperature before 30 μl of Caspase-Glo® 3/7 Reagent (Promega, Oslo, Norway, room temperature, in accordance with the manufacturers' protocol) was added to each well. The samples were mixed on a plate-shaker at 500 rpm for about 30 s and were subsequently incubated at room temperature for 1 h before

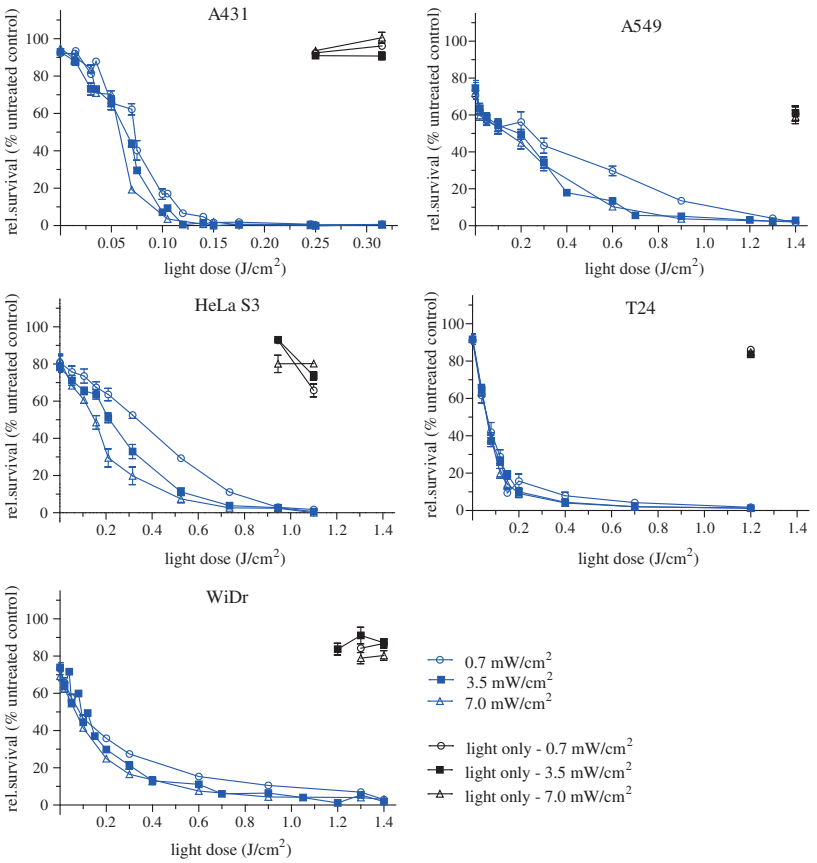

Fig. 2 Dose–response curves for five human cancer cell lines treated with blue light (410 nm) HAL-PDT (20 μM, 3 h, serum free). Three different irradiance values (0.7, 3.5 and 7.0 mW/cm^2) were used for all cell lines. Cell viability is relative to an untreated control in the same microplate (no HAL, no light) and the 0 J/cm^2 point is the "HAL no light" value. Each point is the average of two to five experiments (each in sextuplicate) with standard error of the mean (SEM) indicated by error bars.

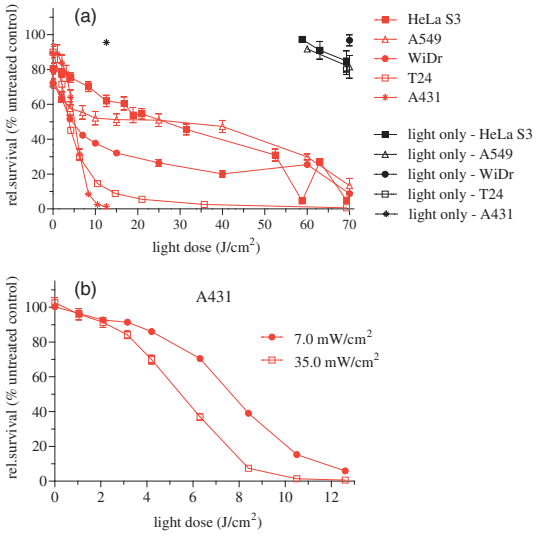

Fig. 3 Dose–response curves for five human cancer cell lines treated with red light (624 nm) HAL-PDT (20 μM, 3 h). In (a) all five cell lines were illuminated at 35 mW/cm^2 and in (b) A431 cells were illuminated with 7 mW/cm^2 in addition ($n = 6$, small SEMs on error bars). Cell viability is relative to an untreated control in the same microplate (no HAL, no light) and the 0 J/cm^2 point is the "HAL no light" value. Each point in (a) is the average of two to five experiments (each in sextuplicate) with standard error of the mean (SEM) indicated by error bars.

luminescence was measured in the plate reader (BMG Labtech FluoStar Omega).

2.9 *Calculations and Statistics*

All calculations for LD values are based on Figs. 2 and 3. The LD's are simply read out, such as LD_{25} equals the dose needed to obtain 25% cell death, LD_{50} equals the dose needed to obtain 50% cell death and so on. Unfortunately, the exact same doses were not used for all experiments. This made it difficult to make a statistical comparison between the curves in Figs. 2 and 3. The reason that doses were sometimes slightly altered between the independent experiments was to improve the measurement points in order to show the expected sigmoidal shape of the curve. Normally one expects an experimental error of 10% to 15% in MTT and resazurin assays. For calculating the mean and standard error of the means (SEMs) in Figs. 2 and 3, the values from sextuplicate measurements in all three to five biological replicates were added together and used to calculate mean values and SEMs.

3 Results

3.1 *Dose–Response Curves of Five Human Cancer Cell Lines after Blue Light HAL-PDT*

To address the question of whether the cytotoxicity of blue light illumination of HAL-induced PpIX (abbreviated as HAL-PDT_{410} is dependent only on total light dose or on total light dose and irradiance, we measured dose–response curves of five human cancer cell lines using three different irradiance values (0.7, 3.5 or 7.0 mW/cm^2) under otherwise identical PDT procedures.

As shown in Fig. 2, the overall light dose required to kill close to 100% of the cells varies from 0.2 to 1.4 J/cm^2, depending on the cell line. The most sensitive cell line is A431 both in terms of the irradiance and light dose required for complete cell killing, whereas the other cell lines are substantially more resistant. The shape of the dose–response curves differs among the different cell lines. The viability of T24 cells drops rapidly with increasing light dose, while the dose–response curve for HeLa S3 cells has a slight slope (depending on the irradiance) with a near complete cell kill at >1.1 J/cm^2. WiDr displays a notable similarity to T24 cells regarding curve characteristics, excluding the HAL-only measurement. Unexpectedly, a less steep dose–response curve was observed when using a lower irradiance (0.7 mW/cm^2) compared to a 10-fold higher irradiance (7 mW/cm^2). This was observed for all five cell lines.

The dark toxicity of 20-μM HAL varied from 35% (A549) to negligible (A431, T24). Blue light illumination without PS using the maximal light dose resulted in up to 40% cell death for A549 cells, and almost no cell killing for A431 and WiDr cells. Hyperthermia from illumination could potentially cause some of the differences between high and low irradiance. However, the temperature in growth medium did not change measurably for 410 nm (7 mW/cm^2, 30 min) illumination and increased only 2 deg for 624 nm (35 mW/cm^2, 30 min), data not shown. Since illumination is carried out at room temperature, the cells will consequently not be exposed to hyperthermia during the PDT protocols employed.

3.2 *Dose–Response Curves of Five Human Cancer Cell Lines after Red Light HAL-PDT*

Red light is commonly used for ALA-based PDT in the clinic. As a result of PpIX's low absorption of red light compared to blue light and the irradiance range of the lamp, only the highest lamp output irradiance (35 mW/cm^2) was used for red light HAL-PDT (HAL-PDT_{624}). An exception is the A431 cells which required the lowest light doses. Therefore it was possible to establish a dose–response curve for 7 mW/cm^2 illumination as well. For an irradiance of 35 mW/cm^2, the illumination time required to achieve near complete cell destruction was below 30 min for all cell lines tested. Except for irradiance and wavelength, the PDT parameters were identical to those in the HAL-PDT_{410} experiments. Dose–response curves for all five cell lines after HAL-PDT_{624} are presented in Fig. 3(a).

Similar to the dose–response curves for HAL-PDT_{410}, the dose–response curves of the individual cell lines to HAL-PDT_{624} differ in both shape and the light doses needed to achieve close to 100% cell killing. The required light doses for near complete cell kill varied from 12.6 J/cm^2 for A431 to >70 J/cm^2 for WiDr and A549. Interestingly, the order of sensitivity of the cell lines to PDT estimated from $LD_{\sim 100}$ values (A431 > HeLa S3 > T24 > WiDr > A549) is comparable for HAL-PDT_{410} and HAL-PDT_{624}. Furthermore, A549 cells showed a biphasic response to HAL-PDT_{624} (and not a biphasic response to HAL-PDT_{410}): a rapid drop in viability below 10 J/cm^2 is followed by a plateau up to 40 J/cm^2. At an even higher light dose (70 J/cm^2), the viability of A549 cells drops to nearly zero. For the cell line with highest sensitivity to HAL-PDT_{624}, A431, the influence of irradiance on the overall cytotoxicity was tested. The results from this experiment are presented again in Fig. 3(b), where lower irradiance

Table 1 Calculated LD values based on Fig. 2 and Fig. 3, LD values are given in J/cm^2. In the upper part of the table, LD values for HAL-PDT$_{410}$ are presented and the corresponding LD-values for HAL-PDT$_{624}$ are presented in the lower part of the table. For a few measurements, the dark toxicity was too high to make a LD$_{25}$-calculation, the missing values are denoted "–".

HAL-PDT$_{410}$	A431			A549			HeLa S3			T24			WiDr		
[mW/cm^2]	0.7	3.5	7.0	0.7	3.5	7.0	0.7	3.5	7.0	0.7	3.5	7.0	0.7	3.5	7.0
LD$_{25}$	0.04	0.03	0.03	–	–	–	0.07	0.02	0.03	0.02	0.02	0.02	–	–	–
LD$_{50}$	0.07	0.06	0.06	0.25	0.19	0.14	0.34	0.22	0.15	0.06	0.06	0.06	0.08	0.09	0.07
LD$_{75}$	0.09	0.08	0.07	0.69	0.36	0.41	0.58	0.39	0.26	0.13	0.13	0.11	0.36	0.26	0.20
LD$_{90}$	0.12	0.10	0.09	1.05	0.64	0.62	0.77	0.56	0.48	0.35	0.20	0.19	0.96	0.62	0.52
LD$_{\sim 100}$	0.25	0.25	0.25	1.40	1.40	1.40	1.10	1.10	1.10	1.20	1.20	1.20	1.40	1.40	1.40

HAL-PDT$_{624}$	A431		A549	HeLa S3	T24	WiDr
[mW/cm^2]	7	35	35	35	35	35
LD$_{25}$	5.7	3.4	–	4.4	1.7	–
LD$_{50}$	7.7	5.1	28.9	26.3	3.8	4.5
LD$_{75}$	9.6	6.9	63.0	56.3	7.5	28.4
LD$_{90}$	11.7	8.3	72.1	66.0	13.8	69.2
LD$_{\sim 100}$	12.6	12.6	–	69.3	69.3	70.0

(7 mW/cm^2) results in less efficient cell destruction for intermediate doses when compared to the fivefold higher irradiance (35 mW/cm^2).

As expected, the dark toxicity of 20 μM HAL in these experiments was about the same as in the HAL-PDT$_{410}$ experiments. Furthermore, red light illumination without PS using the maximal light dose for each cell line induced no cell death within the experimental error, except for A549, which showed about a 30% drop in viability.

To make comparison between the different cell lines and photophysical parameters easier, we have assembled the values from Figs. 2 and 3 in Table 1. We have tabulated the values resulting in 25%, 50%, 75%, and 90% cell death, for LD$_{25}$, LD$_{50}$, LD$_{75}$, and LD$_{90}$, respectively. Since the slope of the dose–response curves is very flat when approaching 100% cell death, the definition of LD$_{100}$ is somewhat subjective, and we chose to use the term "LD$_{\sim 100}$" instead. At LD$_{\sim 100}$, close to 100% of the cells were dead in all experiments when measured by resazurin assay and there were no signs of viability on visual inspection of the cells.

3.3 *Spectra of Intracellular HAL-Induced PpIX*

In order to identify PpIX and possible its derivatives by spectroscopy, fluorescence excitation [Fig. 4(a)] and emission spectra [Fig. 4(b)] of HAL-induced intracellular PS were recorded in A431 and T24 cells.

A431 and T24 were chosen as models for a PDT sensitive and a more resistant cell line, respectively. A431 is the most sensitive to HAL-PDT of all tested cell lines for both blue and red light illumination, while T24 is one of the most resistant cell lines when one compares doses required to achieve close to

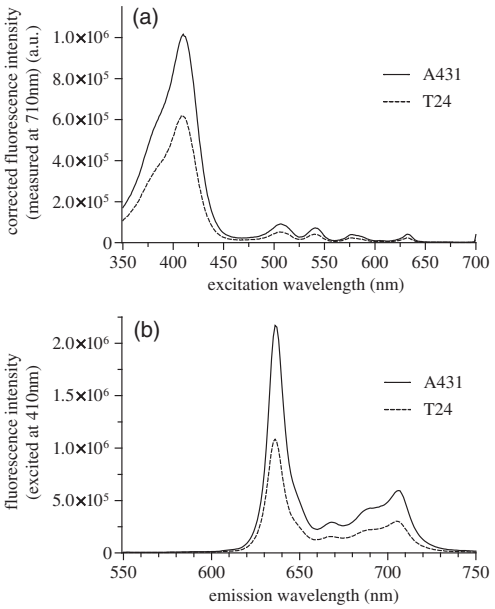

Fig. 4 Spectra of intracellular HAL-induced (20 μM, 3 h) PpIX and possible derivatives thereof in A431 and T24 cells (4×10^6 cells/ml). The spectra from untreated cells are subtracted from the presented PpIX spectra. (a) Fluorescence at 710 nm was measured for excitation wavelengths from 350 to 700 nm at 1 nm steps in signal/reference mode, making the spectra equivalent to absorption spectra. (b) Cells were excited at 410 nm and emission measured at 1 nm steps from 550 to 750 nm.

100% cell killing. Both fluorescence excitation and emission spectra of untreated cells were measured (negligible values) and subtracted from the spectra measured from the incubated cells [Figs. 4(a) and 4(b)]. For both cell lines, the Soret peak is clearly visible at 410 nm and the maximum of the Q-band in the red wavelength range is close to 633 nm under the conditions used [Fig. 4(a)]. The ratio of the fluorescence excitation peaks (equivalent to absorption peaks) at 410 and 633 nm between the two cell lines A431 and T24 is 0.6 (T24:A431).

At 624 nm, the red light fluorescence excitation peak has dropped to 55% from its maximum at 633 nm. Therefore, the overall illumination period could be reduced by roughly one half if a light source with a maximum at 633 nm was used for illumination instead of the 624 nm as used in the present experiments.

The ratio between the peak heights of 410 and 624 nm is 56.3 for A431 and 56.4 for T24 cells, under the conditions used in this study [Fig. 4(a)].

T24 cells had lower fluorescence emission than A431 cells [Fig. 4(b)]. Red light fluorescence emission peaks at 636 nm for both cell lines, while a smaller maximum was determined at 706 nm. For both peaks, the overall fluorescence from T24 cells is about half of the fluorescence value from A431 cells.

3.4 *Caspase 3/7 Activity in A431 and T24 Cells Induced by HAL-PDT$_{410}$ and HAL-PDT$_{624}$*

To test whether different illumination parameters influence apoptosis induction in A431 and T24 cells, caspase 3/7 activity was measured at 2, 5 and 8 h post HAL-PDT. These time points were chosen according to the results of a pilot study. Caspase 3/7 activity is considered a hallmark of apoptosis. Both cell lines were selected due to their property to show the full apoptotic phenotype, clear caspase induction, and comparable susceptibility toward HAL-PDT [see Figs. 2 and 3(a)]. A431 and T24 cells were again used to represent sensitive and more resistant cell lines to HAL-PDT, respectively. All LD values in this study are based on interpolated data from Figs. 2 and 3, therefore, biological and technical variations in these experiments are carried on into the LD values. In addition, the caspase measurements were first done based on the LD values from one dose-response experiment. The light doses were kept fixed in all three independent experiments, but it turned out after all dose-response experiments were done for Figs. 2 and 3 that the light doses used to obtain the bars in Figs. 5 and 6 did not result in identical LD values for all different photophysical parameters. As a result, the doses are assembled in subranges in Figs. 5 and 6. All values shown in Figs. 5 and 6 are relative to an untreated control (no light, no PS) set as 100%.

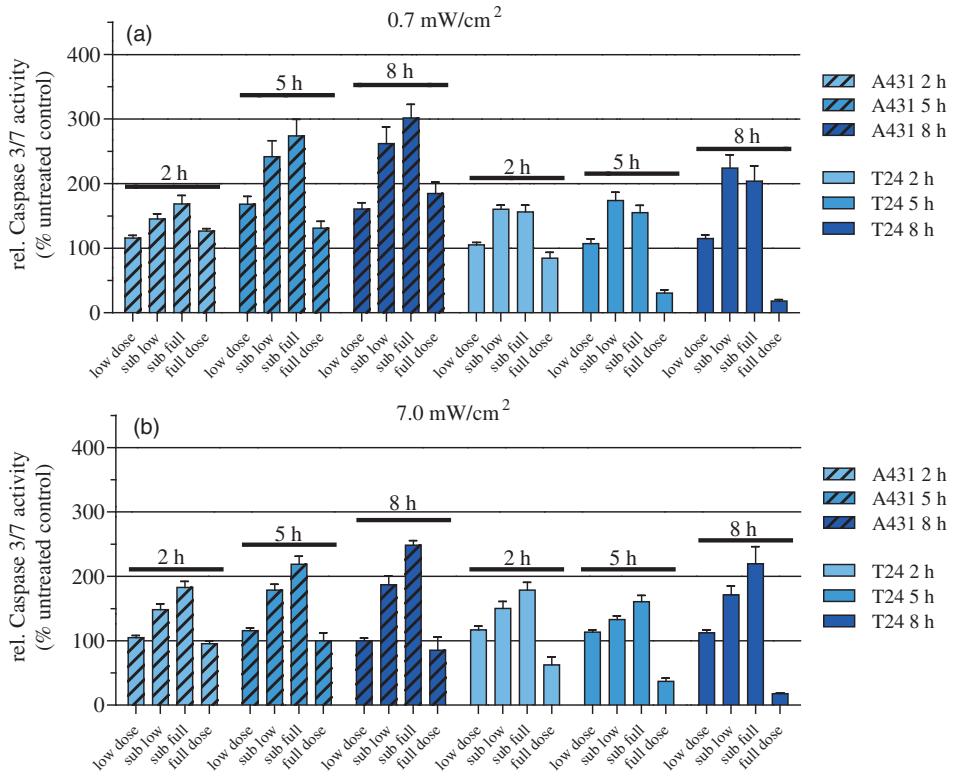

Fig. 5 Caspase 3/7 activity of A431 and T24 cells following HAL-PDT with 410-nm light and (a) 0.7 mW/cm^2 and (b) 7.0 mW/cm^2. Values are related to an untreated control, set as 100%. Caspase 3/7 activity was measured for different light doses at 2, 5, and 8 h after completed illumination. Bars represent averages from three independent experiments with triplicates in each experiment and SEMs are indicated.

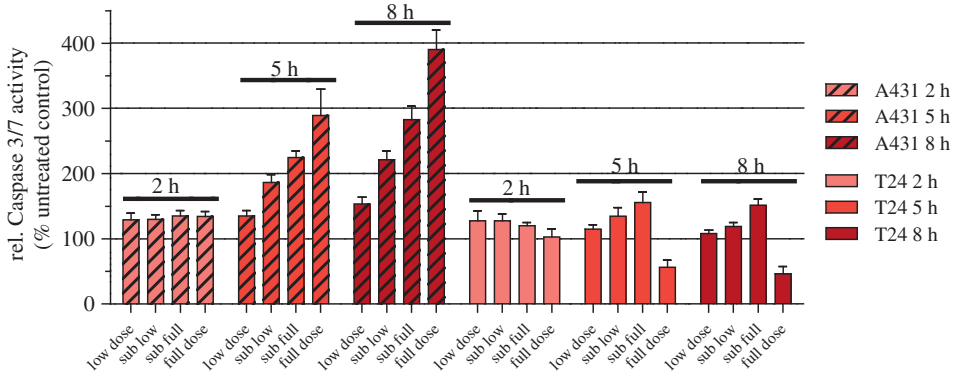

Fig. 6 Caspase 3/7 activity in A431 and T24 cells following HAL-PDT with 624 nm light at 35.0 mW/cm^2. Values are related to an untreated control, set as 100%. Caspase 3/7 activity was measured for different light doses at 2, 5, and 8 h after completed illumination. Bars represent averages from three independent experiments with triplicates in each experiment and SEMs are indicated.

3.4.1 *HAL-PDT$_{410}$*

In order to determine the effect of varying irradiance, HAL-PDT$_{410}$ was performed using irradiance values of either 0.7 mW/cm^2 [Fig. 5(a)] or 7.0 mW/cm^2 [Fig. 5(b)]. In Fig. 5(a), a low dose corresponds to about LD$_{35}$, a sub-low to LD$_{65}$, a sub-full to LD$_{85}$, and a full dose close to 100% cell death. In Fig. 5(b), the variance in the dose ranges is somewhat larger: the low dose corresponds to about LD$_{20}$ (A431) and LD$_{30}$ (T24), the sub-low to LD$_{35}$ (A431) and LD$_{60}$ (T24), the sub-full to LD$_{85}$, and the full dose close to 100% cell death.

Among the light doses tested, sub-full doses generally induced the highest caspase 3/7 activity in A431 cells at all three time points for both irradiance values. The results are similar for T24 cells but the less pronounced and for the lowest irradiance for the sub-low doses seem to induce the highest caspase 3/7 activity. Furthermore, caspase 3/7 activity increases with increasing time post HAL-PDT in the time range tested. A431 generally shows higher caspase 3/7 activity when compared to T24.

3.4.2 *HAL-PDT$_{624}$*

In Fig. 6, a low dose corresponds to about LD$_{20}$ (A431) and LD$_{30}$ (T24), a sub-low to LD$_{40}$ (A431) and LD$_{50}$ (T24), a sub-full to LD$_{65}$ (A431) and LD$_{75}$ (T24), and a full dose close to 100% cell death. Following red light illumination, T24 cells show almost no increased caspase 3/7 activity for any of the light doses and time points tested in this study (Fig. 6). Only a marginal increase was observed at 5 and 8 h for sub-low and sub-full doses. By contrast, A431 displayed increasing caspase 3/7 activity with increasing light doses at 5 and 8 h post HAL-PDT$_{624}$.

Interestingly, when comparing HAL-PDT$_{410}$ to HAL-PDT$_{624}$, the most pronounced differences of caspase 3/7 activity are that (i) blue light induces the highest activity at sub-full doses (except for T24 0.7 mW/cm^2) but red light does so at full doses (except for T24 which showed only minor caspase 3/7 activity after HAL-PDT$_{624}$) and (ii) blue light induces a maximum threefold increase in the activity when compared to untreated controls while red light induces a maximum fourfold increase.

4 Discussion

Although the basic principle of PDT is simple, a number of physical, chemical and biological parameters may influence its efficacy. Different light sources with diverse characteristics are used both in research and in clinical applications.[25,26] By altering the illumination period, different irradiance values can be used to deposit one specific light dose. However, the tumor response may not solely depend on the light dose but may also depend on the irradiance. In clinical application, lower irradiances turned out to be more effective than higher ones (above a specific threshold) due to a limitation of the (tissue) oxygen supply.[27–30] This effect is assumed not to be the case for *in vitro* experiments, where the oxygen supply is much better than in tissues. In HAL-PDT, the effective photosensitizer is endogenous PpIX, which has its largest absorption around 410 nm and a smaller peak of absorption around 630 nm. Red light is commonly used in PDT due to its longer penetration depth in tissue. In the present study, all cells were monolayer cells and were irradiated from below. Hence, scattering, depth of penetration, and cell density would not make a large impact on light delivery. The significance of these parameters is, however, of great importance in clinical treatment. In a study from 2011, the efficacies of different light sources used in the clinic to activate PpIX were compared and demonstrated that blue light sources were the most efficient.[31] Blue light was also used successfully in several dermatological conditions.[32–35]

We have used two in-house made lamps to examine whether there is a difference in the outcome of HAL-PDT with red and blue light and after illumination with different irradiances in five different human cancer cell lines. The following discussion is divided into three main topics: irradiance and wavelength, cell-line specific response, and apoptosis induction.

4.1 *Irradiance and Wavelength*

Interestingly, our cell survival studies indicate that when using blue light and identical total light doses, high irradiance is more efficient in cell killing than low irradiance. This tendency is most strongly pronounced for A431 and HeLa S3 cells. In addition, at least for A431 cells, high irradiance red light induces a

higher cytotoxicity than low irradiance at an identical total light dose. This observation may be (at least partially) ascribed to the counteracting effect of the cellular reactive oxygen species (ROS) defense systems, which have been shown to antagonize PDT when fractionated illumination is applied.[36] It seems likely that during longer illumination at lower irradiance, the ROS defense may have sufficient capacity to partially detoxify the PDT-induced oxidants. By contrast, high-irradiance PDT might overwhelm the antioxidative mechanisms.

The absorption ratios between 410 and 624 nm were ~56 for both cell lines, A431 and T24 [Fig. 4(a)]. This generally correlates quite well with killing efficiencies (Table 1), although there is some variation at different LD values. Wavelength-dependent light absorption by PpIX is probably a major parameter in PDT, but probably not the only one. Other factors likely to contribute are ROS detoxification, such as superoxide dismutase, as well as DNA repair and autophagy.

A difference in killing dependent on irradiance but with a constant dose has also been studied when using another sensitizer. Thus, a photofrin II PDT study on A549 cells demonstrated lower efficacy at lower irradiance values.[37] Although a lower irradiance may reduce killing in PDT treatment, that reduction might then to some extent be compensated by an improved oxygenation.[38]

4.2 *Cell-Line Specific Responses*

Essentially, the response to PDT treatment differs notably between cell lines, both regarding sensitivity and shape of survival curves (Figs. 2 and 3). Similar observations were made by others using different cell lines and PDT protocols.[39] Obviously, generation of increased amounts of PpIX is essential for efficient PDT. However, T24 has only half the amount of total PpIX when compared to A431 (Fig. 4), but is more than twice less sensitive to light (at least at wavelength 410 nm) than A431, again pointing to a complex basis for sensitivity to PDT treatment. Difference in the survival of different cell lines could possibly be explained by different intracellular distributions of PpIX. However, confocal microscopy of HAL-incubated cells (20 μM, 3 h) co-stained with MitoTracker Green performed in this study indicated that PpIX is mainly localized in mitochondria in all cell lines used here. After another hour of HAL-incubation, some PpIX is redistributed to the cell membrane, without notable differences between the cell lines (data not shown). To explore the basis for the different sensitivities would require substantial efforts beyond the scope of the present paper, but it is likely that cell-specific differences in response of cancer cell lines also apply to tumors.

4.3 *Apoptosis Induction*

Apoptosis and necrosis are two major modes of cell death. We have specifically examined apoptosis and have assigned cell death that was not clearly apoptotic to most likely be necrotic. We consequently assume that the difference between the resazurin results and the caspase 3/7 activity measurements is caused by necrosis. However, there are additional mechanisms of cell death, including mitotic catastrophe and autophagy, both of which may, in fact, have a role in PDT.[21,40] The cell death mode apparently may depend both on the type of sensitizer and properties of the cells being treated. Apoptosis and mitotic catastrophe have some common and some unique properties.[41,42] PDT was shown to trigger immune suppression at high irradiances but immune stimulation at low irradiances in normal skin.[22] This is interesting from the perspective of different death modes observed at high and low irradiance in our study. Stimulation of antitumor immunity after PDT is recognized, but the details/trigger mechanisms are still discussed.[43–46] Exploration of the effect of different illumination protocols on cell death mode *in vitro* may help in establishing a better basis for the choice of illumination parameters.

To examine the influence of different illumination parameters on the cell death mode, caspase 3/7 activity was measured at 2, 5 and 8 h post-illumination. These results demonstrate that the cellular response depends on the target cells as well as illumination protocol. The most pronounced difference in caspase 3/7 activity between blue and red light PDT was that HAL-PDT_{410} showed maximal caspase 3/7 activity at sub-full doses and HAL-PDT_{624} maximum at full doses, which appears to be quite unique. For comparison, an ALA-PDT study on five different cell lines showed that the time course of apoptosis varied between the different cell lines and that the amount of apoptosis and necrosis varied with the cell line and dose, which is in line with the results presented in our study.[47]

In conclusion, the shape of the dose survival curve, the LD values, and the amount of apoptotic cells vary significantly between the different cell lines examined. When comparing blue and red light illumination, the light absorbance of the respective wavelength corresponds well to the light sensitivity of the cells. Furthermore, there has been some uncertainty as to whether one could make a direct comparison or not between studies when different wavelengths or irradiances have been used. This study shows that if one compares results between studies with either different irradiances or wavelengths, one should be especially aware of the differences at sublethal doses.

Acknowledgments

We would like to thank Prof. Thor Bernt Melø for his contribution to Fig. 4 and fruitful discussions, the Group of applied optics and laser physics by Prof. Mikael Lindgren for support and lending of the laser measurement system, and Aloys Munyeshyaka for contributing to the pilot experiments. L. Helanders work was funded by the Functional Genomics Program of Research Council of Norway, and the Svanhild and Arne Must fund for medical research. PhotoCure has kindly provided hexyl 5-aminolevulinate powder for this study.

References

1. B. Krammer and K. Plaetzer, "ALA and its clinical impact, from bench to bedside," *Photochem. Photobiol. Sci.* **7**(3), 283–289 (2008).
2. P. Agostinis et al., "Photodynamic therapy of cancer: an update," *CA Cancer J. Clin.* **61**(4), 250–281 (2011).
3. N. Fotinos et al., "5-Aminolevulinic acid derivatives in photomedicine: characteristics, application and perspectives," *Photochem. Photobiol.* **82**(4), 994–1015 (2006).
4. N. Dognitz et al., "Comparison of ALA- and ALA hexyl-ester-induced PpIX depth distribution in human skin carcinoma," *J. Photochem. Photobiol. B* **93**(3), 140–148 (2008).
5. A. Marti et al., "Comparison of aminolevulinic acid and hexylester aminolevulinate induced protoporphyrin IX distribution in human bladder cancer," *J. Urol.* **170**(2 Pt 1), 428–432 (2003).
6. L. Rodriguez et al., "Porphyrin synthesis from aminolevulinic acid esters in endothelial cells and its role in photodynamic therapy," *J. Photochem. Photobiol. B* **96**(3), 249–254 (2009).
7. C. Perotti et al., "Porphyrin synthesis from ALA derivatives for photodynamic therapy. In vitro and in vivo studies," *Br. J. Cancer* **90**(8), 1660–1665 (2004).

8. V. Zenzen and H. Zankl, "Protoporphyrin IX-accumulation in human tumor cells following topical ALA- and h-ALA-application in vivo," *Cancer Lett.* **202**(1), 35–42 (2003).
9. J.-L. Soret, "Analyse spectrale: Sur le spectre d'absorption du sang dans la partie violette et ultra-violette," *Comptes rendus de l'Académie des sciences* **97**(2), 1269–1270 (1883).
10. H. W. Wang et al., "Broadband reflectance measurements of light penetration, blood oxygenation, hemoglobin concentration, and drug concentration in human intraperitoneal tissues before and after photodynamic therapy," *J. Biomed. Opt.* **10**(1), 014004 (2005).
11. K. Plaetzer et al., "Photophysics and photochemistry of photodynamic therapy: fundamental aspects," *Lasers Med. Sci.* **24**(2), 259–268 (2008).
12. L. O. Svaasand, "Optical dosimetry for direct and interstitial photoradiation therapy of malignant tumors," *Prog. Clin. Biol. Res.* **170**, 91–114 (1984).
13. P. Juzenas et al., "Noninvasive fluorescence excitation spectroscopy during application of 5-aminolevulinic acid in vivo," *Photochem. Photobiol. Sci.* **1**(10), 745–748 (2002).
14. S. H. Kaufmann and W. C. Earnshaw, "Induction of apoptosis by cancer chemotherapy," *Exp. Cell Res.* **256**(1), 42–49 (2000).
15. R. Baskar et al., "Cancer and radiation therapy: current advances and future directions," *Int. J. Med. Sci.* **9**(3), 193–199 (2012).
16. M. Rebucci and C. Michiels, "Molecular aspects of cancer cell resistance to chemotherapy," *Biochem. Pharmacol.* **85**(9), 1219–1226 (2013).
17. K. Plaetzer et al., "Apoptosis following photodynamic tumor therapy: induction, mechanisms and detection," *Curr. Pharm. Des.* **11**(9), 1151–1165 (2005).
18. T. Kushibiki et al., "Responses of cancer cells induced by photodynamic therapy," *J. Healthcare Eng.* **4**(1), 87–108 (2013).
19. A. C. Moor, "Signaling pathways in cell death and survival after photodynamic therapy," *J. Photochem. Photobiol. B* **57**(1), 1–13 (2000).
20. P. Agostinis et al., "Regulatory pathways in photodynamic therapy induced apoptosis," *Photochem. Photobiol. Sci.* **3**(8), 721–729 (2004).
21. P. Mroz et al., "Cell death pathways in photodynamic therapy of cancer," *Cancer* **3**(2), 2516–2539 (2011).
22. G. A. Frost, G. M. Halliday, and D. L. Damian, "Photodynamic therapy-induced immunosuppression in humans is prevented by reducing the rate of light delivery," *J. Invest. Dermatol.* **131**(4), 962–968 (2011).
23. P. K. Pieslinger et al., "Characterization of a simple and homogenous irradiation device based on light-emitting diodes: a possible low cost supplement to conventional light sources for photodynamic treatment," *Med. Laser Appl.* **21**(4), 277–283 (2006).
24. Roithner Lasertechnik, Vienna, Austria, "Properties of diverse LEDs," http://www.roithner-laser.com/led_diverse.html (31 July 2014).
25. M. A. Calin and S. V. Parasca, "Light sources for photodynamic inactivation of bacteria," *Lasers Med. Sci.* **24**(3), 453–460 (2009).
26. L. Brancaleon and H. Moseley, "Laser and non-laser light sources for photodynamic therapy," *Lasers Med. Sci.* **17**(3), 173–186 (2002).
27. T. M. Sitnik and B. W. Henderson, "The effect of fluence rate on tumor and normal tissue responses to photodynamic therapy," *Photochem. Photobiol.* **67**(4), 462–466 (1998).
28. B. W. Henderson, T. M. Busch, and J. W. Snyder, "Fluence rate as a modulator of PDT mechanisms," *Lasers Surg. Med.* **38**(5), 489–493 (2006).
29. H. W. Wang et al., "Effect of photosensitizer dose on fluence rate responses to photodynamic therapy," *Photochem. Photobiol.* **83**(5), 1040–1048 (2007).
30. S. Iinuma et al., "In vivo fluence rate and fractionation effects on tumor response and photobleaching: photodynamic therapy with two photosensitizers in an orthotopic rat tumor model," *Cancer Res.* **59**(24), 6164–6170 (1999).
31. R. M. Sayre, J. C. Dowdy, and R. W. Gottschalk, "Comparative effectiveness of clinically used light sources for cutaneous protoporphyrin IX-based photodynamic therapy," *J. Cosmetic Laser Ther.* **13**(2), 63–68 (2011).
32. A. F. Taub, "Photodynamic therapy for the treatment of acne: a pilot study," *J. Drugs Dermatol.* **3**(6 Suppl), S10–S14 (2004).
33. S. L. Marcus and W. R. McIntyre, "Photodynamic therapy systems and applications," *Expert Opin. Emerg. Drugs* **7**(2), 321–334 (2002).
34. J. E. Lane et al., "Unilateral Basal cell carcinomas: an unusual entity treated with photodynamic therapy," *J. Cutan. Med. Surg.* **9**(6), 336–340 (2005).
35. A. M. Chapas and B. A. Gilchrest, "Broad area photodynamic therapy for treatment of multiple basal cell carcinomas in a patient with nevoid basal cell carcinoma syndrome," *J. Drugs Dermatol.* **5**(2 Suppl), 3–5 (2006).
36. C. B. Oberdanner et al., "Photodynamic treatment with fractionated light decreases production of reactive oxygen species and cytotoxicity in vitro via regeneration of glutathione," *Photochem. Photobiol.* **81**(3), 609–613 (2005).
37. W. Matthews et al., "In vitro photodynamic therapy of human lung cancer: investigation of dose-rate effects," *Cancer Res.* **49**(7), 1718–1721 (1989).
38. T. M. Sitnik, J. A. Hampton, and B. W. Henderson, "Reduction of tumour oxygenation during and after photodynamic therapy in vivo: effects of fluence rate," *Br. J. Cancer* **77**(9), 1386–1394 (1998).
39. J. V. Moore, C. M. L. West, and C. Whitehurst, "The biology of photodynamic therapy," *Phys. Med. Biol.* **42**(5), 913–935 (1997).
40. S. Rello-Varona et al., "Mitotic catastrophe induced in HeLa cells by photodynamic treatment with Zn(II)-phthalocyanine," *Int. J. Oncol.* **32**(6), 1189–1196 (2008).
41. M. Castedo et al., "Cell death by mitotic catastrophe: a molecular definition," *Oncogene* **23**(16), 2825–2837 (2004).
42. I. Vitale et al., "Mitotic catastrophe: a mechanism for avoiding genomic instability," *Nat. Rev. Mol. Cell Biol.* **12**(6), 385–392 (2011).
43. P. Mroz, Y.-Y. Huang, and M. R. Hamblin, "Photodynamic therapy for cancer and activation of immune response," in *Biophotonics and Immune Responses*, V. W. R. Chen, Ed., SPIE, San Francisco, California (2010).
44. A. P. Castano, P. Mroz, and M. R. Hamblin, "Photodynamic therapy and anti-tumour immunity," *Nat. Rev. Cancer* **6**(7), 535–545 (2006).
45. P. Mroz and M. R. Hamblin, "The immunosuppressive side of PDT," *Photochem. Photobiol. Sci.* **10**(5), 751–758 (2011).
46. A. D. Garg et al., "Photodynamic therapy: illuminating the road from cell death towards anti-tumour immunity," *Apoptosis* **15**(9), 1050–1071 (2010).
47. L. Wyld, M. W. Reed, and N. J. Brown, "Differential cell death response to photodynamic therapy is dependent on dose and cell type," *Br. J. Cancer* **84**(10), 1384–1386 (2001).

Linda Helander received her MSc degree in Trondheim at NTNU (Norwegian University of Science and Technology) in 2004. She studied biophysics and after her degree she worked as a staff engineer within molecular biology at University of Tromsø and is currently working as head of laboratory of NTNU Nanolab and finishing her PhD within the program of molecular medicine at NTNU.

Hans E. Krokan received his MD and PhD degrees in Oslo and Tromsø. He was a postdoctoral fellow at Harvard University and guest scientist at the National Cancer Institute, NIH. He is now a professor in molecular medicine at Norwegian University of Science and Technology and has authored approximately 200 scientific papers. He is an EMBO member and has been awarded prestigious national and international prizes for his research within DNA repair and cancer.

Anders Johnsson received his PhD at Lund University, Sweden. He has spent research periods in USA and Germany, specializing in physics and biophysics. He is now professor em. in the Department of Physics, Norwegian University of Science and Technology, Trondheim, Norway. His research interest focuses on oscillatory physiological processes in organisms, on photobiology and PDT of bacteria, and on balance system of plants. He has authored /coauthered about 190 papers and book chapters.

Odrun A. Gederaas is a senior research scientist who obtained her Dr. Philos degree in medical technology from the Norwegian University of Science and Technology, in collaboration with the University of Leiden, The Netherlands, and the Norwegian Radium Hospital in Oslo, Norway. The interdisciplinary field in photodynamic therapy has been developed during her postdoctoral fellow periods in Ohio, Irvine, Salzburg, and Lyon; together with two pharmacology companies in Oslo (Photo Cure AS and PCI Biotech AS).

Kristjan Plaetzer earned his PhD and venia docendi in biophysics at the University of Salzburg, Austria. He is interested in the cell death modes induced by PDT and cellular energetics of photo-treated cells and acquired expertise in application of photodynamic procedures based on natural substances as photosensitizers against microorganisms. He is now head of the Laboratory of Photodynamic Inactivation at the University of Salzburg (PDI-PLUS).

Paper III

View Online
Dynamic Article Links

Photochemical & Photobiological Sciences

Cite this: DOI: 10.1039/c0pp00369g

www.rsc.org/pps

PAPER

Photodynamic therapy with hexyl aminolevulinate induces carbonylation, posttranslational modifications and changed expression of proteins in cell survival and cell death pathways

Yan Baglo, Mirta M. L. Sousa, Geir Slupphaug, Lars Hagen, Sissel Håvåg, Linda Helander, Kamila A. Zub, Hans E. Krokan and Odrun A. Gederaas*

Received 8th December 2010, Accepted 3rd March 2011
DOI: 10.1039/c0pp00369g

Photodynamic therapy (PDT) using blue light and the potent precursor for protoporphyrin IX, hexyl aminolevulinate (HAL), has been shown to induce apoptosis and necrosis in cancer cells, but the mechanism remains obscure. In the present study, we examined protein carbonylation, expression levels and post-translational modifications in rat bladder cells (AY-27) after PDT with HAL. Altered levels of expression and/or post-translational modifications induced by PDT were observed for numerous proteins, including proteins required for cell mobility, energy supply, cell survival and cell death pathways, by using two-dimensional difference gel electrophoresis (2D-DIGE) and mass spectrometry (MS). Moreover, 10 carbonylated proteins associated with cytoskeleton, transport, oxidative stress response, protein biosynthesis and stability, and DNA repair were identified using immunoprecipitation, two-dimensional gel electrophoresis and MS. Overall, the results indicate that HAL-mediated PDT triggers a complex cellular response involving several biological pathways. Our findings may account for the elucidation of mechanisms modulated by PDT, paving the way to improve clinic PDT-efficacy.

1. Introduction

5-Aminolevulinic acid (ALA) is an endogenous precursor for protoporphyrin IX (PpIX) formed *via* the heme biosynthetic pathway. It has been shown that certain tumor cells have a large capacity to synthesize the photosensitizer PpIX in mitochondria when exposed to adequate concentrations of exogenous ALA because of low activity of ferrochelatase and elevated porphobilinogen deaminase.[1] Hexyl aminolevulinate (HAL) is an ester of ALA that is effectively converted into free ALA by esterases in cytosol before entering into the heme biosynthetic pathway.[2,3] The uptake mechanisms of ALA and ALA methyl ester have been extensively studied in human colon carcinoma cells (WiDr).[4–6]

In recent years, a number of studies on HAL-mediated PDT have been conducted. The improved penetration of HAL due to its high lipophilicity was demonstrated by comparison of distribution of ALA, whilst kinetics and intracellular localization of HAL-induced PpIX were investigated in human and rat bladder cancers *in vivo* and several human cancer cell lines.[7–18] The effect of illumination was examined in rat ovarian cancer and porcine bladder mucosa.[19,20] Moreover, tissue response to HAL-PDT was monitored in rat bladder. The results revealed a clear treatment response *in vivo* including decreased tissue oxygenation and PpIX photobleaching.[21] Later, PpIX photobleaching was proven to be a useful tool to predict the tissue response to HAL-PDT.[22] A clinical study comprising 24 patients demonstrated that HAL-PDT was a non-invasive, repeatable procedure for cervical intraepithelial neoplasia and no severe side effects were encountered.[23] Mechanisms of cell killing in PDT remain obscure, but are most likely complex and apparently involve both caspase-dependent and -independent apoptotic pathways.[24–26]

PDT results in a sequence of photochemical processes in photosensitized cells. Cellular antioxidant mechanisms are apparently overloaded by high levels of reactive oxygen species (ROS) and radicals. This leads to ROS-induced protein modifications and dysfunction, and eventually affects pathways resulting in cell death.[27] The most thoroughly characterized oxidative modifications of proteins subsequent to PDT are irreversible and non-enzymatic carbonylation and oxidation of thiol groups.[28,29] Magi *et al.* found that a specific set of proteins, including structural proteins and chaperones, were carbonylated and their results supported the concept that oxidative damage to proteins was selectively induced by PDT with Purpurin-18.[30]

The aim of the present study was to identify proteins with altered expression levels and/or altered post-translational status 2 h subsequent to HAL-mediated PDT in rat bladder cancer cells (AY-27), using 2D difference gel electrophoresis (2D-DIGE) and mass spectrometry (MS). To detect protein carbonylation and altered expression in less abundant proteins, carbonylated proteins were labeled with 2,4-dinitrophenyl hydrazine (DNPH)

Department of Cancer Research and Molecular Medicine, Norwegian University of Science and Technology, N-7491, Trondheim, Norway. E-mail: odrun.gederaas@ntnu.no; Fax: +4772576400; Tel: +4772573015

and immunoprecipitated with anti-DNP antibody prior to 2D-GE and MS.[31,32]

2. Materials and methods

2.1 Cell culture and HAL-mediated light treatment

Rat bladder cancer cells (AY-27) were maintained in RPMI-1640 culture medium (BioWhittaker) supplemented with 5% L-glutamine, 1% penicillin/streptomycin, 0.1% fungizone and 10% fetal bovine serum (FBS) in a humidified atmosphere of 95% air and 5% CO_2 at 37 °C.

About 3.5×10^6 cells were seeded per Petri dish (diameter: 10 cm) and cultured for one day. Subsequent to wash cells with PBS twice, RPMI-1640 culture medium (FBS-free) containing 10 μM HAL (PhotoCure AS, Norway) was added to cells and kept in the dark for 3.5 h. The medium was then replaced with PBS, and the cells were exposed to blue light (435 nm) for 35 s (0.45 J cm^{-2}, Lumi Source, PCI Biotech AS, Norway). Subsequent to 2 h incubation in the dark in FBS-free medium, cells were harvested by scraping in ice-cold PBS and centrifuged (450 g, 5 min, 4 °C).

Three groups of cell samples were analyzed in parallel: HAL; cells incubated with HAL only. PDT; cells treated with blue light after HAL incubation, and controls; without any treatment, neither HAL incubation nor light exposure.

This protocol was chosen based on our earlier unpublished results that the HAL-incubation time (3–3.5 h) gave a stable production of PpIX inside the AY-27 cancer cells and light treatment at the same experimental conditions led to about LD_{80} close to clinic target.

2.2 Protein extraction

Cell pellets were resuspended in 0.3× packed cell volume (PCV) of buffer I (10 mM Tris-HCl pH 8.0, 200 mM KCl, 1 mM DTT, 1% phosphatase inhibitor cocktail 1 and 2 (Sigma), 2% Complete protease inhibitor cocktail (Roche) and mixed with a volume of buffer II (10 mM Tris-HCl pH 8.0, 200 mM KCl, 2 mM EDTA, 40% glycerol, 0.5% NP40, 1 mM DTT and phosphatase- and protease inhibitors as above) corresponding to the combined volumes of the pellet and buffer I. The mixture was incubated on a roller (45 min, 4 °C) and sonicated (2 min, dark) using Branson Sonifier250 (output 2, duty cycle 20). Subsequent to centrifugation (10 min, 16100 g, 4 °C) supernatants (control, HAL and PDT) were collected and protein concentrations were determined using the Bio-Rad protein assay (BioRad Laboratories, USA).

2.3 Two dimensional difference gel electrophoresis (2D-DIGE)

Protein lysates (Control, HAL and PDT), 50 μg of each, were diluted in 2× lysis buffer (7 M urea, 4% CHAPS, 30 mM Tris, 2 M thiourea pH 8–8.5) and labelled with a specific CyDye (Cy2, Cy3 and Cy5, respectively), according to manufacturer's instructions (GE Healthcare). The reaction was quenched by adding 10 mM lysine (1 μl) following incubation for 10 min on ice in the dark. Each labelled protein sample was diluted 2-fold with 2× sample buffer (7 M urea, 4% CHAPS, 30 mM Tris, 130 mM DTT) and incubated on ice for 10 min. The three protein samples were mixed together and 1× sample buffer was added to reach a final volume of 450 μl. Then, 1% IPG buffer pH 3–11 (GE Healthcare) was added to the sample and rehydrated overnight into an IPGstrip (pH 3–11, 24 cm). Isoelectric focusing (IEF) was carried out according to the manufacturer's instructions (GE Heathcare). For the second dimension, strip was first incubated with equilibration stock buffer (50 M Tris-HCl pH 8.8, 6 M urea, 30% glycerol and 2% SDS) containing 1% DTT for 15 min and then with the equilibration stock buffer containing 2.5% iodoacetamide for 15 min under agitation at room temperature. The equilibrated strip was sealed on top of a 10% polyacrylamide gel using colorless liquid agarose. The electrophoresis was run overnight using Ettan DALT electrophoresis system (400 V, 20 mA, 2 W/gel, 20 °C).

Spots were visualized using the Typhoon™ Trio Imager (GE Healthcare) at wavelengths of 520 nm, 580 nm and 620 nm. Images were analyzed using DeCyder™ 2D software, which provides a 3D view of each protein spot. The spots are plotted as peaks that represent directly both the distribution (peak area) of the spot in the gel and its amount (peak volume). The relative peak volumes of protein spots were used to calculate the volume ratio of protein spots pairs (Cy3 and Cy5). Changes in volume ratio of protein spots pairs were used to determine proteins differentially expressed due to PDT treatment. Proteins of interest were then selected using DeCyder™ 2D software and picked using Ettan Spot Picker.

2.4 Two dimensional gel electrophoresis (2D-GE)

The HAL and PDT lysates (300 μg of each) were mixed together and DeStreak rehydration solution (GE Healthcare) was added to reach a final volume of 450 μl. The IPGstrip (pH 3–11, 24 cm) was rehydrated and protein separation by IEF and SDS-PAGE was performed as described above.

After 2D-GE separation, the gel was stained with silver according to the protocol established by Shevchenko[33] with minor modifications. Spots of interest were excised manually.

2.5 Protein identification by mass spectrometry (MS)

Protein spots were in-gel digested with trypsin as described by Shevchenko.[33] Peptides were extracted from the gel and desalted using StageTIP.[34] The eluted peptides were mixed with HCCA (α-cyano-4-hydroxycinnamic acid) matrix (7 g l^{-1} in 50% Acetonitrile, 50% ethanol) and loaded onto a MALDI-plate. Peptide mass fingerprints and MS/MS spectra were obtained using an Ultraflex III MALDI-TOF/TOF instrument (BRUKER Daltonics GmbH, Germany). Protein identification was performed by MSDB database searches using the Mascot software (Matrix Science).

2.6 Carbonylated protein labeling with 2,4-dinitrophenyl hydrazine (DNPH)

Protein lysates (1.5 mg each) were diluted (1 : 1) with 10% SDS and incubated for 5 min prior to addition of an equal volume of 10 mM DNPH in 10% TFA and further incubation for 30 min at room temperature under rotation. Reactions were stopped and the products (DNP-protein) precipitated by adding 2 volumes of 20% ice-cold trichloroacetic acid (TCA) and incubation on ice for 45 min. Precipitated DNP-proteins were pelleted (20 min, 5900 *g*, 4 °C), and pellets were washed three times with acetone (5 min, 4500 g, 4 °C) and resuspended in 600 μl of a 1 : 1 mixture of buffer I and II.

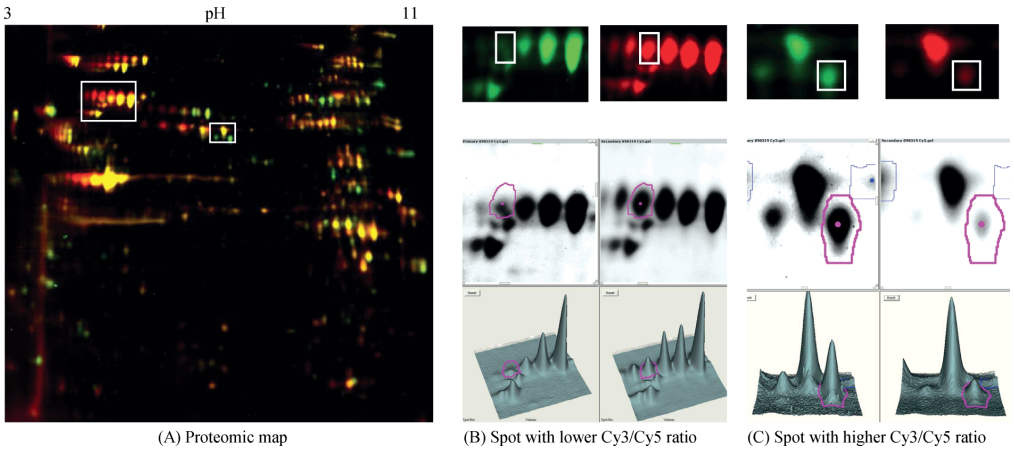

Fig. 1 Proteomic map of HAL and PDT lysate samples of AY-27 cells. (A) Proteins under-expressed (green spots) or over-expressed (red spots) in the PDT sample (HAL and light treatment) compared to control (only HAL treatment); (B) spot with lower Cy3/Cy5 ratio (DeCyder analysis) shown as red in the proteomic map was up-regulated in the PDT sample. This spot together with other 3 spots to the right were identified as heat shock protein 60 kDa later by MS indicating pI-shift.; (C) Spot with higher Cy3/Cy5 ratio shown as green in the proteomic map was down-regulated in the PDT sample.

2.7 Immunoprecipitation using anti-DNP antibody

Anti-DNP antibodies were covalently coupled to paramagnetic Dynabeads protein A beads according to the manufacturer's protocol (Dynal). DNP-labelled protein samples were incubated with crosslinked beads (150 µl) overnight at 4 °C with constant agitation. The beads were washed three times with 10 mM Tris-HCl (pH 8.3), 50 mM KCl (pH 8.3) and DNP-proteins eluted with 1× Novex LDS loading buffer (13 µl, Invitrogen) and the beads were further incubated overnight in 1× sample buffer (117 µl). The combined eluates were then subjected to 2D-GE using 7 cm IPGstrip (pH 3–11) and a 4–12% gradient NuPAGE gel (Invitrogen). The gel was stained with Krypton protein stain according to the manufacturer's protocol (Pierce, USA) and the spots were visualized using a Typhoon scanner (GE Healthcare).

3. Results and discussion

3.1 PDT treatment causes marked changes in protein expression and apparent post-translational modification status

Alterations in the apparent post-translational modification (PTM) status of proteins two hours subsequent to HAL alone or HAL/PDT treatment of rat bladder cancer cells (AY-27) were monitored in three parallel experiments using 2D-DIGE. Since our primary objective was to identify altered migration of proteins that could indicate differential PTM status, a Cy2-labelled internal control was not included in the experiments. Nevertheless, a marked difference in the overall expression level of several proteins was evident from the Cy3/Cy5 ratios. Moreover, the proteomic maps obtained from the parallel experiments were very similar, indicating that the procedure is highly reproducible. A representative proteomic map of HAL and PDT lysate samples is shown in Fig. 1 (a), in which clear red spots represent up-regulated proteins (Fig. 1, b) and clear green spots represent down-regulated proteins (Fig. 1, c) in the PDT-treated cells as compared to cells treated with HAL only. Yellow spots represent proteins expressed at similar level in both samples. The 2D-DIGE image clearly demonstrates that additional exposure of the HAL-treated cells to blue light causes a striking change in the expression of some proteins. Moreover, several proteins exhibited apparently different migration in the 2D-gel, typically in the form of species having an acidic pI-shift (Fig. 1, b). Such acidic shifts might be the result of enzymatic modifications mediating gain of negative charge by, for example, phosphorylation, or loss of positive charge by, for example, acetylation. However, shifts towards the acidic side may also result from non-enzymatic oxidative modifications, such as oxidation of cysteine to cysteine sulfenic- or sulfinic acid.

In order to increase protein concentration and enhance protein identification in MS analysis, a 2D-GE was run with higher amount of both HAL and PDT lysate samples (Fig. 2), and proteins were excised from the silver-stained gel using the 2D-DIGE gels as reference. A total of 40 proteins were identified and assigned in the 2D-DIGE gel (Fig. 3). Among these, 15 proteins were markedly up-/down-regulated or displayed modified post-translational status, as suggested by their altered migration. As shown in Table 1, heterogeneous nuclear ribonucleoprotein (hnRNP) L and pre-mRNA-processing factor 19 were markedly up-regulated, while pyruvate kinase isozymes M1/M2, vimentin, and tubulin alpha-1 chain were markedly down-regulated. The remaining 10 proteins displayed acidic pI-shifts, as illustrated for HSP60 (Fig. 1, b).

Apparent down-regulation of vimentin could be a consequence of vimentin cross-linking resulting from carbonylation. This has previously been observed in A549 cells subsequent to acrolein-induced carbonylation,[35] and would mediate a loss of vimentin monomers in 1D-GE and 2D-GE gels. Interestingly, several of the most abundant cytoskeletal and chaperone proteins such as β-actin, protein disulfide-isomerase A6 and A3, HSP70/90 and

Table 1 Proteins and biological processes/pathways in AY-27 cells affected by HAL-mediated PDT, based on the 24 proteins subject to post-translational modification and differential expression, analyzed using Uniprot and PANTHER software (www.pantherdb.org)

Gene ID	Name of protein	Cellular location	PDT response[a]	Main molecular function	Main biological process/pathway	Reference
P11980	pyruvate kinase isozymes M1/M2	cytosol	D	carbohydrate kinase	glycolysis/pyruvate metabolism	
P68370	tubulin alpha-1A chain	microtubule	D	tubulin	intracellular protein traffic, cell structure and motility, cell cycle, developmental process, *etc*.	30,37,38
P31000	vimentin	nucleus, cytoplasm	D	structural protein	ectoderm development; cell structure	35,39
Q5U1Y5	hnRNP L[b]	nucleus	U	ribosomal protein	mRNA splicing	
Q9JMJ4	pre-mRNA-processing factor 19	nucleus	U	RNA-binding protein	mRNA splicing	
Q63081	protein disulfide isomerase (PDI) A6	ER	P	other isomerase	disulfide-isomerase reaction	43,52
P11598	PDI A3 (p58)	ER	P	isomerase	disulfide-isomerase reaction	43,52
P11884	aldehyde dehydrogenase	mitochondria	P	dehydrogenase	phenylethylamine degradation (carbon metabolism)	
Q66HD0	endoplasmin (GRP94, HSP90)	ER	P	chaperone	protein folding, stress response	43–46,50,51
P63039	60kDa heat shock protein (HSP60)	mitochondria	P	chaperonin	protein folding	30,43–47,49–51
P10719	F1-ATPase beta chain	mitochondria	P	other ion channel, hydrogen transporter, ATP synthase; hydrolase	purine metabolism, electron transport (ATP synthesis)	
Q6P136	hyou1 protein	cytosol	P	chaperone	stress response	
P48721	stress-70 protein (GRP75)	mitochondria	P	chaperone	protein folding; Stress response (apoptosis signaling pathway)	43–46
P14659	heat shock cognate 71kDa protein (HSP70)	cytosol, organelles	P	chaperone	protein folding; Stress response (apoptosis signaling pathway)	30,43–46,48–51
P60711	β-actin	cytoplasm	C, P, U	actin and actin related protein	transport; cytokinesis; cell structure, *etc*.	30–40
P15178	aspartyl-tRNA synthetase	cytoplasm	C, U	aminoacyl-tRNA synthetase	protein biosynthesis	
P02563	myosin-6 heavy chain	cytoplasm	C, U	motor protein, muscle protein	muscle contraction/development, (Wnt signaling pathway, cytokine signaling pathway, *etc*)	

Table 1 *(Contd.)*

Gene ID	Name of protein	Cellular location	PDT response[a]	Main molecular function	Main biological process/pathway	Reference
P32089	tricarboxylate transport protein (TCC)	mitochondria, membrane	C, U	mitochondrial carrier protein	small molecule transport	
A7VJC2	hnRNP A2/B1	nucleus, cytoplasm	C, U	ribonucleoprotein	mRNA splicing	
P04256	hnRNP A1	nucleus, cytoplasm	C, U	ribonucleoprotein	mRNA splicing, mRNA transport	
Q7TP52	carboxymethylene-butenolidase homolog	cytoplasm	C, U	hydrolase; other miscellaneous function protein	carbohydrate metabolism	
Q5M7T9	threonine synthase-like 2	cytosol	C, U	synthase	threonine biosynthesis; vitamin B6 metabolism	
P54758	ephrin type-A receptor 6	membrane	C, U	tyrosine protein kinase, receptor; transferase	protein phosphorylation; cell proliferation and differentiation; receptor protein tyrosine kinase signaling pathway	
Q06226	serum and glucocorticoid -regulated kinase (sgk1)	ER, nucleus, cytoplasm	C, D	kinase activity	Protein phosphorylation; Inhibition of apoptosis; Other homeostasis activities and intracellular signaling cascade	

[a] D: down-regulated; U: up-regulated; P: pI-shift; C: carbonylated. [b] hnRNP: heterogeneous nuclear ribonucleoprotein.

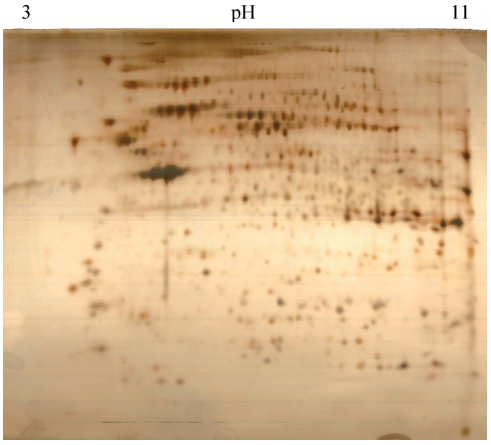

Fig. 2 Silver-stained gel. HAL and PDT lysate samples (300 μg of each) of AY-27 cells were mixed and subjected to IEF in a 24 cm IPGstrip pH 3–11 and separated in a 10% polyacrylamide gel. Proteins selected from the DIGE reference gel were excised from the silver stained gel for MS identification.

Grp75 all display marked acidic pI-shifts after HAL-mediated PDT. It is tempting to speculate that these abundant proteins may be quantitatively dominating targets for direct oxidative attack within the cell during HAL-mediated PDT, and that the observed pI-shifts may represent such covalent modifications that are not reversed by the reducing conditions employed during 2D-DIGE. Cysteine sulfonic acid is such an irreversible modification, whereas cysteine sulfenic acid and reaction products thereof such as glutathioylations, are reversible,[36] and would most likely have been reverted during the procedure of two dimensional gel-electrophoresis. Moreover, carbonylation should not mediate pI shifts since they do not introduce charge differences in the proteins. An alternative explanation would be that these proteins, at least in part, are modified enzymatically as part of the oxidative stress response. At least the protein disulfide isomerases, β-actin, HSP70/90 may become phosphorylated as a consequence of various forms of cellular stress, and for the chaperone group of protein this apparently is part of a regulatory mechanism modulating the substrate specificity.

Damage to several structural proteins induced by PDT was previously reported using other cell lines and photosensitizers. Moor *et al.* and Lee *et al.* stated that cellular structures having high sensitizer and a high oxygen concentration would be preferentially damaged upon illumination.[37,38] Belichenko *et al.* investigated the role of vimentin in apoptosis after PDT with the silicon phthalocyanine Pc4 in human Jurkat T cells and found that the full-length vimentin confers resistance to nuclear apoptosis.[39]

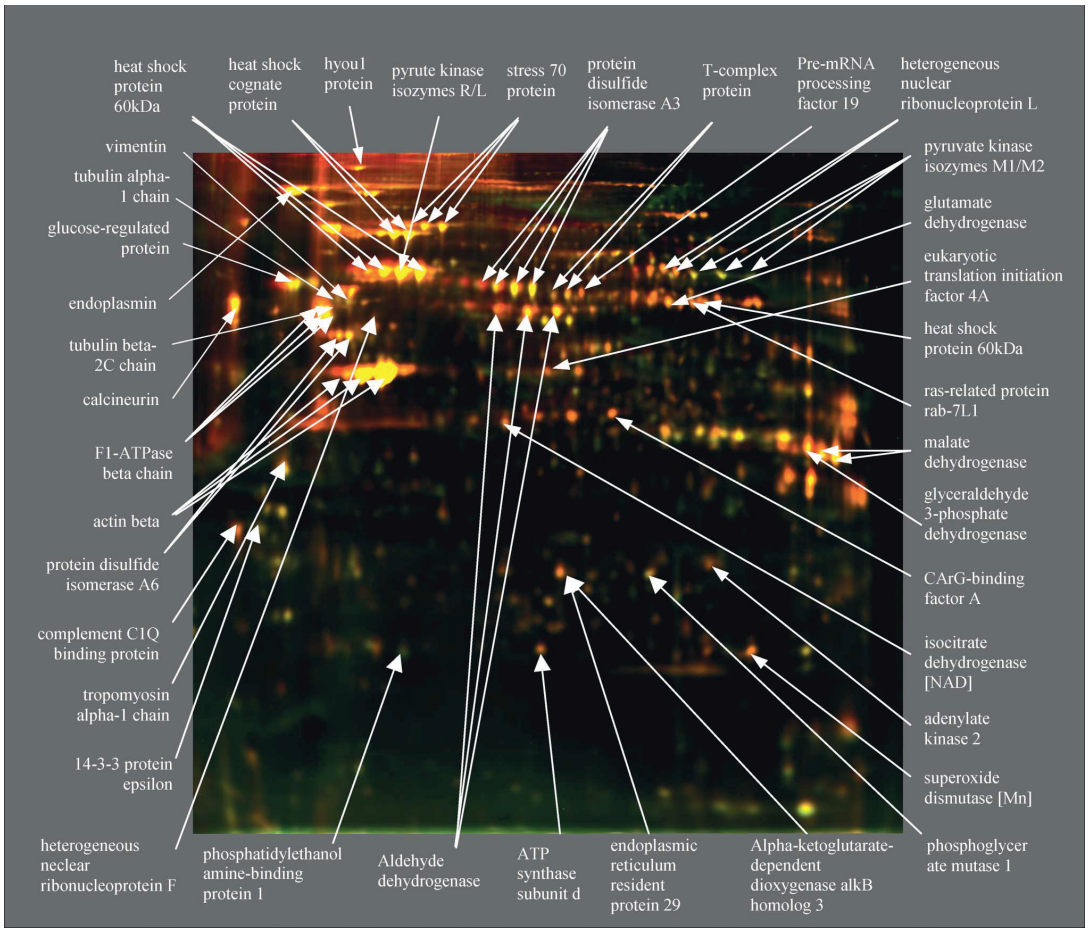

Fig. 3 Mapping of 40 identified proteins in AY-27 cells (DIGE, 10% polyacrylamide gel). Protein spots of interest were picked from both 2D-DIGE gels and silver stained 2D-GE gels and identified by MALDI-TOF/TOF (Ultraflex III, BRUKER Daltonics GmbH, Germany).

Later, Tsaytler *et al.* concluded that more structural proteins were oxidatively modified in human epidermoid carcinoma cells A431 after Pc4-PDT,[40] and Magi *et al.* described that tubulin α-1 chain and β-actin were modified *via* carbonylation after PDT with Purpurin-18 in human HL60 cells.[30]

It has been demonstrated that some cell lines can respond to photodynamic damage by initiating a rescue response[41,42] to induce expression of stress proteins containing a number of heat shock proteins (HSPs) and glucose-regulated proteins (GRPs).[43–46] The contribution by HSP60 increased the resistance to Photofrin-mediated PDT in human colon cancer cell line (HT29),[47] while HSP70 was demonstrated to inhibit apoptosis mediated by PDT with either dihematoporphyrin ether or Purpurin-18 in human leukemia cells (HL60).[48] Elevated expression of both HSP60 and HSP70 after ALA-PDT was observed in several human cell lines by Yanase *et al.*,[49] and these proteins were carbonylated during Purpurin-18 mediated PDT, as reported by Magi *et al.*[30] Moreover, it has been demonstrated that the amounts of HSP60, HSP70 and GRP94 (endoplasmin, HSP90) increased at the cell surface, contributing to enhanced immune responses in mouse tumor cells (SCCVII) after Photofrin-mediated PDT.[50,51] Our results show that several rescue/stress proteins were modified in the rat cell line AY-27 after HAL-PDT, including HSP60, HSP70, GRP94, GRP75 and hyou1 protein. These proteins have important chaperone functions in the cell and apparently may shield the cells from oxidative damage. Interestingly, Magi *et al.*[30] hypothesized that cellular chaperones may actually bind to oxidized proteins and that a protein-protein radical transfer can occur from oxidized proteins to chaperones. Thus, certain chaperones trying to reduce the toxic effect of oxidative stress are themselves oxidized.

Among proteins involved in energy metabolism, pI-shift was observed for hyou1 protein and F1-ATPase beta chain. Additionally, pyruvate kinase isozymes M1/M2 were shown to be down-regulated. These modifications might contribute to energy insufficiency and cell death by inhibiting the hypoxia responses.

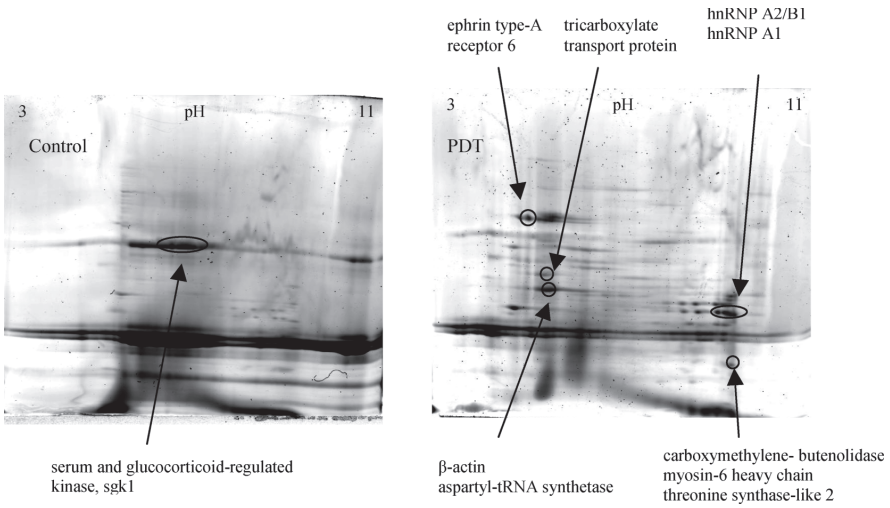

Fig. 4 Mapping of carbonylated proteins of AY-27 cells 2 h subsequent to HAL-mediated PDT. Nine up-regulated proteins are shown in PDT sample (right) and one down-regulated is shown in Control sample (left). Each sample (1.5 mg) was labeled with 10mM DNPH in 10% TFA and immunoprecipited with 150 µl cross-linked protein A beads with anti-DNP antibodies before 2D-GE separation. Protein spots of interest were excised from krypton-gels and 10 carbonylated proteins were identified by MALDI-TOF/TOF.

Moreover, the modifications on the rescue/stress proteins might lose their protective effect against oxidative stress triggering the suicide mechanism after PDT.

Three proteins associated with Ca^{2+} signaling pathways were shown to be affected by ALA-PDT,[43,52] including calreticulin precursor, protein disulfide isomerase (p55) and protein disulfide isomerase A3 (p58).[43] In our study, although protein p58, p55 and calcineurin subunit B have been identified, only p58 was confirmed to be modified by showing a pI-shift. More experiments are required to identify possible HAL-PDT effects on this signaling pathway.

3.2 Detection of carbonylated proteins

The most widely used marker for oxidative damage to proteins is the presence of carbonyl groups. Carbonyls can be introduced into proteins either by direct oxidation of Pro, Arg, Lys, and Thr side chains or by Michael addition reactions with products of lipid peroxidation or glycol-oxidation. Elevation in the total level of protein carbonyls has been documented after PDT, but the identities of the proteins modified by carbonylation or other types of oxidation remain largely incompletely understood. Since carbonylation, in contrast to oxidation of cysteine to cysteine sulfonic or sulfinic acid, do not mediate a change in pI, control and PDT samples were derivatized with DNPH and immunoprecipitated using an anti-DNP antibody prior to separation by 2D-GE. By using this experimental outline we were able to identify 9 proteins with increased carbonylation and, surprisingly, one protein with reduced carbonylation (Fig. 4).

According to our results, β-actin was confirmed to be carbonylated after HAL-PDT, in agreement with results after PDT with Purpurin-18 in HL60.[30] However, carbonylation is apparently not the only modification induced in β-actin by HAL-PDT. The pI-shift towards the acidic side indicates that alternative oxidations such as cysteine sulfinic acid, or secondary enzymatic modifications such as phosphorylation, may be present.

Moreover, protein hnRNP A1 and hnRNP A2/B1 were confirmed to be up-regulated and oxidized. Together with pre-mRNA processing factor 19 and hnRNP L (Table 1), four up-regulated proteins in our results are related to DNA-repair, pre-mRNA processing and mRNA splicing. These results may suggest that transcription, translation or stability may have been increased in response to protein and DNA damages under oxidative stress induced by HAL-mediated PDT.

Interestingly, mitochondrial tricarboxylate carrier protein (TCC) and serum and glucocorticoid-regulated kinase 1 (sgk1) were found to display altered expression or modification after PDT. Both of them are supposed to play a key role in oxidative stress conditions in rat brain.[53,54] Our results demonstrate that both proteins were carbonylated. TCC was up-regulated, while sgk1 was down-regulated already at 2 h post-PDT.

3.3 Proteins, pathways and processes affected by HAL-PDT

ROS-induced modifications may change protein functions, thereby affecting biological processes and signaling pathways.[27] A total of more than 200 post-translational modifications have been identified.[55] Furthermore, increasing evidence suggests that many proteins carry multiple and distinct modifications. These may in some cases antagonize or synergize each other, with important biological consequences.[55] Thus, the PANTHER classification system was used to gain information of potential affected biological processes after HAL-PDT. Clearly, the complex responses indicate that no single mechanism can be responsible for the effects of HAL-PDT (Table 1).

In AY-27 cells the endogenous photosensitizer PpIX is synthesized and accumulated in mitochondria, and moves to other membrane-rich organelles when a certain concentration

is reached.[1] Classification of proteins by cellular localization (Table 1) demonstrates that the majority of the modified proteins by HAL-PDT were from mitochondria, ER and membranes. However, in the study of Pc4-PDT,[40] the majority of affected proteins were cytosolic, likely reflecting a somewhat different cellular targeting of PpIX and Pc4.[56] So far, nuclear localization of PpIX has not been observed. Nevertheless, several cytoplasmic and nuclear proteins were shown to be affected in our study, likely caused by indirect oxidation or intracellular translocation subsequent to HAL-mediated PDT.

4. Conclusions

Our results demonstrate that a number of proteins in AY-27 cells are differentially expressed or chemically or enzymatically modified after HAL-mediated PDT, thus most likely affecting important processes, such as cell motility, energy metabolism, and signaling pathways for survival and cell death. The results support previous studies employing other photosensitizers,[30,40] in that numerous cellular pathways are likely to be affected by PDT. The majority of proteins identified subsequent to 2D-DIGE displayed acidic pI-shifts, indicating altered phosphorylation status or oxidative thiol modifications. Notably, these proteins mainly belong to the mitochondrial/ER molecular chaperones and stress proteins, indicating that these cellular compartments are major targets for HAL-mediated PDT. These results have extended our understanding of the clinic effects associated with ALA-PDT, and may pave the way for potential new adjuvant drugs. Our further studies are, however, warranted to elucidate to what degree these modifications are associated with the apoptotic signaling events induced by HAL-PDT. By better understanding mechanisms of PDT-mediated cytotoxicity in AY-27 bladder cancer cells, we aim at improving efficacy of PDT in the *in vivo* rat model[21] and ultimately in treatment of human bladder. This may also pave the way for targeted use of other treatment modalities, such as siRNA and photochemical internalization (PCI).[57]

Acknowledgements

We are grateful to our colleague Kristian Wollen Steen for his excellent laboratory assistance; to Photocure ASA and PCI Biotech AS (Oslo, Norway) for HAL (Hexvix®) and Lamp resource supply; to the FUGE Proteomics Laboratory at NTNU (Trondheim, Norway), and to Professor Steven H. Selman (Medical College of Ohio, USA) for AY-27 cell line supply.

References

1 N. Schoenfeld, O. Epstein, M. Lahav, R. Mamet, M. Shaklai and A. Atsmon, The heme biosynthetic pathway in lymphocytes of patients with malignant lymphoproliferative disorders, *Cancer Lett.*, 1988, **43**(1–2), 43–8.
2 J. Kloek, W. Akkermans and G. M. Beijersbergen van Henegouwen, Derivatives of 5-aminolevulinic acid for photodynamic therapy: enzymatic conversion into protoporphyrin, *Photochem. Photobiol.*, 1998, **67**(1), 150–4.
3 G. Di Venosa, H. Fukuda, A. Batlle, A. Macrobert and A. Casas, Photodynamic therapy: regulation of porphyrin synthesis and hydrolysis from ALA esters, *J. Photochem. Photobiol., B*, 2006, **83**(2), 129–36.
4 E. Rud, O. Gederaas, A. Hogset and K. Berg, 5-aminolevulinic acid, but not 5-aminolevulinic acid esters, is transported into adenocarcinoma cells by system BETA transporters, *Photochem. Photobiol.*, 2000, **71**(5), 640–7.
5 O. A. Gederaas, A. Holroyd, S. B. Brown, D. Vernon, J. Moan and K. Berg, 5-Aminolaevulinic acid methyl ester transport on amino acid carriers in a human colon adenocarcinoma cell line, *Photochem. Photobiol.*, 2001, **73**(2), 164–9.
6 O. A. Gederaas *Biological mechanisms involved in 5-aminovulinic acid based photodynamic therapy*, PhD thesis, NTNU and The Norwegian Radium Hospital, 2000.
7 N. Dognitz, D. Salomon, M. Zellweger, J. P. Ballini, T. Gabrecht and N. Lange, *et al.*, Comparison of ALA- and ALA hexyl-ester-induced PpIX depth distribution in human skin carcinoma, *J. Photochem. Photobiol., B*, 2008, **93**(3), 140–8.
8 A. Marti, P. Jichlinski, N. Lange, J. P. Ballini, L. Guillou and H. J. Leisinger *et al.*, Comparison of aminolevulinic acid and hexylester aminolevulinate induced protoporphyrin IX distribution in human bladder cancer, *J. Urol.*, 2003, **170**(2), 428–32.
9 A. Juzeniene, K. P. Nielsen, L. Zhao, G. A. Ryzhikov, M. S. Biryulina and J. J. Stamnes *et al.*, Changes in human skin after topical PDT with hexyl aminolevulinate, *Photodiagn. Photodyn. Ther.*, 2008, **5**(3), 176–81.
10 R. W. Wu, E. S. Chu, C. M. Yow and J. Y. Chen, Photodynamic effects on nasopharyngeal carcinoma (NPC) cells with 5-aminolevulinic acid or its hexyl ester, *Cancer Lett.*, 2006, **242**(1), 112–9.
11 S. M. WU, Q. G. Ren, M. O. Zhou and Y. Wei, Photodynamic Effects of 5-Aminolevulinic Acid and Its Hexylester on Several Cell Lines, *Acta Biochim. Biophys. Sin.*, 2003, **35**(7), 655–60.
12 A. Casas, C. Perotti, M. Saccoliti, P. Sacca, H. Fukuda and A. M. Batlle, ALA and ALA hexyl ester in free and liposomal formulations for the photosensitisation of tumour organ cultures, *Br. J. Cancer*, 2002, **86**(5), 837–42.
13 S. Berrahmoune, N. Fotinos, L. Bezdetnaya, N. Lange, J. C. Guedenet and F. Guillemin *et al.*, Analysis of differential PDT effect in rat bladder tumor models according to concentrations of intravesical hexyl-aminolevulinate, *Photochem. Photobiol. Sci.*, 2008, **7**(9), 1018–24.
14 L. Zhao, K. P. Nielsen, A. Juzeniene, P. Juzenas, V. Lani and L. W. Ma *et al.*, Spectroscopic measurements of photoinduced processes in human skin after topical application of the hexyl ester of 5-aminolevulinic acid, *J. Environ. Pathol. Toxicol. Oncol.*, 2006, **25**(1-2), 307–20.
15 A. Juzeniene, P. Juzenas, L. W. Ma, V. Iani and J. Moan, Topical application of 5-aminolaevulinic acid, methyl 5-aminolaevulinate and hexyl 5-aminolaevulinate on normal human skin, *Br. J. Dermatol.*, 2006, **155**(4), 791–9.
16 V. Zenzen and H. Zankl, Protoporphyrin IX-accumulation in human tumor cells following topical ALA- and h-ALA-application in vivo, *Cancer Lett.*, 2003, **202**(1), 35–42.
17 S. El Khatib, J. Didelon, A. Leroux, L. Bezdetnaya, D. Notter and M. D'Hallewin, Kinetics, biodistribution and therapeutic efficacy of hexylester 5-aminolevulinate induced photodynamic therapy in an orthotopic rat bladder tumor model, *J. Urol.*, 2004, **172**(5), 2013–7.
18 G. Kirdaite, N. Lange, N. Busso, H. Van Den Bergh, P. Kucera and A. So, Protoporphyrin IX photodynamic therapy for synovitis, *Arthritis Rheum.*, 2002, **46**(5), 1371–8.
19 M. Ascencio, J. P. Estevez, M. Delemer, M. O. Farine, P. Collinet and S. Mordon, Comparison of continuous and fractionated illumination during hexaminolaevulinate-photodynamic therapy, *Photodiagn. Photodyn. Ther.*, 2008, **5**(3), 210–6.
20 L. Vaucher, P. Jichlinski, N. Lange, C. Ritter-Schenk, H. van den Bergh and P. Kucera, Hexyl-aminolevulinate-mediated photodynamic therapy: how to spare normal urothelium. An in vitro approach, *Lasers Surg. Med.*, 2007, **39**(1), 67–75.
21 E. L. Larsen, L. L. Randeberg, O. A. Gederaas, C. J. Arum, A. Hjelde and C. M. Zhao *et al.*, Monitoring of hexyl 5-aminolevulinate-induced photodynamic therapy in rat bladder cancer by optical spectroscopy, *J. Biomed. Opt.*, 2008, **13**(4), 044031.
22 M. Ascencio, P. Collinet, M. O. Farine and S. Mordon, Protoporphyrin IX fluorescence photobleaching is a useful tool to predict the response of rat ovarian cancer following hexaminolevulinate photodynamic therapy, *Lasers Surg. Med.*, 2008, **40**(5), 332–41.
23 P. Soergel, X. Wang, H. Stepp, H. Hertel and P. Hillemanns, Photodynamic therapy of cervical intraepithelial neoplasia with hexaminolevulinate, *Lasers Surg. Med.*, 2008, **40**(9), 611–5.
24 S. Shahzidi, T. Stokke, H. Soltani, J. M. Nesland and Q. Peng, Induction of apoptosis by hexaminolevulinate-mediated photodynamic therapy in

human colon carcinoma cell line 320DM, *J. Environ. Pathol. Toxicol. Oncol.*, 2006, **25**(1-2), 159–71.
25 I. E. Furre, M. T. Moller, S. Shahzidi, J. M. Nesland and Q. Peng, Involvement of both caspase-dependent and -independent pathways in apoptotic induction by hexaminolevulinate-mediated photodynamic therapy in human lymphoma cells, *Apoptosis*, 2006, **11**(11), 2031–42.
26 I. E. Furre, S. Shahzidi, Z. Luksiene, M. T. Moller, E. Borgen and J. Morgan *et al.*, Targeting PBR by hexaminolevulinate-mediated photodynamic therapy induces apoptosis through translocation of apoptosis-inducing factor in human leukemia cells, *Cancer Res.*, 2005, **65**(23), 11051–60.
27 K. England and T. G. Cotter, Direct oxidative modifications of signalling proteins in mammalian cells and their effects on apoptosis, *Redox Rep.*, 2005, **10**(5), 237–45.
28 E. R. Stadtman and R. L. Levine, Protein oxidation, *Ann. N. Y. Acad. Sci.*, 2000, **899**, 191–208.
29 I. Dalle-Donne, M. Carini, M. Orioli, G. Vistoli, L. Regazzoni and G. Colombo *et al.*, Protein carbonylation: 2,4-dinitrophenylhydrazine reacts with both aldehydes/ketones and sulfenic acids, *Free Radical Biol. Med.*, 2009, **46**(10), 1411–9.
30 B. Magi, A. Ettorre, S. Liberatori, L. Bini, M. Andreassi and S. Frosali *et al.*, Selectivity of protein carbonylation in the apoptotic response to oxidative stress associated with photodynamic therapy: a cell biochemical and proteomic investigation, *Cell Death Differ.*, 2004, **11**(8), 842–52.
31 T. Reinheckel, S. Korn, S. Mohring, W. Augustin, W. Halangk and L. Schild, Adaptation of protein carbonyl detection to the requirements of proteome analysis demonstrated for hypoxia/reoxygenation in isolated rat liver mitochondria, *Arch. Biochem. Biophys.*, 2000, **376**(1), 59–65.
32 I. V. Kjaersgard and F. Jessen, Two-dimensional gel electrophoresis detection of protein oxidation in fresh and tainted rainbow trout muscle, *J. Agric. Food Chem.*, 2004, **52**(23), 7101–7.
33 A. Shevchenko, M. Wilm, O. Vorm and M. Mann, Mass spectrometric sequencing of proteins silver-stained polyacrylamide gels, *Anal. Chem.*, 1996, **68**(5), 850–8.
34 M. Mann and O. N. Jensen, Proteomic analysis of post-translational modifications, *Nat. Biotechnol.*, 2003, **21**(3), 255–61.
35 P. C. Burcham, A. Raso and C. A. Thompson, Intermediate filament carbonylation during acute acrolein toxicity in A549 lung cells: functional consequences, chaperone redistribution, and protection by bisulfite, *Antioxid. Redox Signaling*, 2010, **12**(3), 337–47.
36 N. L. Reynaert, A. van der Vliet, A. S. Guala, T. McGovern, M. Hristova and C. Pantano *et al.*, Dynamic redox control of NF-kappaB through glutaredoxin-regulated S-glutathionylation of inhibitory kappaB kinase beta, *Proc. Natl. Acad. Sci. U. S. A.*, 2006, **103**(35), 13086–91.
37 A. C. Moor, Signaling pathways in cell death and survival after photodynamic therapy, *J. Photochem. Photobiol., B*, 2000, **57**(1), 1–13.
38 C. Lee, S. S. Wu and L. B. Chen, Photosensitization by 3,3′-dihexyloxacarbocyanine iodide: specific disruption of microtubules and inactivation of organelle motility, *Cancer Res.*, 1995, **55**(10), 2063–9.
39 I. Belichenko, N. Morishima and D. Separovic, Caspase-resistant vimentin suppresses apoptosis after photodynamic treatment with a silicon phthalocyanine in Jurkat cells, *Arch. Biochem. Biophys.*, 2001, **390**(1), 57–63.
40 P. A. Tsaytler, M. COF, D. V. Sakharov, J. Krijgsveld and M. R. Egmond, Immediate protein targets of photodynamic treatment in carcinoma cells, *J. Proteome Res.*, 2008, **7**(9), 3868–78.
41 T. J. Dougherty, C. J. Gomer, B. W. Henderson, G. Jori, D. Kessel and M. Korbelik *et al.*, Photodynamic therapy, *J. Natl. Cancer Inst.*, 1998, **90**(12), 889–905.
42 C. J. Gomer, A. Ferrario, N. Hayashi, N. Rucker, B. C. Szirth and A. L. Murphree, Molecular, cellular, and tissue responses following photodynamic therapy, *Lasers Surg. Med.*, 1988, **8**(5), 450–63.
43 D. Grebenova, P. Halada, J. Stulik, V. Havlicek and Z. Hrkal, Protein changes in HL60 leukemia cells associated with 5-aminolevulinic acid-based photodynamic therapy. Early effects on endoplasmic reticulum chaperones, *Photochem. Photobiol.*, 2000, **72**(1), 16–22.
44 C. J. Gomer, S. W. Ryter, A. Ferrario, N. Rucker, S. Wong and A. M. Fisher, Photodynamic therapy-mediated oxidative stress can induce expression of heat shock proteins, *Cancer Res.*, 1996, **56**(10), 2355–60.
45 C. J. Gomer, A. Ferrario, N. Rucker, S. Wong and A. S. Lee, Glucose regulated protein induction and cellular resistance to oxidative stress mediated by porphyrin photosensitization, *Cancer Res.*, 1991, **51**(24), 6574–9.
46 P. M. Curry and J. G. Levy, Stress protein expression in murine tumor cells following photodynamic therapy with benzoporphyrin derivative, *Photochem. Photobiol.*, 1993, **58**(3), 374–9.
47 J. G. Hanlon, K. Adams, A. J. Rainbow, R. S. Gupta and G. Singh, Induction of Hsp60 by Photofrin-mediated photodynamic therapy, *J. Photochem. Photobiol., B*, 2001, **64**(1), 55–61.
48 M. Nonaka, H. Ikeda and T. Inokuchi, Inhibitory effect of heat shock protein 70 on apoptosis induced by photodynamic therapy in vitro, *Photochem. Photobiol.*, 2004, **79**(1), 94–8.
49 S. Yanase, J. Nomura, Y. Matsumura, K. Nagai, M. Kinoshita and H. Nakanishi *et al.*, Enhancement of the effect of 5-aminolevulinic acid-based photodynamic therapy by simultaneous hyperthermia, *Int. J. Oncol.*, 2005, **27**(1), 193–201.
50 M. Korbelik, J. Sun and I. Cecic, Photodynamic therapy-induced cell surface expression and release of heat shock proteins: relevance for tumor response, *Cancer Res.*, 2005, **65**(3), 1018–26.
51 I. Cecic and M. Korbelik, Deposition of complement proteins on cells treated by photodynamic therapy in vitro, *J. Environ. Pathol. Toxicol. Oncol.*, 2006, **25**(1-2), 189–203.
52 O. A. Gederaas, K. Thorstensen and I. Romslo, The effect of brief illumination on intracellular free calcium concentration in cells with 5-aminolevulinic acid-induced protoporphyrin IX synthesis, *Scand. J. Clin. Lab. Invest.*, 1996, **56**(7), 583–9.
53 A. L. Wadey, H. Muyderman, P. T. Kwek and N. R. Sims, Mitochondrial glutathione uptake: characterization in isolated brain mitochondria and astrocytes in culture, *J. Neurochem.*, 2009, **109**(Suppl 1), 101–8.
54 B. Schoenebeck, V. Bader, X. R. Zhu, B. Schmitz, H. Lubbert and C. C. Stichel, Sgk1, a cell survival response in neurodegenerative diseases, *Mol. Cell. Neurosci.*, 2005, **30**(2), 249–64.
55 N. Khidekel and L. C. Hsieh-Wilson, A 'molecular switchboard'–covalent modifications to proteins and their impact on transcription, *Org. Biomol. Chem.*, 2004, **2**(1), 1–7.
56 M. Lam, N. L. Oleinick and A. L. Nieminen, Photodynamic therapy-induced apoptosis in epidermoid carcinoma cells. Reactive oxygen species and mitochondrial inner membrane permeabilization, *J. Biol. Chem.*, 2001, **276**(50), 47379–86.
57 P. K. Selbo, A. Weyergang, A. Hogset, O. J. Norum, M. B. Berstad, M. Vikdal and K. Berg, Photochemical internalization provides time- and space-controlled endolysosomal escape of therapeutic molecules, *J. Controlled Release*, 2010, **148**(1), 2–12.

Paper IV

Is not included due to copyright